1975

A high temperature vaporization and thermodynamic study of the scandium-sulfur system

Richard Timothy Tuenge
Iowa State University

A high temperature vaporization and thermodynamic study of the scandium-sulfur system

by

Richard Timothy Tuenge

A Dissertation Submitted to the
Graduate Faculty in Partial Fulfillment of
The Requirements for the Degree of
DOCTOR OF PHILOSOPHY

Department: Chemistry
Major: Physical Chemistry

Approved:

Signature was redacted for privacy.

In Charge of Major Work

Signature was redacted for privacy.

For the Major Department

Signature was redacted for privacy.

For the Graduate College

Iowa State University
Ames, Iowa

1975

TABLE OF CONTENTS

LIST OF TABLES

LIST OF FIGURES

I. INTRODUCTION

The transition-metal sulfur systems have been the subject of extensive investigation largely because they exhibit a wide variety of stoichiometries, structures and properties. Jellinek (1) has reviewed the literature through 1968 on the structures and properties of the binary and ternary transition-metal and rare-earth sulfides. The sesquisulfides and higher sulfides are generally semiconductors while the monosulfides and metal-rich sulfides are mostly metallic. The magnetic behavior of the sulfides varies from diamagnetic to Pauli paramagnetic. The rare-earth sulfides and some of the transition-metal sulfides are very stable thermally and have very high melting points. The thermal properties of the rare-earth sulfides have been reviewed by Samsonov (2). This review emphasizes that the physical and thermal properties of these sulfides make them suitable for many high-temperature technological applications. The metallic monosulfides may be used as containers for high temperature heat sources (in nonoxidizing atmospheres) or as electrode materials. The sesquisulfides may find use in semiconductor technology, in conversion of thermal energy to electrical energy or in heterogeneous catalysis.

A knowledge of the vaporization behavior, accurate

vapor pressures and thermodynamic properties of these compounds is required in order to evaluate them for use at high temperatures for extended periods of time. Vaporization studies require a knowledge of both the vapor species and solid phases present at elevated temperatures. Information on the chemical composition as a function of temperature and time is also necessary in order to obtain accurate thermodynamic data.

Because they possess a wide range of structures and properties, the transition-metal sulfides also provide excellent systems for investigating the nature of chemical bonding in nonmolecular solids. Although various bonding models have been proposed by a number of workers including Pauling (3), Rundle (4), Hume-Rothery (5), Brewer (6) and Jellinek (1), they are still incomplete. Vaporization studies of the transition-metal and rare-earth sulfides may provide additional insights into the nature of the bonding in nonmolecular solids. Thermodynamic data for the stabilities of the solid phases can be important in testing the ability of various models to describe the bonding.

Scandium, by virtue of its position in the periodic table, is related to both lanthanum and the lanthanides and also titanium and other members of the first transition-metal series. Therefore, the compounds which it forms,

especially those with nonmetals including sulfur, are in certain aspects similar to both the corresponding rare-earth compounds and also other transition-metal compounds. Lanthanum and some of the elements of lanthanide series have the electronic configuration $(Xe)4f^{q}5d^{1}6s^{2}$ which, except for the f electrons, is analogous to the $(Ar)3d^{1}4s^{2}$ electronic configuration of scandium. In compounds of the lanthanide elements the 4f electrons are localized about the metal, therefore, the bonding and electrical properties of these compounds are determined mainly by the s and d valence electrons of the metal (along with the valence electrons of the nonmetal) and thus are similar to those of the corresponding scandium compounds. The metals of the first transition series have an increasing number of 3d electrons with increasing atomic number. The structure and properties of the compounds of these elements will strongly depend on the concentration and configuration of the d electrons.

The purpose of this study of the scandium-sulfur system was to obtain information on the stoichiometry, structure, vaporization behavior and thermodynamic properties of the solid phases at high temperatures. Comparisons of thermodynamic data for the stability of scandium sulfides with those for rare-earth and first transition-

metal series sulfides were found to yield information relating to electronic or other effects. The thermodynamic results will be compared with predictions based on various bonding models in order to test the appropriateness of the models.

II. PREVIOUS WORK

A. Phase Study of the Scandium-Sulfur System

The phase Sc_2S_3 was first prepared by Klemm, Meisel and von Vogel (7) in 1930 by the reaction of H_2S with $ScCl_3$ at an elevated temperature. They were unable to determine the crystal structure by X-ray powder diffraction. Men'kov et al. (8) prepared Sc_2S_3 in 1961 and using powder data erroneously concluded that the compound had the tetragonal β-In_2S_3 structure. In 1958 Hahn (9, pp. 263-283) stated, with reference to a private communication from Klemm, that Sc_2S_3 crystallizes in a defect NaCl-type structure with random voids in the metal sublattice and that ScS crystallizes in the NaCl structure. Hahn postulated that a range of homogeneity exists between them.

In 1964 Dismukes and White (10) determined the crystal structure of Sc_2S_3 using single crystal data and also reported the existence of the phases ScS and $Sc_{1.37}S_2$. They prepared pure Sc_2S_3 by passing H_2S through finely divided Sc_2O_3 in a graphite crucible for 2-3 hours at 1550°C or higher. They also prepared stoichiometric crystals of the sesquisulfide by transport with I_2 in a quartz ampoule from a hot zone of about 1150°C to a cold zone of 950°C. The transported Sc_2S_3 crystals were yellow to transmitted light. The crystal structure of Sc_2S_3 is closely related to that of

NaCl with a unit cell 12 times as large due to a complex ordering of the positions at which one-third of the cations are missing. The orthorhombic unit cell parameters are $a \tilde{=} 2a_o$, $b \tilde{=} \sqrt{2}\, a_o$, and $c \tilde{=} 3\sqrt{2}\, a_o$, where the NaCl-type cell parameter $a_o = 5.21$ Å. Dismukes and White (10) prepared the phase $Sc_{1.37}S_2$, a black powder, by heating a pressed pellet of Sc_2S_3 powder at less than 10^{-3} mm pressure at 1650°C for 2 hours in a carbon crucible. The X-ray powder pattern of $Sc_{1.37}S_2$ was indexed on the basis of a rhombohedral unit cell with $a = 6.331$ Å and $\alpha = 34.57°$. Intensities calculated on the basis of one cation site filled and the other with 0.37 occupancy gave good agreement with the observed intensities. The structure of $Sc_{1.37}S_2$ is a partially disordered cation-deficient NaCl structure. Dismukes and White (10) postulated that it could exist continuously over the range to ScS by filling the vacant sites. Dismukes and White (10) prepared scandium monosulfide by reacting a 0.25 g piece of scandium metal with a stoichiometric amount of sulfur contained in an alumina boat in an evacuated quartz tube at 1150°C for 70 hr. The gold-colored product had the NaCl-type structure with $a_o = 5.19$ Å.

Dismukes and White (10) also measured some electrical properties of ScS and $Sc_{1.37}S_2$. They obtained a value of the resistivity of ScS of less than 10^{-3} ohm cm and a

thermoelectric power of 0.5 μV/deg at 300 K. They found a metallic-type temperature dependence of the resistivity and thermoelectric power for $Sc_{1.37}S_2$ and, with an estimated charge carrier mobility at 300 K of $\mu = 14\ cm^2V^{-1}sec^{-1}$, postulated that conduction is by electrons in a 3d band. Optical absorption measurements by Dismukes (11) gave a direct band gap for Sc_2S_3 of 2.78 eV and Hall measurements established that Sc_2S_3 was an n-type semiconductor. Lashkarev et al. (12) measured the resistivity of Sc_2S_3 and obtained the value of 10^{10} ohm-cm at 300 K. They obtained a higher value for the energy band gap of Sc_2S_3 (3.6 eV) based on their electrical resistance data. Table 2.1 lists some of the properties and also structural data for the three known scandium-sulfur phases.

B. Characterization of Vaporization of Scandium Sulfides

According to Dismukes and White (10), scandium sesquisulfide melts at 1775 ± 25°C. They reported that Sc_2S_3 loses sulfur when heated in a vacuum above 1100°C. The existence of any congruently vaporizing composition in the scandium-sulfur system has not been reported.

The dissociation energy of ScS(g) was reported in 1967 by Coppens, Smoes and Drowart (CSD) (13) and more recently by Steiger and Cater (SC) (14), both employing mass

Table 2.1. Structure and properties of phases in the scandium-sulfur system

Phase	$\frac{Sc}{S}$	Crystal System and Space Group	Unit Cell Dimensions (Å)	Cal. Density (Measured Density) (g/cm^3)	Resistivity[a] (ohm-cm)	Thermo-electric power ($\mu V/deg$)	References
Sc_2S_3	.667	orthorhomic F_{ddd}	a = 10.42 b = 7.37 c = 22.10	2.917 (2.897)	10^{10}		10, 11, 12
$Sc_{1.37}S_2$	.685	trigonal $R\bar{3}m$	a = 6.331 $\alpha = 33.57^{\circ}$	2.95	0.3×10^{-3}	10	10
ScS	1.0	cubic Fm3m	a = 5.19	3.66 (3.59)	$< 10^{-3}$	0.5	10

[a]Value of resistivity at 300°C.

spectrometric isomolecular exchange reactions. The results of the former study (CSD) were based on the standard dissociation energies of GeS and SiS, 130.9 ± 0.6 and 148.6 ± 1.5 kcal/mole respectively, and yield a value for D_0° (ScS) of 113.4 ± 2.5 kcal/mole. The results of the latter study (SC) were based on the values D_0° (US) = 124.0 ± 2.3 kcal/mole, D_0° (YS) = 125.4 ± 2.5 kcal/mole and D_0° (YO) = 170.0 ± 3 kcal/mole, yielding values for the dissociation energy at 0 K for ScS of 111.6 ± 3.8 and 113.8 ± 3.9 kcal/mole by second and third law treatments respectively. Electron spin resonance and optical spectra of ScS(g) obtained by McIntyre et al. (15) using matrix isolation gave a vibrational frequency of 554 cm^{-1} and an electronic ground state of $^2\Sigma^+$ for the scandium sulfide molecule.

III. EXPERIMENTAL

A. Sample Preparation

The scandium sulfides investigated in this research were prepared from 99.999% pure crystalline sulfur obtained from the American Smelting and Mining Company and scandium metal obtained from the Ames Laboratory. The scandium had been purified by sublimation and the purity obtained was 99.9 wt % including both metallic and nonmetallic impurities. The chemical analysis of the bulk scandium is shown in Table 3.1.

The general method of preparation of transition metal sulfides described by Conard (16) and Smeggil (17) in which metal filings are reacted with sulfur was not used for scandium sulfide, since it has been shown by Spedding and Beaudry (18) that scandium in a finely divided state is a powerful "getter" for nonmetallic elements, especially oxygen, nitrogen and hydrogen. Analysis of scandium filings prepared in an argon filled glove box showed an oxygen impurity of 1.2 at %. In the preparation of scandium sulfides described below, special care was taken to minimize oxygen contamination.

The bulk scandium was machined on a lathe in a helium filled glove box by Paul Palmer. The turnings produced were generally 2-8 mm long and about .1 mm thick and were

Table 3.1. Chemical analysis of scandium metal (AL Code No. Sc-12572) by spark source mass spectrometer

Element	Atomic ppm	Element	Atomic ppm	Element	Atomic ppm
Li	<.01	Cu	9	Sb	<.08
Be	--	Zn	<.1	Te	<.1
B	.02	Ga	--	I	<.06
Na	40	Ge	<.2	Cs	<.04
Mg	<.4	As	<.04	Ba	<.08
Al	1	Se	<.5	Hf	< 1
Si	.3	Br	--	Ta	100
P	<.1	Rb	<.1	W	.3
S	< 3	Sr	<.6	Re	< 1
Cl	1	Zr	<.6	Os	< 1
K	.2	Nb	--	Ir	<.6
Ca	.03	Mo	< 2	Pt	<.6
Ti	<.2	Ru	< 10	Au	<.1
V	<.1	Rh	--	Hg	<.2
Cr	2	Pd	<.4	Tl	<.1
Mn	.1	Ag	.07	Pb	.3
Ge	--	Cd	<.2	Bi	<.08
Co	.1	In	<.08	Th	<.2
Ni	10	Sn	.2	U	<.2

Table 3.1 (Continued)

Element	Atomic ppm	Element	Atomic ppm	Element	Atomic ppm
		Rare Earth Impurities			
Y	4	Sm	.3	Ho	6
Lu	4.9	Eu	<.2	Er	1.2
Ce	2.2	Gd	2.4	Tm	<.2
Pr	.6	Tb	.5	Yb	.5
Nd	.5	Dy	1.1	Lu	41
		Other Impurities			
O[a]	343	N[a]	10	H[a]	76
C[b]	176	F[c]	185	Fe[c]	29[c]

[a]Vacuum fusion results.
[b]Combustion analysis.
[c]Atomic absorption spectroscopy.

kept under a helium atmosphere until reaction with sulfur in the following preparations.

(1) ScS_{1+x} , $x \simeq .5$

Two samples with an initial composition of S/Sc = 1.5 were prepared by the reaction of scandium turnings with sulfur in a quartz tube 20 mm in diameter and five inches

long. The quartz tube was previously outgassed at 1000°C for 3 hours and then transferred to a nitrogen atmosphere glove box where the reactants were introduced. The reaction tube was then transferred to a vacuum line, evacuated to approximately 10^{-5} torr and sealed. The tube was placed in a resistance furnace at 300°C and the temperature of the furnace was gradually raised to 900°C in about 5 days. After about 4 days at this temperature, most of the sulfur had reacted and the tube was removed from the furnace and broken open, taking care to prevent contamination of the sample by quartz fragments. Samples prepared in this manner were generally grey in color with small areas of blue, red and gold and were very brittle on the outside. Unreacted scandium metal could be observed when the sample was crushed.

(2) ScS_x , $x \simeq 1.0$

Four samples were prepared with initial composition, S/Sc, between 0.95 and 1.05. The preparation was similar to that described previously for ScS_{1+x}. The ScS_x samples were heated at 900°C for 5 days after which all of the sulfur had reacted and the product was uniformly grey in color. Unreacted scandium metal was also present in these samples.

(3) Sc_xS , $1 < x < 4$

Scandium sulfide samples with initial compositions, Sc/S of 1.5, 2, 2.5, 3 and 4 were prepared using the same procedure described above for the ScS_{1+x} and ScS_x preparations. The sulfur reacted completely with the scandium turning after about 5 days at 900°C. Varying amounts of unreacted scandium were present depending on the stoichiometry.

All of the scandium sulfide samples prepared in quartz tubes resulted in nonhomogeneous samples. These samples were subsequently annealed at high temperature in order to obtain homogeneous materials. A radio-frequency induction heating unit and a high vacuum system was used in this work and will be described later.

B. Phase Analysis

1. X-ray analysis

X-ray analysis of the scandium sulfide samples was principally performed using the Debye-Scherrer powder technique. Samples were ground and loaded into a 0.2 mm diameter capillary and aligned in a Norelco Debye-Scherrer powder camera having a diameter of 114.6 mm. The radiation used was nickel filtered CuKα. A Siemens film measuring device was used to measure the linear diffraction length

of the reflections, which were recorded to .005 mm. Front reflections ($\lambda = 1.54178$ Å) were used to identify phases and back reflections ($CuK\alpha_1 = 1.54051$ Å) were used to determine lattice parameters. The powder patterns were indexed by comparison of observed $\sin^2\theta$ values and relative intensities with those calculated from a computer program by Yvon et al. (19) using atomic scattering factors of Hanson et al. (20) and atom positions reported by Dismukes and White (10). Lattice parameters were obtained from sin θ values by a least squares treatment.

Single crystals of some of the scandium sulfide samples were obtained by vaporization and annealing procedures. A Weissenberg camera was used to investigate the X-ray diffraction of the crystals. The single crystal technique was used to determine if the vacancies in the lattice positions were ordered. Such vacancies would give rise to superstructure reflections. The intensity of these reflections is generally rather low and single crystal diffraction may be necessary to observe them.

2. Combustion analysis

The composition of the scandium-sulfide samples could be determined by heating the sample in air to produce Sc_2O_3. Between 45 and 70 mg of sample were heated in a platinum crucible using Meeker burner at about 800-900°C

until the product reached a constant weight, generally within about 2 days. X-ray powder diffraction of the residue showed that it was only Sc_2O_3 with possibly a trace of platinum. This method is thus considered to be satisfactory for obtaining accurate compositions of scandium sulfides. The only disadvantage of the method is the relatively large amount of sample required for the analysis.

3. Electron microprobe analysis

Electron microprobe analysis of the scandium sulfide samples was performed by Francis Laabs of the Ames Laboratory, Spectrochemical Services Group I. The samples were mounted in a copper and epoxy disk and polished with diamond paste by Harlan Baker. The intensities of the characteristic X-rays of scandium and sulfur emitted upon excitation from the well-defined electron beam were measured. Since the electron microprobe monitors intensities from a sample volume of the order of cubic microns, six to ten independent intensity observations were made at different beam positions in order to obtain representative analysis of the samples. The composition of the samples was determined by comparison of the X-ray intensities with those from a sample with composition determined by combustion analysis. The X-ray intensity analysis was performed

using the computer program MAGIC IV (21).

C. Characterization of the Vaporization Behavior of Scandium Sulfides

A major problem of high temperature vaporization studies is to find a container material that will not interact with the sample at the temperatures of the investigation. A tungsten crucible was chosen for this study for the following reasons: (a) Published data on binary systems of scandium-tungsten and sulfur-tungsten as reported by Shunk (22) and Elliott (23) respectively show that there are no stable intermediate phases in the scandium-tungsten system and the solubility of scandium in tungsten at 1625°C is probably less than one ppm. There are two phases, WS_2 and WS_3, in the latter system, and neither of which are stable at high temperatures. (b) Measurement of the weight of the tungsten crucible before and after scandium sulfide vaporizations showed no weight change. (c) The tungsten surface which had been in contact with the sample at temperatures where the sample was nearly molten was visibly unchanged. (d) Results of a spark source mass spectrometric analysis of one of the scandium sulfide samples annealed in the tungsten crucible indicated that only about 3 ppm of tungsten were present in the sample. The complete results of this analysis are given in Table 3.2.

Table 3.2. Spark source mass spectrometric analysis of scandium sulfide sample ScS-2-26

Element	Atomic ppm	Element	Atomic ppm	Element	Atomic ppm
Li	--	Ga	--	Nd	< 2
Be	--	Ge	--	Sm	< 1
B	--	As	<.2	Eu	<.2
C	--	Se	--	Ge	≤ 10
N	2	Br	--	Tb	1
O	--	Rb	--	Dy	300
F	2	Sr	.1	Ho	4
Na	1	Y	8	Er	≤ 1
Mg	--	Zr	--	Tm	.3
Al	--	Nb	--	Yb	<.6
Si	10	Mo	< 2	Lu	20
P	2	Ru	--	Hf	--
S	~ 10^6	Rh	--	Ta	150
Cl	5	Pd	--	W	3
K	2	Ag	<.6	Re	< 1
Ca	3	Cd	<.1	Os	< 1
Sc	10^6	In	--	Ir	<.8
Ti	5	Sn	< 8	Pt	<.6
V	<.4	Sb	<.4	Au	.2
Cr	1	Te	--	Hg	.2
Mn	.2	I	.1	Tl	<.1
Fe	30	Cs	.02	Pb	<.5
Co	.8	Ba	1	Bi	<.1
Ni	6	La	7	Th	3
Cu	4	Ce	4	U	<.3
Zn	< 4	Pr	1		

The vacuum line used to determine the vaporization behavior of the scandium sulfides is shown in Figure 3.1. A residual pressure of 10^{-6} to 10^{-7} torr was maintained with the use of a silicone-oil diffusion pump connected to a mechanical forepump. The crucible was heated by induction using a Lepel 20 kw, 200-480 kc generator to power a 3.5 in. diameter, 11 turn, water cooled work coil, constructed from .25 in. copper tubing. The temperature was measured by a Leeds and Northrop single adjustment vanishing filament optical pyrometer by sighting through a prism and pyrex window onto a black-body hole in the center of the bottom of the crucible. This pyrometer was calibrated by Bruce Conard at Argonne National Laboratory using the technique of sectored disks described by Thorn and Winslow (24) and Conard (16). The corrections between the true temperatures calculated via Wien's radiation equation and the pyrometer temperature scale for the three optical pyrometer scales are plotted in Figure 3.2. A temperature correction for the absorbance of the prism and pyrex window was made using the relation

$$\frac{1}{T_w} - \frac{1}{T_c} = C \quad , \tag{3.1}$$

where T_c is the true temperature of the black-body hole and T_w is the observed temperature with the window and

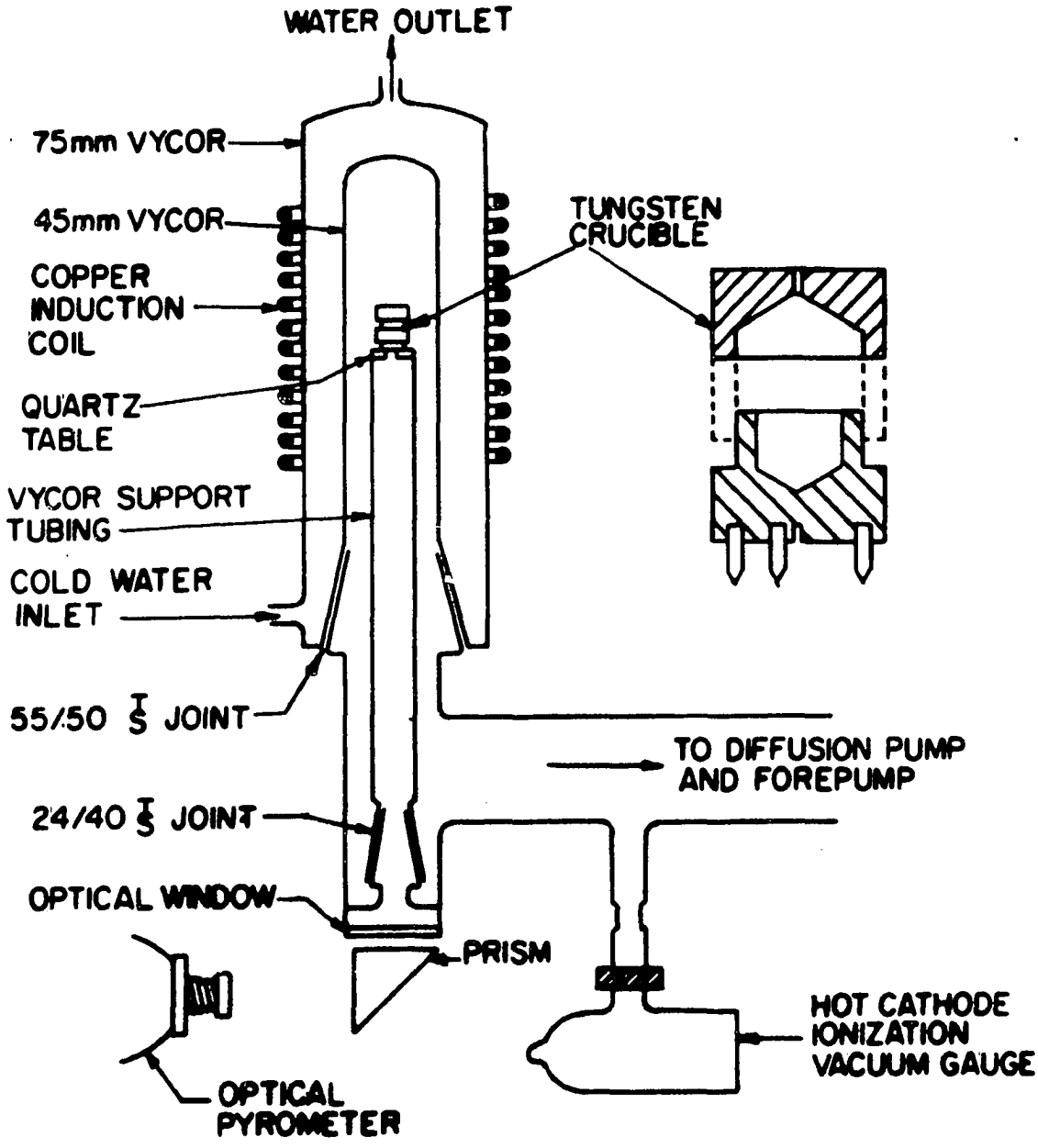

Figure 3.1. Schematic diagram of vacuum line used for high temperature annealing and vaporization of scandium sulfides

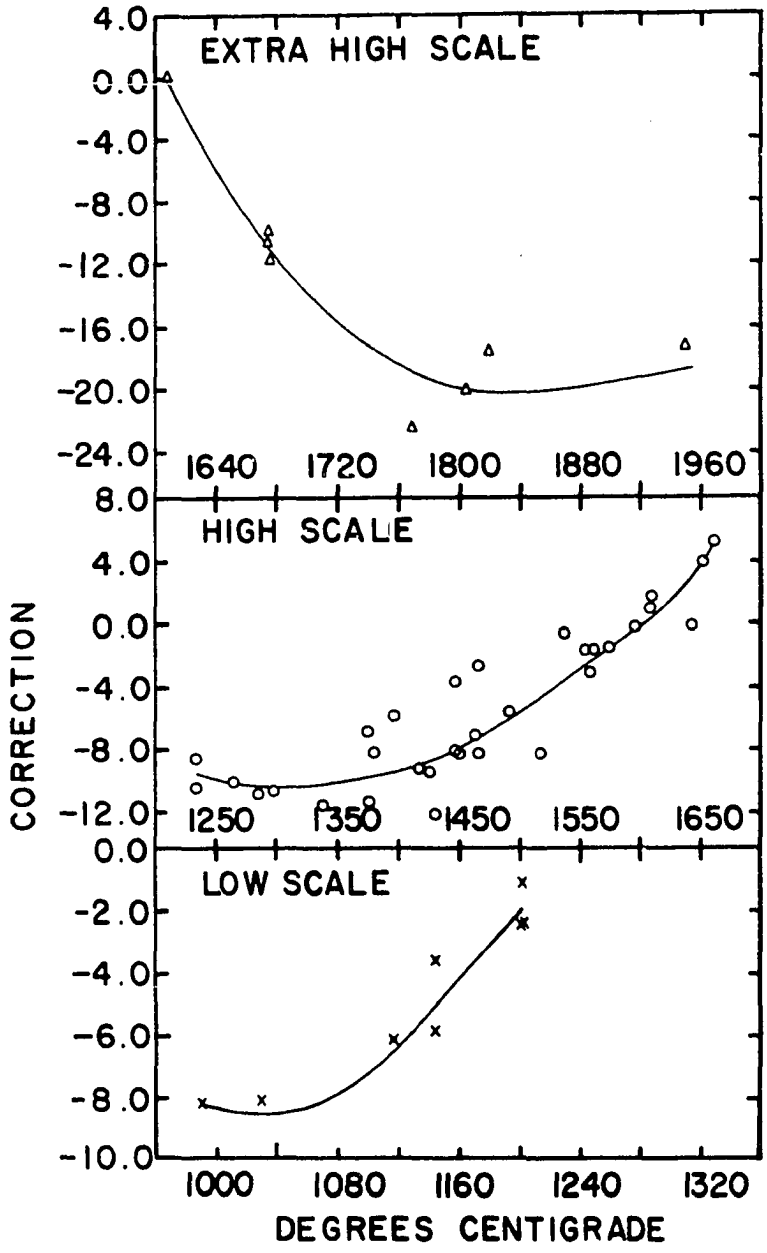

Figure 3.2. Plots of temperature correction vs. observed temperature for LOW, HIGH, and XHIGH scales of manual optical pyrometer (AEC 9415). Calibration by Conard (16) using sectored wedge technique

prism in the path. The values of C at various temperatures were obtained by comparing the measured temperatures of a tungsten strip lamp with and without the window and prism. The results are listed in Table 3.3.

The experimental procedure used to determine the mode of vaporization of scandium sulfides was as follows: A known amount of sulfide was placed in a previously outgassed tungsten crucible. After the system had been evacuated to a residual pressure of about 10^{-6} torr, the crucible and sample were heated for several hours at a temperature at which the vapor pressure was high enough to produce a darkening of the vacuum cap as the result of condensation from the vapor phase. The residue left in the crucible was analyzed for phases present and composition by X-ray and chemical analysis previously described. The mass loss by vaporization of the samples was also determined by weighing the crucible and sample before and after the vaporizations. This procedure was repeated a number of times for each of the initial scandium sulfide compositions. The results are given in Chapter V.

D. Knudsen Effusion Vapor Pressure Measurement

The vapor pressure of scandium sulfide was measured as a function of temperature with all other conditions invariant including the composition of the solid. The target

Table 3.3. Temperature correction constant for window and prism for induction heating vacuum line

Temperature w/o window & prism			Temperature with window & prism			Constant
Mean ^{o}C	Pyrometer corr(^{o}C)	T_c(K)	Mean(^{o}C)	Pyrometer corr(^{o}C)	T_w(K)	($x10^{-5}K^{-1}$)
1034	-9	1298	1014	-8	1279	1.20
1076	-8	1341	1053	-8	1318	1.30
1104	-7	1370	1078	-8	1343	1.47
1151	-5	1419	1124	-6	1391	1.44
1190	-3	1460	1162	-4	1431	1.41
1251	-10	1514	1224	-9	1488	1.28
1293	-10	1556	1263	-10	1526	1.25
1335	-10	1598	1300	-10	1563	1.42
1366	-10	1629	1331	-10	1594	1.36
1406	-9	1670	1366	-10	1629	1.49
1448	-8	1713	1406	-9	1670	1.51
1463	-7	1729	1420	-9	1684	1.53
						ave. = 1.43 ± .1

collection technique was used for this experiment. This technique has been recently described by Cater (25). The scandium sulfide sample (ScS-2-91) used for this vapor pressure measurement had been previously characterized as congruently vaporizing. The scandium content of the effusate collected on the targets was analyzed by the electron microprobe technique. The electron microprobe was calibrated for microgram quantities of scandium by measuring the intensity of the characteristic X-ray radiation emitted from known quantities of scandium deposited from the vapor of pure scandium metal.

1. Apparatus

The target collection apparatus constructed and used in this study is shown in Figure 3.3. The target magazine was made from a 8.89 cm long copper tube, 3.18 cm outer and 2.79 inner diameter. The magazine holds as many as 19 targets. The targets were held in position by a stainless steel target support brazed to the copper tube. The stainless steel support had a knife-edged opening 1.49 cm in diameter that defined the area of deposit on the targets. The target magazine was cooled by liquid nitrogen in the dewar connected to the top of the magazine. The targets used were aluminum discs 2.22 cm diameter, 4.3 mm thick. One surface of the targets was made flat and smooth by

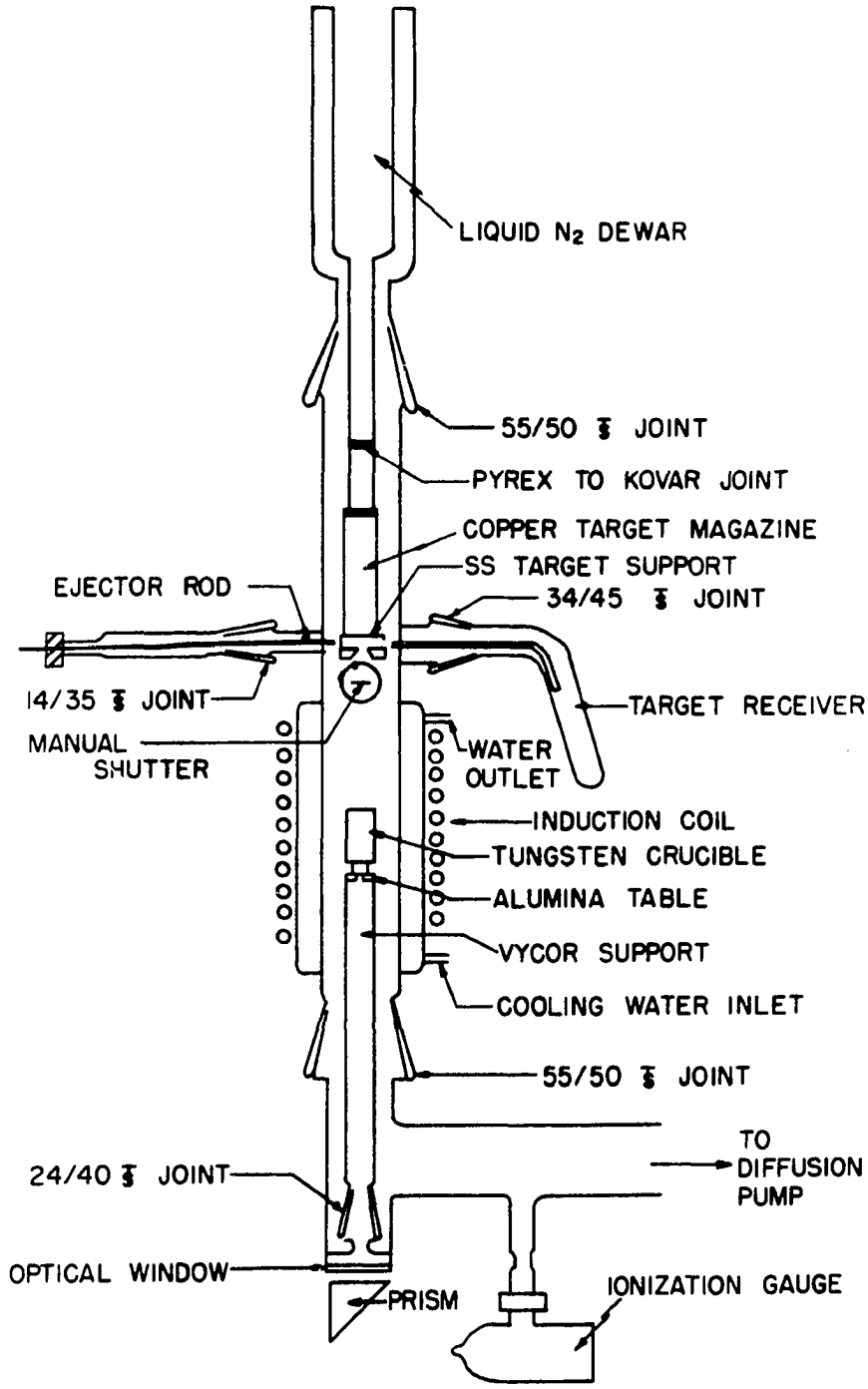

Figure 3.3. Schematic diagram of vacuum line apparatus used for target collection experiments on scandium sulfides

Harlan Baker using a mechanical polishing technique in which the surface was first ground with 600 grit diamond powder followed by stepwise polishing with 2 micron and .5 micron particle diamond paste. Each target was then press-fit into an aluminum ring 2.22 cm i.d. and 2.54 o.d. that was 4.6 mm thick to prevent the deposits from being scratched when the targets were ejected from the magazine.

The tungsten crucible designated RTT-2-172 used for the target collection experiments is shown in Figure 3.4. The crucible was made nearly symmetric with respect to a horizontal plane through the center in order to obtain a more nearly uniform temperature throughout the cell. The sample was placed in the top compartment and the temperature was measured by sighting the pyrometer into the bottom compartment of the cell. The area of the top orifice was determined by measuring the distance on a 75 x micrograph of the orifice. The outside diameter was .90 $\pm$ .01 mm and the inside diameter was .88 $\pm$ .01 mm. Thus, the area of the orifice was taken to be 6.22 $\pm$ .1 x 10^{-3} cm^2. The length of the orifice was determined using a small steel ball as shown in Figure 3.5, measuring the appropriate distance with a micrometer. The length of the orifice was determined to be .411 $\pm$ .01 mm.

The target collection apparatus was set up in the vacuum line used for vaporization experiments by replacing

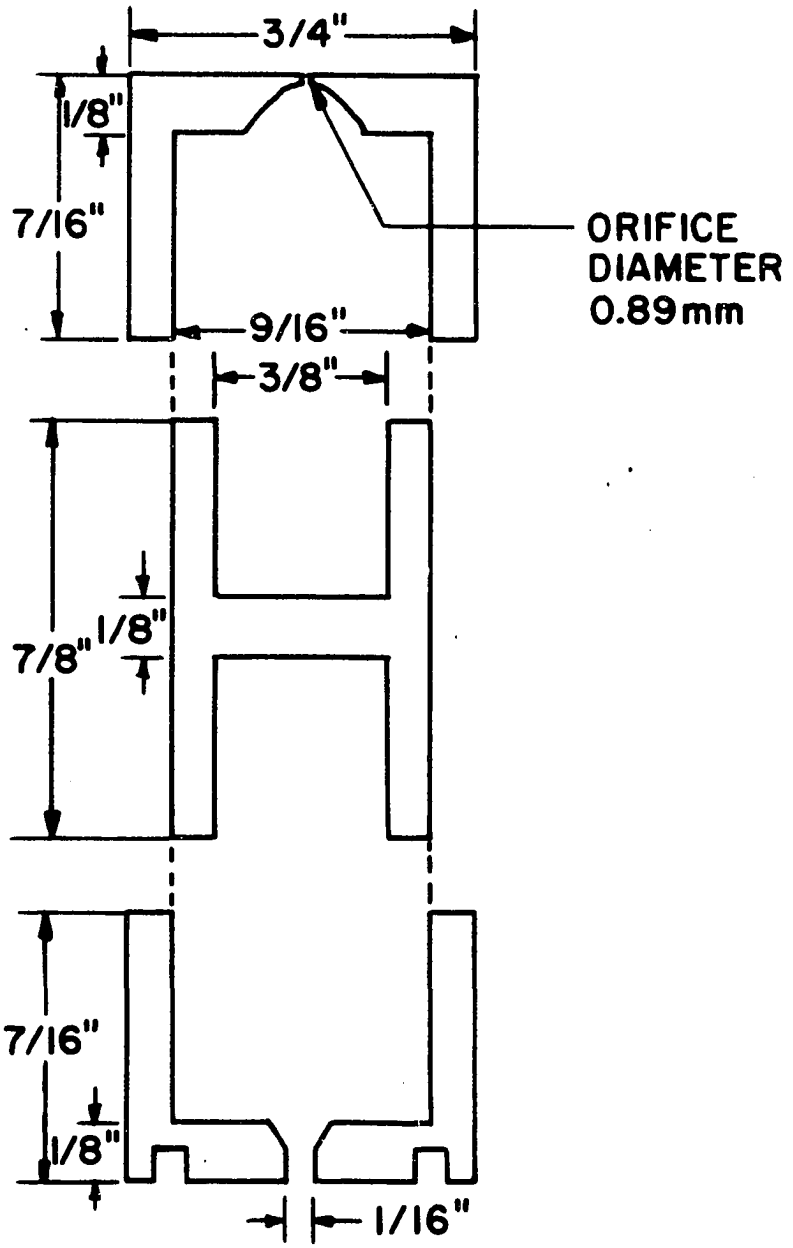

Figure 3.4. Cross section of the cylindrical tungsten crucible used for scandium sulfide target collection experiments

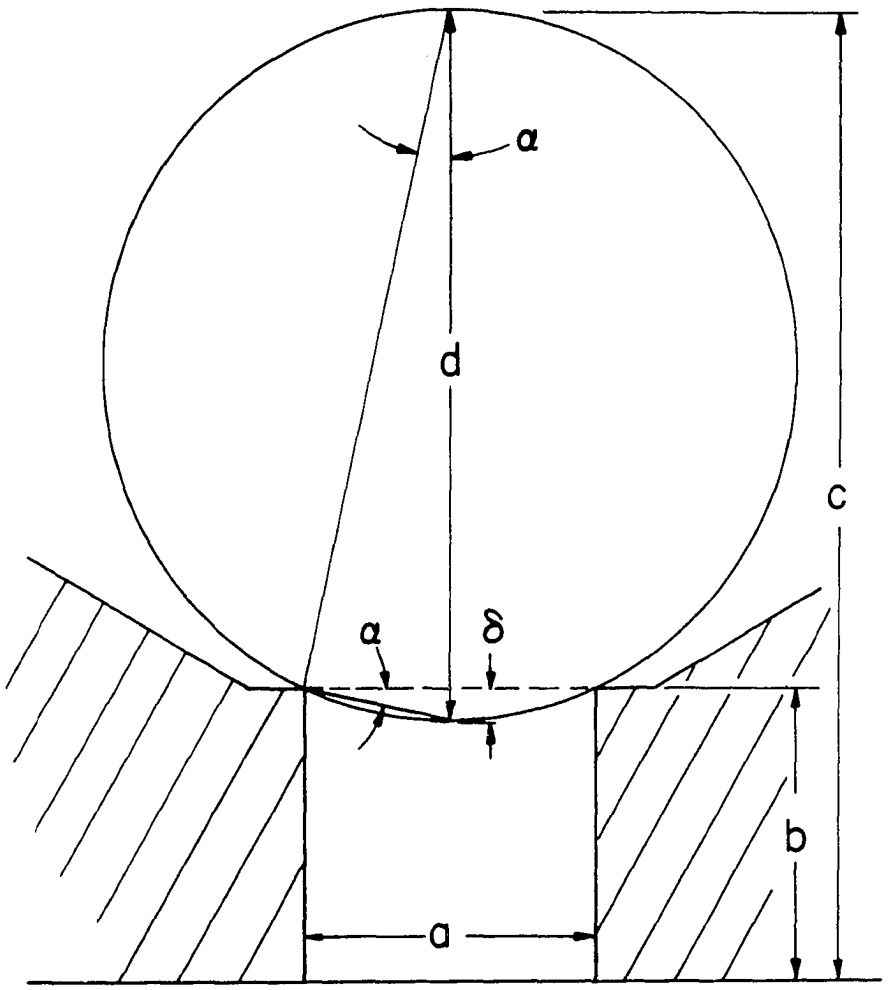

$$c = b + d - \delta$$

$$\delta = \frac{d - \sqrt{(d+a)(d-a)}}{2}$$

STEEL BALL 3/32 DIAMETER

Figure 3.5. Determination of the length (b) of the orifice by the small ball method

the vycor water jacket shown in Figure 3.1. The crucible was heated by radio frequency induction using a ten-turn copper load coil. Figure 3.6 shows a schematic of the temperature regulating and measuring system used. A Leeds and Northrup Mark I automatic optical pyrometer was used to measure the temperature by sighting through a prism and a pyrex window into the bottom compartment of the crucible. The millivolt signal from the pyrometer was compared with the setpoint voltage of a Leeds and Northrup Electromax IV current-adjusting type controller. The output of the controller was used to drive the Lepel T-660 thyratron regulator which closed the loop to give a feedback system for regulating the temperature of the crucible. In order to reduce the effect of the rf field of the induction coil on the operation of the automatic pyrometer, a shielding enclosure consisting of one layer each of sheet metal, copper and μ-metal was constructed for the pyrometer. In order to calibrate the automatic pyrometer, the section of the apparatus containing the copper magazine and liquid nitrogen dewar was replaced with a cap topped by a flat pyrex plate. The disappearing filament pyrometer previously described was sighted into the orifice in the top of the crucible using a mirror and pyrex plate optics. Thus, the automatic pyrometer was calibrated in situ against the manual pyrometer. By sighting the disappearing filament pyrometer

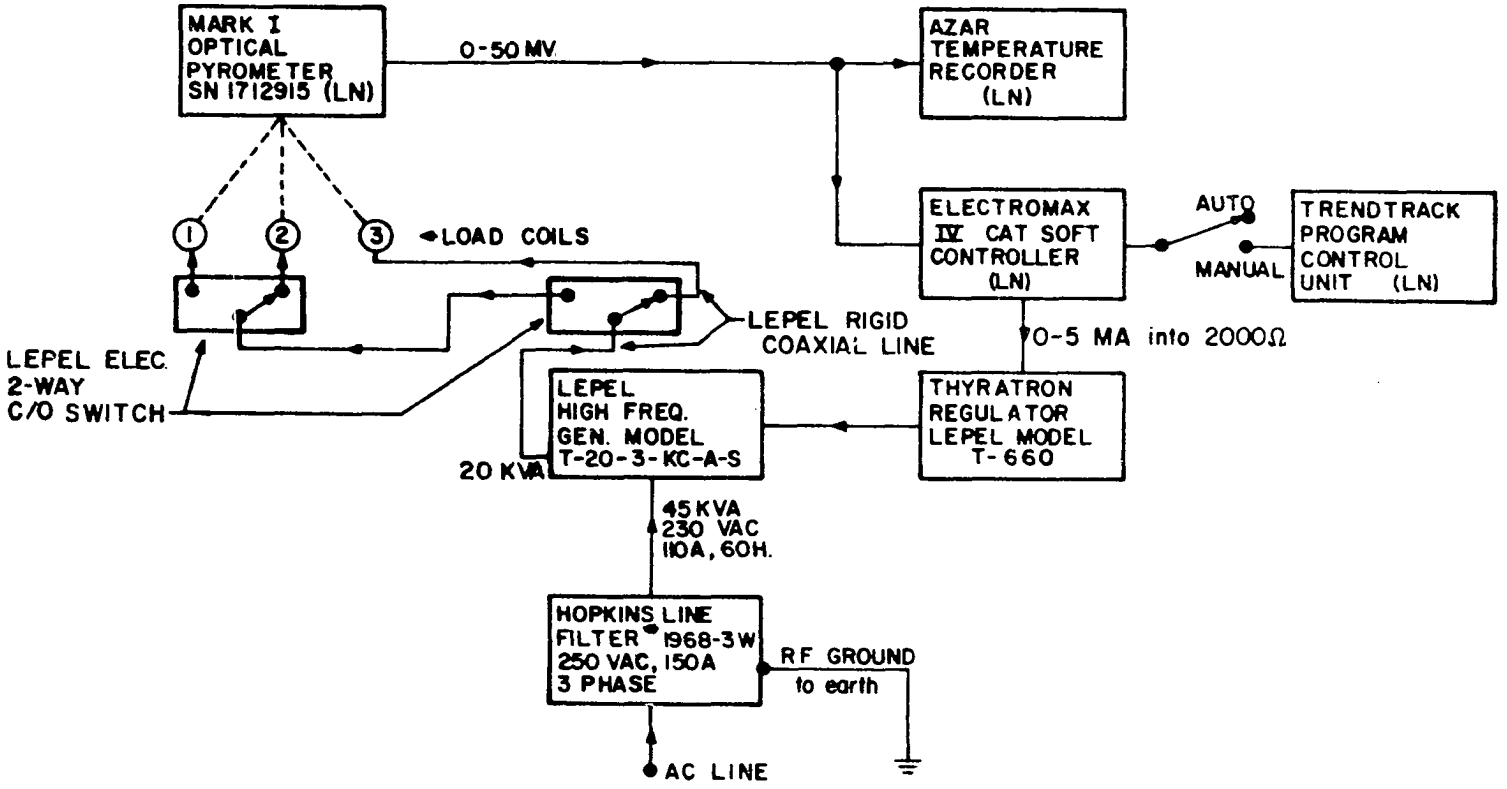

Figure 3.6. Schematic of temperature regulating and shielding system for Lepel rf heating system

successively into the top and bottom orifices, the temperature of the two compartments was determined to be the same within the precision of the instrument. A calibration curve was obtained between the millivolt output of the automatic pyrometer, sighted into the bottom orifice through a window and prism having a combined correction constant of $1.43 \times 10^{-5}\ K^{-1}$, and the corrected temperature measured by the disappearing filament pyrometer previously calibrated, sighted into the top orifice through a window and mirror having a combined correction constant of $1.53 \times 10^{-5}\ K^{-1}$. Appendix A tabulates the results for the in situ calibration of the automatic pyrometer.

The stability of the automatic pyrometer and temperature regulating system was checked by recording the output of the automatic pyrometer as a function of time with the set point of the controller on some selected value. The drift in temperature with time was $\pm\ 2^{\circ}C$ or less over periods up to 5 hours.

2. Procedure

About 150 mg of the congruently vaporizing scandium sulfide (ScS-2-91) was loaded into crucible RTT-2-172, which had been previously outgassed, and the target collection apparatus was assembled according to Figure 3.3. After evacuating the system, the distance between the

crucible orifice and aluminum target was measured by a cathetometer. The radio-frequency generator was turned on when the residual pressure was about 10^{-6} torr and the temperature was slowly increased (manual control on rf generator) until the temperature was about 100° below the lower limit of the temperature range used for data collection. The set point of the Electromax controller was set to the millivoltage value corresponding to the output of the automatic pyrometer at that temperature and the rf generator control was switched to automatic. Adjustment of the proportional band control of the Electromax was necessary to obtain a good control of the temperature as measured by the output of the automatic optical on a digital voltmeter, and also on a Leeds and Northrup AZAR recorder. The temperature was then varied over the interval 1960-2220 K by changing the set point of the controller. When a particular constant temperature was obtained the manually operated beam shutter was opened and at the same time a precision timer was turned on. The molecular beam effusing from the orifice could then condense on the aluminum target which was coaxial with the incident beam. After a certain exposure time at a given temperature, the beam shutter was closed and the timer was turned off. A manually operated rod was used to eject the exposed target from the magazine into a glass target

receiver.

The temperature of the crucible was then varied until another constant temperature was obtained. The above procedure was repeated and another fresh aluminum target was exposed. When the experiment was completed the crucible was allowed to cool for eight to ten hours before the apparatus was opened to atmosphere. The targets were then removed from the receiver and stored in a vacuum desiccator until they could be analyzed by the electron microprobe technique.

The electron microprobe analysis of the deposits on the aluminum targets was again performed by Fran Laabs. Both scandium and sulfur analyses were attempted but only the scandium gave quantitative results with the electron microprobe. Since the scandium sulfide deposits were thin films about 70-700 Å thick, a good measurement of the background was necessary to accurately determine the amount of scandium present. Thus, both scandium and aluminum characteristic X-ray intensities were measured. A rastered electron beam was used and the accelerating potential was 6 kV. The samples were moved at 96 microns per minute to minimize the destruction of the sample by the electron beam. To allow for inhomogeneity of the effusate on the discs and to obtain a more accurate counting rate, each disc was exposed to the primary electron beam at four

different positions. Each exposure was made for 100 seconds and the resulting number of counts was registered simultaneously on the spectrometers detecting the scandium and aluminum characteristic radiation. The average value of the counts from the four exposures was used for the analysis of the quantity of scandium deposited on the disc.

A calibration curve relating the number of counts of scandium and the amount of scandium present on the target was obtained by collecting data from a series of targets with deposits from the vapor of pure scandium metal. Known quantities of scandium deposited on the targets were calculated from the Knudsen effusion equation using values for the vapor pressure of scandium metal at each temperature obtained from the JANAF Thermochemical Tables (26).

3. Specific experiments

The first experiment performed with the target collection apparatus was the vaporization of scandium metal to obtain known amounts of scandium deposits in order to calibrate the electron microprobe. About 0.5 gram of scandium metal, obtained from Bernard Beaudry of the Ames Laboratory, was loaded into crucible RTT-2-172 and 13 targets were collected with deposits from the vapor over a temperature range of 1574 to 1773 K following the procedure described in the previous section. The targets were

then analyzed by the electron microprobe technique and the scandium calibration curve was determined as described above.

In the second target collection experiment data were collected from five targets with deposits from the vapor of the congruently subliming scandium sulfide. In this experiment the temperature of the crucible was held at 1799 $\pm$ 1°C and the targets were exposed for various lengths of time from one to five hours. The purpose of this experiment was to determine if the amount of scandium on the target was proportional to time of deposition and to obtain an accurate value for the vapor pressure of the congruently vaporizing scandium sulfide at this temperature.

The third target collection experiment was performed in order to measure the vapor pressure of congruently vaporizing scandium sulfide as a function of temperature over the range 1960 to 2220 K. Eighteen targets were collected following the procedure described in section D2 of this chapter.

E. Mass Spectrometric Investigation of Scandium Sulfides

1. Introduction

In order to obtain thermodynamic properties for vaporization in the scandium sulfide system, the vaporization processes (chemical reactions) must be determined. This requires the identification of all of the vapor species produced. Gilles (27) has discussed various methods of characterization of vaporization processes. At the present time, the high temperature mass spectrometer is the major tool used in these studies. Chupka and Inghram (28) were among the first to use the technique in their determination of the heat of sublimation of graphite and dissociation energies of $C_2(g)$ and $C_3(g)$. Since then many vaporization studies have employed this technique and a number of review articles including those by Inghram and Drowart (29), Grimley (30) and Drowart and Goldfinger (31) have appeared. The main goals of the mass spectrometric investigation of the scandium sulfides were: (1) to identify the gaseous species and determine the vaporization processes for the congruently vaporizing solid scandium sulfide, (2) to determine the partial pressures of the various gaseous species as a function of temperature in order to obtain thermodynamic properties for the congruently vaporizing scandium

sulfide and (3) to determine how the partial pressures of the various gaseous species vary as the composition of the solid scandium sulfide varies over a specified range.

A number of different mass spectrometric runs with various samples was performed to accomplish these purposes.

2. Apparatus

The mass spectrometer used in this study was an Electronics Associates, Inc. (EAI) model 200 quadrupole analyzer. The quadrupole instrument was first developed by Paul and coworkers (32) and since then has been used for a a number of high temperature vaporization studies. The high temperature mass spectrometer consists of four regions; (1) vapor source, (2) ionizer, (3) analyzer and (4) detector.

The function of the vapor source is to provide a representative sample of the solid or liquid in a form of a molecular beam to the ion source. The high temperature Knudsen effusion assembly used is a modification of a design by Rauh et al. (33) and is shown in Figure 3.7. The assembly consisted of the crucible, the supporting frame, the heating filament, and the radiation shields. The crucible used was fabricated from a tungsten rod. The dimensions of the crucible (RTT-2-98) are given in Figure 3.8. The orifice diameter and length were determined by

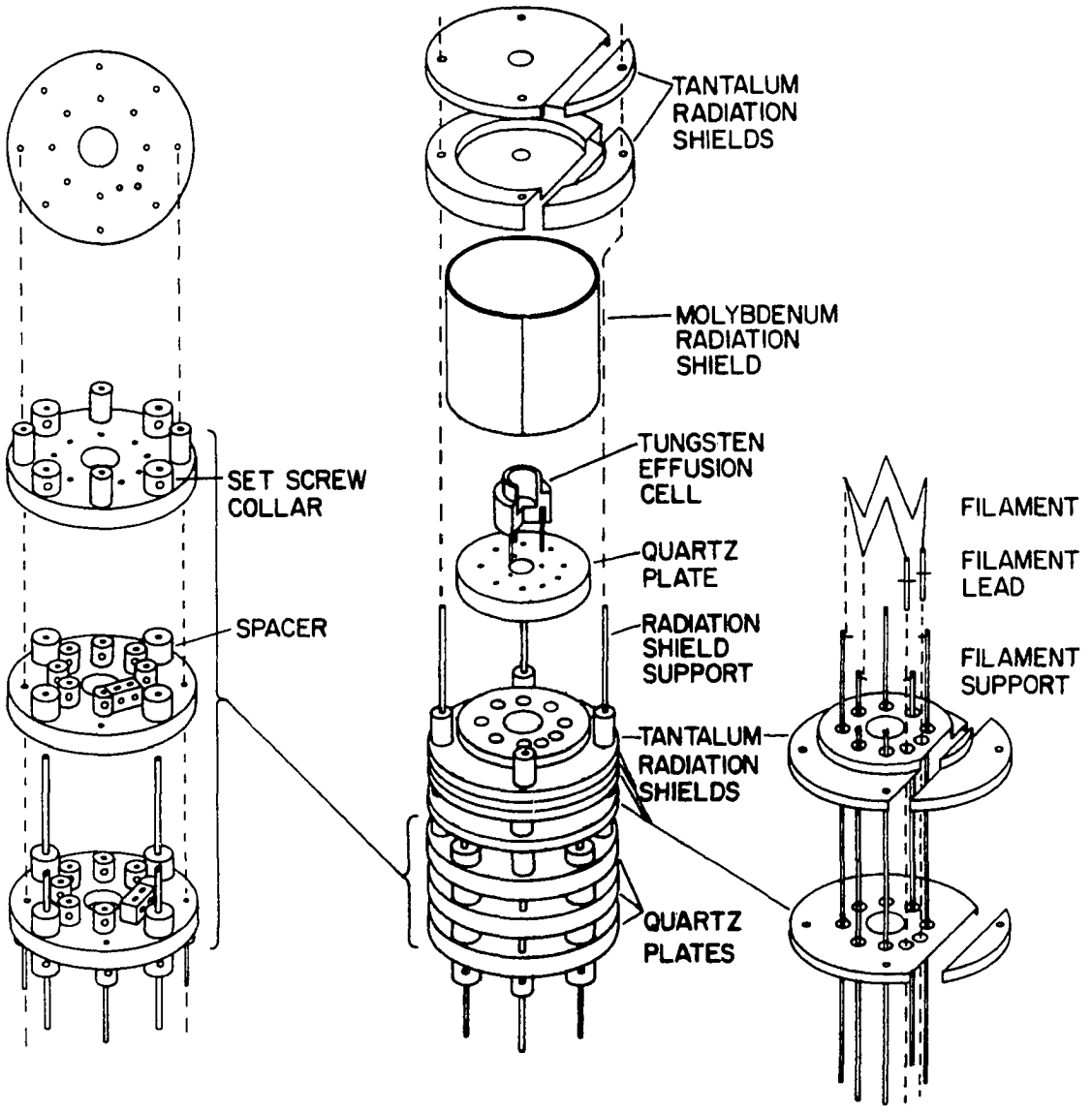

Figure 3.7. High temperature Knudsen effusion cell assembly used for mass spectrometric experiments, modified after Rauh et al. (33)

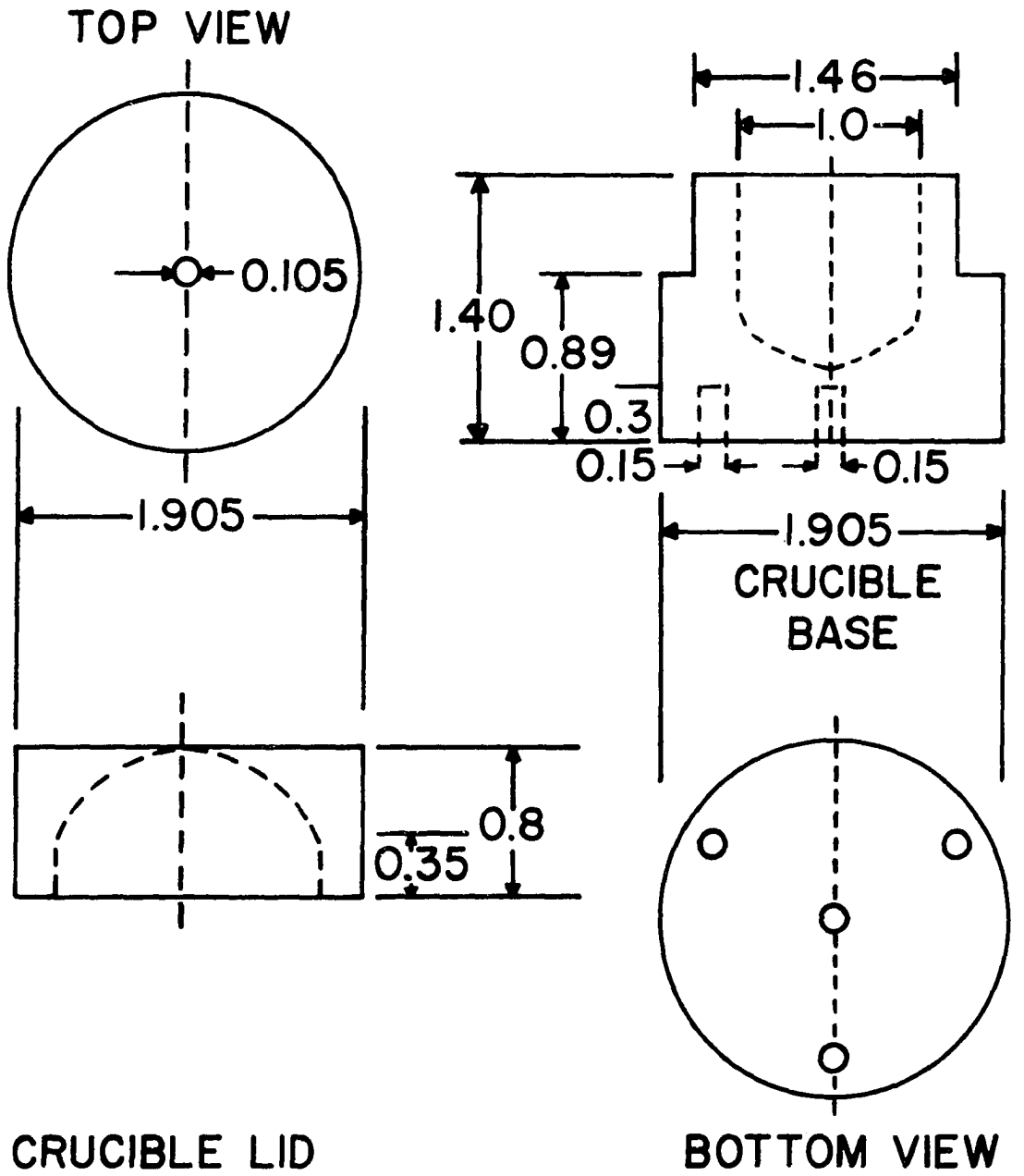

Figure 3.8. Construction of the tungsten crucible used for mass spectrometric vaporization studies of scandium sulfides, dimensions in centimeters

the same procedures described in section C1 of this chapter for crucible RTT-2-172. The orifice diameter was found to be 1.05 ± .01 mm and the orifice length was 0.575 ± .01 mm. The tungsten crucible was mounted on three tungsten rods which were positioned in holes in an alumina disc. The crucible was heated by a 10 mil diameter tungsten filament fabricated by the procedure described by Owzarski (34). The filament was supported by six tungsten rods slit axially with a spark cutter. The crucible was grounded to the support frame. A Universal Voltronics "BRE" precision regulated power supply was used to heat the crucible by electron bombardment. A negative dc potential of 500 to 1500 volts was superimposed on the 0-50 volt ac, 0-20 amp output to provide acceleration of emitted electrons in the direction of the crucible. The dc voltage was stable to within 0.1% and the ac output was stabilized by using a Stabiline voltage regulator to regulate the input line voltage. The temperature of the crucible remained constant within ± 4°C for periods up to eight hours at a particular voltage setting. The temperature was even more constant during periods from midnight to 6 a.m. (± 2°C). Three layers of shield cans made from molybdenum or tantalum surrounded the crucible in order to maintain a uniform temperature of the crucible. The shields were insulated from ground potential by quartz plates. There was a water

cooled copper block between the crucible and ion source with a movable shutter over a hole in the middle of the block. The shutter could be controlled from outside of the vacuum system by either manual or motor-driven mode.

The main function of the ion source is to produce ions from neutral atomic or molecular species originating from the crucible and to focus the ions into the analyzer region. Since an axial beam ionizer was used the ion beam produced was coaxial with the molecular beam.

The quadrupole analyzer consists of four stainless steel rods on which rf and dc potentials are superimposed. The transmission and resolution can be varied by changing the U/V ratio of the dc and rf voltages.

The ion current could be detected by use of either a Faraday cup or an electron multiplier. The Faraday cup detects singly charged particles on a one-to-one input to output ratio and is not sufficiently sensitive to measure low partial pressures. The Faraday cup was used mainly to determine the multiplying efficiency of the electron multiplier. The electron multiplier had 14 stages with copper-beryllium dynodes. The electron current output of the multiplier was generally between 10^5 and 10^6 times the input ion current. The multiplier output could be monitored either on an oscilloscope or after amplification with a picoammeter (Keithly 417) on a Brush strip chart recorder.

The temperature of the crucible was measured using the disappearing filament pyrometer previously described by sighting through a mirror and optical window onto the black-body hole in the bottom of the crucible. The absorbance correction for the optics was calculated as described in section C1 of this chapter. Temperature-correction constant measurements were made before and after every mass spectrometric run and the values obtained for the correction constant C in Equation 3.1 were averaged. The values usually agreed to within 10%.

3. Mass spectrometer operation

The operation of the EAI quadrupole mass spectrometer used in this study has been previously described by Owzarski (34). Conditions specific to the spectrometer operation for this investigation will be given here.

A known amount of sample under investigation was loaded into the tungsten crucible, the crucible was mounted on the supporting frame of the Knudsen cell assembly and the tungsten filament was positioned uniformly around the crucible. The orifice of the crucible and the holes in the shield cans were aligned with respect to the hole in the copper cooling block. The Knudsen cell assembly was attached to the mass spectrometer and the system was roughed down with a cryogenic sorption pump and a trapped

rotary pump. The stainless steel system walls were baked out using a heating tape, tubular heaters, and infrared lamps. After about three hours of bakeout the pressure was sufficiently low that the ion pump (Ultek Model 10-402) would operate. The system bakeout was continued usually overnight. After bakeout the residual pressure in the system was generally 3-4 x 10^{-9} torr.

A portion of the mass spectrum was obtained on the scope by selecting either the low, medium or high mass range and adjusting the sweep width (SW) and center of mass (CM). The resolution control was adjusted to give adequate resolution on the medium mass range (masses 10-150) without sacrificing too much sensitivity. A resolution setting of 6.06 was chosen. Optimum values for the extractor, focus, and ion energy were obtained by maximizing the ion intensity. Values used were: 30V, extractor; 45V, focus; and 30V, ion energy. The mass spectrum was then displayed on the strip chart recorder by choosing appropriate sweep frequency and chart speed settings. A mass scan on the medium mass range shown in Figure 3.9 exhibits deliberately deteriorated resolution of lower masses and enhanced sensitivity of higher masses. Since the ion intensity decreases with increasing sweep frequency for sweep frequencies less than 0.5 sec/amu, data were always recorded at sweep frequencies lower than this

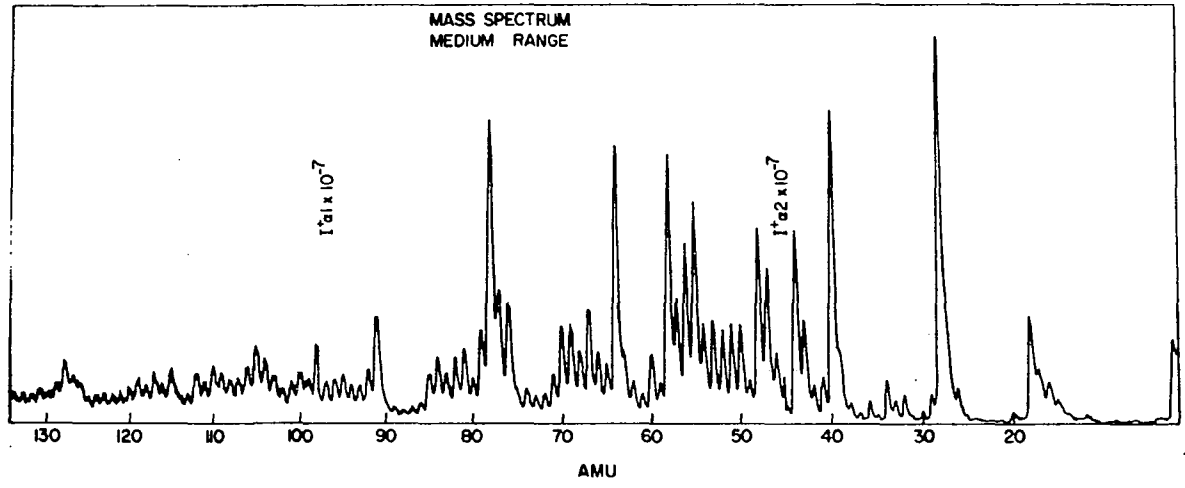

Figure 3.9. Background mass spectrum, medium mass range, sensitivity of higher masses is enhanced

value. The emission current of the ionizer filament was always kept at two milliamps or below in order to maintain the filament lifetime. The value of the electron energy used in most of the mass spectrometer operation was 50 electron volts. This value was selected because it resulted in relatively high ion currents, could be maintained for a long period of time without burning out the filament, and hopefully did not produce serious fragmentation of molecules under investigation.

The intensities of ion species of interest at the instrumental settings selected were determined by measuring the heights of the particular mass peaks on the strip chart recorder. The net intensity due to species effusing from the crucible was determined by subtracting the background intensity recorded with the shutter closed from that with the shutter fully open. It was found that the electron multiplier efficiency was a function of mass of the ion and time, exhibiting at times severe deterioration upon opening of the shutter. In order to determine the multiplier gain during the experiment, the gain of a reference peak (CO^+, $\frac{m}{e}=28$) was measured frequently, usually immediately before and after each shutter-open intensity.

The shutter assembly was used to determine which ions were formed from the molecular beam effusing from the

crucible by the determination of shutter profiles. The shutter was manually closed by fractional amounts of the shutter translation and the ion intensity of the particular mass under investigation was monitored after each decrement. The shape of the shutter profile obtained could be used to identify the origin of the species.

4. Specific experiments

A total of nine vaporization experiments was performed employing the mass spectrometer. Detailed descriptions of the experiments are given below.

The first experiment (MS-1) was designed to determine the vapor species formed from vaporization of the congruently subliming scandium sulfide. About 30.6 mg of scandium sulfide (ScS-2-91) previously characterized as congruently vaporizing was used in this experiment. Mass scans were taken on the medium mass ranges (masses 10-154) with shutter open and closed at various temperatures from 1500°-1700°C observed. Shutter profiles were taken for the shutterable species. Electron multiplier gains were measured for some of the shutterable species and compared with the multiplier gain of the reference ion (CO^+, $\frac{m}{e} = 28$).

Experiments MS-2 and MS-3 were performed in order to calibrate the ion intensity of a particular species in the mass spectrometer to the absolute pressure of the species.

The calibrant used was silver. In MS-2 4.45 mg of 99.9% pure silver wire were loaded into the same crucible (RTT-2-98) used for containing the scandium sulfide in the mass spectrometer. The crucible support was assembled and aligned and placed in the mass spectrometer. The crucible was heated to about 880°C where a small shutterable intensity of $Ag^+(107)$ was observed. After outgasing for several hours the temperature was increased to 1008°C and held constant $\pm$ 2°C. The shutter was opened and the ion intensity was measured until the sample was exhausted. The purpose of MS-3 was to determine if the silver calibration was repreducible after realigning the crucible. In MS-3 2.99 mg of Ag were used following the same procedure used in MS-2. The purpose of MS-4 was to measure the electron multiplier gain for $Ag^+(107)$ relative to the reference ion (CO^+, $\frac{m}{e}=28$).

Mass spectrometric experiments MS-5, MS-6 and MS-7 were performed in order to measure the temperature dependence of the ion intensities of the shutterable species present over the congruently vaporizing scandium sulfide. The medium mass range was employed in these three runs. In MS-5 an 80 mg sample of ScS-2-91 was used. Ion intensity data were collected over a temperature range of 1952-2197 K using 80 eV electron energy and 2 mA emission current. During the run the electron multiplier gain of

the reference ion (CO^+, $\frac{m}{e}=28$) was measured periodically. Another sample of ScS-2-91 (~ 131 mg) was used for MS-6. In this run ion intensity data were collected over a temperature range of 1915-2197 K measuring the multiplier gain immediately before and after each shutter-open scan. MS-7 used the residue of the scandium sulfide sample from MS-6. In this run the sweep frequency and shutter speed were increased to permit faster collection of shutter-open data. Ion intensity data were collected over a temperature range of 1929-2220 K.

The purpose of MS-8 was to collect ion intensity data of shutterable species over a scandium sulfide sample with composition changing from an initial value of S/Sc ≃ 1.0 to the congruently vaporizing composition. About 89.5 mg of ScS-2-175 (S/Sc = 1.006) were used in this experiment. The temperature of the crucible was held at 2035 ± 3 K and the shutter open ion intensities continuously monitored as a function of time until the congruently vaporizing composition was obtained.

The purpose of MS-9 was to collect ion-intensity data as a function of temperature for one of the shutterable species over a scandium-sulfide sample with composition of S/Sc ≃ 1.0. About 85.3 mg of ScS-2-189 (S/Sc = 0.99) were used for this experiment. Ion intensity data were collected over a temperature range of 1110-1300°C. It was assumed

that the composition of the solid did not change significantly during this time. The residue of MS-9 was used in MS-10 in which ion intensity data were collected as the composition varied upon vaporization from the 1:1 composition to the congruently vaporizing composition. An attempt was made to measure the ion currents as quickly as possible after the temperature was increased to 2035 $\pm$ 2 K.

The purpose of MS-11 was to collect ion intensity data of one of the shutterable species over the congruently vaporizing scandium sulfide. The sample used was the residue of MS-10. Data were collected on the low mass range over a temperature range of 1939-2173 K.

IV. THEORY

A. Knudsen Effusion Vapor Pressure Measurement

In a binary system, in which one solid phase and the gas phase are in equilibrium, the Gibbs Phase Rule

$$F = C - P + 2 \qquad (4.1)$$

limits the number of independent intensive variables, F, to two. However, if the chemical composition of the solid phase remains constant during the vaporization process, i.e. if the effusing vapor and the solid phase have the same composition (congruent vaporization), then for a fixed temperature the partial pressures of each gaseous species will be fixed. Thus, measurements of the partial pressures of the species present over the solid as a function of temperature will yield information on the equilibrium constants for the gas-solid equilibria.

Knudsen (35) found that the rate at which molecules effuse from a cell with a small orifice is related to the pressure inside the cell by the equation

$$dN_x/A_o dt = P_x/(2\pi m_x kT)^{1/2} \quad , \qquad (4.2)$$

where $dN_x/A_o dt$ is the rate at which molecules of the x-th species effuse per unit orifice area, A_o, P_x is the pressure of the x-th species inside the cell, m_x is the mass

of the particular gaseous species, k is the Boltzman constant and T the temperature. If the rate of effusion is expressed in terms of the weight of gas per unit area, the Knudsen equation can be expressed in the form

$$dg_x/(A_o M_x dt) = P_x/(2\pi M_x RT)^{1/2} \quad , \qquad (4.3)$$

where dg_x/dt is the weight of gas effusing per second, M_x is the molecular weight of the x-th gaseous species, and R is the gas constant. The Knudsen effusion equation is valid providing that the following conditions hold: (1) the vapor pressure inside the cell is sufficiently low (at least 10^{-3} atm) that the molecules behave as ideal gases, (2) the orifice is sufficiently small so that the ratio of the mean free path of the effusing molecules to the orifice diameter is large (greater than 10), and (3) the orifice is knife-edged. Since the orifice of the tungsten crucible used in the vaporization experiments could not be machined to a knife edge, a correction term called the Clausing factor was used to correct for the molecules that strike the orifice walls and reenter the crucible. For cylindrical orifices, the Clausing factor is a function of the length to radius of the orifice, ℓ/r, and has been tabulated for a variety of ℓ/r values by Dushman and Lafferty (36). The Knudsen pressure with the Clausing correction may be calculated from the equation

$$P_x = dg_x T^{1/2}/(44.33\ A_o W M_x^{1/2} dt) \quad , \qquad (4.4)$$

where W is the Clausing factor.

If the rate of mass transport of the effusing molecules is measured by collecting the effusate on a target located above the orifice, then another correction must be made to the Knudsen pressure. This is the target collection probability correction, which is the probability that a molecule entering the orifice will strike the target. The cosine law can be applied to calculate the target collection probability providing that the target and ideal orifice are parallel, circular, coaxial and the target is sufficiently far from the crucible so that the orifice appears as a point. For an ideal orifice the fraction of the total number of effusing molecules intercepted by the target is $R^2/(L^2 + R^2)$, where R is the radius of the deposit on the target and L is the distance from the orifice to the target. For a nonideal orifice, the angular distribution of the molecular beam may deviate from the cosine law. Edwards (37) obtained an equation with which the target collection probability for a nonideal orifice can be calculated. If the rate of mass collection of the x-th species on the target, dg_x/dt, and target probability W_p are determined, the pressure of the x-th species inside the cell is given by

$$P_x = dg_x T^{1/2}/(44.33\ A_o W_p M_x^{1/2} dt) \quad . \tag{4.5}$$

B. Mass Spectrometer Pressure Calibration

For ions formed by electron impact when an electron beam crosses a molecular beam at right angles, the ion intensity I^+ measured on the collector is given by the equation

$$I_i^+ = n_s i\, \ell \sigma_i\, \eta_i\, \gamma_i\, n_i G \quad , \tag{4.6}$$

where n_s is the density of a molecular beam effusing from a Knudsen cell orifice determined by the cosine law to be

$$n_s = 2nA_o/3\pi^2 L^2 \quad , \tag{4.7}$$

where A_o is the area of the orifice, L is the distance from the orifice and n is the number of molecules per cm^3 inside the cell. The other parameters in Equation 4.6 are: i, the electron emission current; ℓ, the effective path length of the electron beam; σ_i, the ionization cross section of the ion; η_i, the transmission of the mass spectrometer for the ion (which may be a function of the mass of the ion, but this variation is not known for the quadrupole spectrometer and will be neglected); γ_i, the electron multiplier gain for the i-th ion; n_i, the fractional

isotopic abundance; and G, a geometric factor including the alignment of the crucible. Inserting the ideal gas law $P = nkT$ in Equations 4.7 and 4.6 yields

$$I_i^+ T = P_i \sigma_i \gamma_i n_i / C_m = P_i K_i / C_m \quad , \tag{4.8}$$

where C_m, the machine constant, combines all of the instrumental factors assumed to be independent of the mass and nature of the species and the sensitivity constant K_i which contains the ionization cross section, the electron multiplier efficiency and the fractional isotopic abundance.

The method employed for the evaluation of the machine constant in this work was the total exhaustion of a known amount of calibrant from the cell. Combining Equations 4.8 and 4.4 yields

$$P_c = C_m I_c T/(\sigma_c \gamma_c n_c) = (dg_c/dt)T^{1/2}/44.33\ A_o W M_c^{1/2} \quad , \tag{4.9}$$

where the c subscript refers to the calibrant.

Integrating with respect to time from t_1 to t_2, the machine constant may be calculated as

$$C_m = \frac{\sigma_c \gamma_c n_c \Delta g_c}{44.33\ A_o W M_c^{1/2} \int_{t_1}^{t_2} I_c T^{1/2} dt} \tag{4.10}$$

where Δg_c is the weight loss of the calibrant during the time interval. The advantage of this method for determining C_m is that the value obtained is independent of the saturation conditions of the vapor in the cell.

Otvos and Stevenson (38) proposed that the maximum cross section, σ, for single ionization could be calculated as

$$\sigma = \sum_i N_i q_i = \sum_i A N_i \langle r_i^2 \rangle \quad , \tag{4.11}$$

where N_i is the number of electrons in the i-th shell and q_i is the cross section for ionizing one electron in the shell, and $\langle r_i^2 \rangle$ is the mean square radius. Mann (39) revised this calculation by employing a quantum mechanical method for evaluating the mean-square orbital radii. Mann's calculated values agree fairly well with available experimental results and were used in this study for gaseous atoms. For the ionization cross section of molecules, Otvos and Stevenson (38) and Gryzinski (40) both postulated that sum of the cross sections of the constituent atoms is a reasonable approximation.

C. Calculation of Thermodynamic Quantities

The equilibrium constant for a particular vaporization reaction can be obtained from the partial pressures of each of the vapor species involved assuming that the vapor behaves

as a perfect gas. The enthalpy and entropy changes associated with the reaction may be obtained by combining the Gibbs-Helmholz equation

$$\Delta G_T^o = \Delta H_T^o - T\Delta S_T^o \qquad (4.12)$$

and the equilibrium equation

$$\Delta G_T^o = - RT \ln K_{eq} \qquad (4.13)$$

to obtain

$$2.303\ R \log K_{eq} = - \Delta H_T^o/T + \Delta S_T^o \quad . \qquad (4.14)$$

If the variation of C_p with temperature is taken to be zero over the temperature interval of the experiment, a plot of $2.3\ R \log K_p$ vs. T^{-1} will be linear yielding a slope which is the standard enthalpy change, ΔH_T^o, and an intercept which is the standard entropy change, ΔS_T^o, for the vaporization reaction at the mean temperature of the measurements. This is the second-law method of data analysis. The enthalpy and entropy changes at a reference temperature can then be obtained using enthalpy and entropy increments for the products and reactants. Another way of employing the second-law method to obtain ΔH_{298}^o involves using the free energy function change for the reaction, which is defined by

$$\Delta fef = \Delta \left(-\frac{G_T^o - H_{298}^o}{T} \right)$$

$$= - \Delta G_T^o/T + \Delta H_{298}^o/T$$

$$= R \ln K_{eq} + \Delta H_{298}^o/T \quad . \qquad (4.15)$$

Plotting $-R \ln K_{eq} + \Delta fef$ vs. T^{-1} yields a line with slope equal to ΔH_{298}^o.

The third-law method yields a value of

$$\Delta H_{298}^o = - RT \ln K_{eq} + T(\Delta fef) \qquad (4.16)$$

for each measurement of K_{eq} at each experimental temperature. An average value can then be obtained by averaging all of the ΔH_{298}^o values. The third-law method, thus, requires both a knowledge of the free energy functions of the solid and gaseous molecules and also the absolute value of K_p. The second-law method does not require a pressure calibration, since the slope of the plot of $\log\pi(I_i^+ T)^{n_i}$ vs. T^{-1} also corresponds to the enthalpy change for the reaction at the midpoint temperature.

D. Application of the Gibbs-Duhem Equation

For a condensed phase in equilibrium with a perfect gaseous mixture at a constant temperature, the Gibbs-Duhem equation can be expressed as

$$\Sigma N_i \, d \ln p_i = 0 \quad , \tag{4.17}$$

where N_i is the mole fraction of the i-th component. Thus, for the binary scandium-sulfur system, we have

$$N_S \, d \ln P_S + N_{Sc} \, d \ln P_{Sc} = 0 \quad . \tag{4.18}$$

Integrating from composition x' to composition x" yields

$$\ln \frac{P_S(x=x'')}{P_S(x=x')} = - \int_{\ln P_{Sc}(x=x')}^{\ln P_{Sc}(x=x'')} (N_{Sc}/N_S) d \ln P_{Sc} \quad . \tag{4.19}$$

Taking $P_S = K \, P_{ScS}/P_{Sc}$, $x'' = 1.0$ and $x' = .8065$ yields

$$\ln\left(\frac{P_{ScS}(x=1.0) \cdot P_{Sc}(x=.8065)}{P_{ScS}(x=.8065) \cdot P_{Sc}(x=1.0)}\right) = -.8065 \ln \frac{P_{Sc}(x=1.0)}{P_{Sc}(x=.8065)} - A \quad , \tag{4.20}$$

where A is the remaining part of the integral on the right hand side of Equation 4.19.

E. Born-Haber Calculations

The Born-Haber calculation involves the application of the first law of thermodynamics to a thermochemical cycle, which relates the cohesive energy of a compound to the energy of the constituent elements in their standard states. A Born-Haber cycle for the formation of a cystalline metal sulfide MS from its elements is given below.

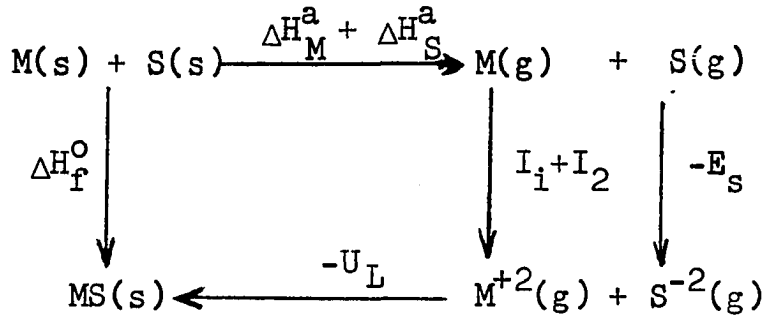

Combining the energy terms associated with the two reaction paths indicated in this diagram yields

$$\Delta H_f^o = \Delta H_M^a + \Delta H_S^a + I_1 + I_2 - E_s - U_L \quad , \qquad (4.21)$$

where ΔH_M^a and ΔH_S^a are the enthalpies of atomization of the metal and sulfur respectively, I_1 and I_2 are the first and second ionization potentials of the metal, E_s is the electron affinity for sulfur (to produce S^{-2}), and U_L is the lattice energy. If all of the energy terms on the right hand side of Equation 4.21 are known (measured or calculated), the heat of formation of the compound can be obtained. The lattice energy is the amount of energy required to convert one mole of the crystal at 0 K into its constituent ions in the gas phase and consists of the coulomb attraction and interatomic repulsion terms. For an isolated univalent ion pair, the potential energy arising from two terms is

$$\Phi = -\frac{e^2}{r} + be^{-r/\rho} \quad , \tag{4.22}$$

where r is the distance between the ions. For a sulfide with a perfect NaCl-type lattice, each metal ion is surrounded by six sulfur ions at a distance r. Twelve other metal ions at a distance of $\sqrt{3}$ r, six more metal ions at a distance 2r, 24 sulfurs at a distance $\sqrt{5}$ r, etc. Thus, the coulomb term for a metal ion in a sodium chloride lattice is

$$\Phi_c = -\frac{6z_1z_2e^2}{r} + \frac{12z_1z_2e^2}{\sqrt{2}\,r} - \frac{8z_1z_2e^2}{\sqrt{3}\,r} + \frac{6z_1z_2e^2}{2r} - \frac{24z_1z_2e^2}{\sqrt{5}\,r} \cdots$$

$$= -\frac{z_1z_2e^2}{r}\left[6 - \frac{12}{\sqrt{2}} + \frac{8}{\sqrt{3}} - \frac{6}{2} + \frac{24}{\sqrt{5}} - \cdots\right] \quad , \tag{4.23}$$

where z_1 and z_2 are the valences of the metal and sulfur ions. The infinite series arising in Equation 4.23 converges to 1.74756 and is the Madelung constant, A, for the sodium chloride structure. The repulsion term for the NaCl lattice obtained similarly is

$$\Phi_r = 6be^{-r/\rho} + 12be^{-\sqrt{2}r/\rho} + 8be^{-\sqrt{3}r/\rho} + 6be^{-2r/\rho}$$

$$\simeq 6be^{-r/\rho} \quad . \tag{4.24}$$

Only the first nearest neighbor term is important, since the repulsive forces are short range dropping off exponentially. Thus, the potential energy associated with bringing a metal ion from infinity to its stable position in the rocksalt lattice is

$$\Phi = - \frac{Az_1z_2e^2}{r} + 6be^{-r/\rho} \quad . \tag{4.25}$$

Since the potential energy is a minimum at the equilibrium distance, $(\partial\Phi/\partial r)_{r_o} = 0$, the potential becomes

$$\Phi_o = - \frac{Az_1z_2e^2}{r_o} (1 - \frac{\rho}{r_o}) \quad . \tag{4.26}$$

The lattice energy for the rocksalt lattice is then

$$U_L = - N_o\Phi_o = \frac{NAz_1z_2e^2}{r_o} (1 - \frac{\rho}{r_o}) \quad , \tag{4.27}$$

where N is the number of ions per mole of solid.

Lattice energy calculations have been refined by including additional terms such as London dispersion energy, crystal field stabilization energy of nonspherical ions and also by including effects due to polarization. Kapustinskii (41) has proposed a semiempirical equation for the lattice energy that compensates for some of these effects. This equation is

$$U_L = \frac{256.1\ n\ z_1 z_2}{r_c + r_a} \quad , \tag{4.28}$$

where n is the total number of ions in the formula and r_c and r_a are ionic radii of the cation and anion respectively.

V. RESULTS

A. Low Temperature Preparation of Scandium Sulfides

Scandium sulfide samples of various compositions were prepared as described in Chapter III, Section A. Table 5.1 lists the phases present in samples which resulted from the low temperature preparations of scandium sulfides. In all preparations except the two with highest sulfur to scandium ratio, ScS-1-179 and ScS-2-16, the sulfur was completely consumed. Some unreacted scandium was present in all preparations. The low temperature product was a brittle greyish-brown colored coating formed on the surface of the scandium turnings. Phase analyses were performed by X-ray diffraction. The phases Sc_2S_3 and $Sc_{1.37}S_2$ were present in all of the low temperature preparations.

B. Characterization of the Vaporization Behavior of Scandium Sulfides

1. Vaporization of sulfur-rich sulfides

The two sulfur-rich samples, ScS-1-179 and ScS-2-16, which have a composition ScS_{1+x} where x is between 0 and 0.5, were used in successive vaporization studies in an inductively heated tungsten crucible. Table 5.2 presents the results of seven successive vaporizations starting with sample ScS-1-179, and four successive vaporizations of

Table 5.1. Results of low temperature preparation of scandium sulfides

Sample	Initial Composition Sc/S	Heating Conditions Temp. (°C)	Heating Conditions Time (days)	Phase Present
ScS-1-179[a]	.67	920	3	Sc_2S_3, $Sc_{1.37}S_2$, Sc
ScS-2-16[a]	.67	925	4	Sc_2S_3, $Sc_{1.37}S_2$, Sc
ScS-2-51	.95	900	5	Sc_2S_3, $Sc_{1.37}S_2$, Sc
ScS-2-80	.95	913	10	Sc_2S_3, $Sc_{1.37}S_2$, Sc
ScS-2-75	1.5	900	8	Sc_2S_3, $Sc_{1.37}S_2$, Sc
ScS-2-93a	2	900	6	Sc_2S_3, $Sc_{1.37}S_2$, Sc
ScS-2-93b	2.5	930	4	Sc_2S_3, $Sc_{1.37}S_2$, Sc
ScS-2-103	3	910	5	Sc_2S_3, $Sc_{1.37}S_2$, Sc
ScS-2-105b	4	915	5	Sc_2S_3, $Sc_{1.37}S_2$, Sc
ScS-2-164	1.0	950	8	Sc_2S_3, $Sc_{1.37}S_2$, Sc
ScS-2-171	1.05	900	8	Sc_2S_3, $Sc_{1.37}S_2$, Sc

[a]Some unreacted sulfur present.

Table 5.2. Results of successive vaporization of sulfur-rich sulfides

Run no.	Temp (°C)[a]	Time (hr)	Wt.Loss (mg)	Appearance	Phases Present	Lattice Parameter (Å)
			A. ScS-1-179			
1	1260	3.5	0.4 (3.5%)	dull grey	Sc_2S_3, $Sc_{1.37}S_2$	
2	1420	1.0	0.2 (2%)	bluish	$Sc_{1.37}S_2$	
3	1500	3.0	0.0	bluish	$Sc_{1.37}S_2$	
4	1560	2.0	0.8 (10.7%)	shiny purple	ScS	
5	1615	4.0	0.1 (1.6%)	shiny purple	ScS	
6	1680	3.0	0.9 (16.1%)	shiny purple	ScS	
7	1710	2.0	1.4 (30%)	shiny purple	ScS	5.166 ± 2
			B. ScS-2-16			
1	1560	2.0	1.2 (0.6%)	shiny copper	ScS	5.172 ± 2
2	1650	4.0	2.6 (1.3%)	redish copper	ScS	5.168 ± 3
3	1710	3.0	6.3 (10.7%)	shiny maroon	ScS	5.166 ± 2
4	1815	3.0	14.6 (28%)	shiny purple	ScS	5.166 ± 2

[a]Observed temperature, without corrections.

sample ScS-2-16. Although the composition of the residue of each vaporization was not determined, the appearance of the residue and the lattice parameters of the cubic phases obtained eventually, after a significant percentage had vaporized, remain unchanged. In the seventh successive vaporization from ScS-1-179, some of the sample sublimed on the crucible lid near the orifice. The sublimate had the same appearance and lattice parameter (5.166 Å) as the residue in the bottom of the crucible. A single crystal was obtained from the sublimate and was investigated by Weissenberg techniques. The symmetry of the crystal was cubic. Intensities of the diffraction maxima were not measured but the absence of superstructure spots indicated that the structure was the NaCl-type previously reported.

2. Vaporization of stoichiometric scandium monosulfide

Four samples were prepared with an initial sulfur to scandium ratio of about 1.0. Sample ScS-2-80 was used for electrical and magnetic measurements. Samples ScS-2-164 and ScS-2-171 were used for mass spectrometric experiments. Sample ScS-2-51 was used for successive vaporizations from an inductively heated tungsten crucible. In this series of vaporizations the composition of the residue of each run was determined as well as the phase(s) and lattice parameter. Table 5.3 presents the results of successive

Table 5.3. Results of successive vaporization of stoichiometric scandium monosulfides

Product (residue)	Temp (°C)[a]	Time (hr)	% Vaporized[b]	Composition S/Sc	Appearance	Phase Present	Lattice Parameter (Å)
ScS-2-60	1525	4.0	0.5	1.092[c]	gold	ScS	5.183 ± 2
ScS-2-63	1595	2.0	1.3	1.05[d]	gold	ScS	5.180 ± 2
ScS-2-66	1650	2.0	2.5	1.27[d]	dark gold	ScS	5.178 ± 2
ScS-2-67	1700	2.0	4.1	1.156[d]	copper	ScS	5.176 ± 2
ScS-2-71	1721	3.0	7.0	1.190[d]	rust	ScS	5.170 ± 2
ScS-2-78	1710	12.0	9.8	1.196[d]	maroon	ScS	5.170 ± 2
ScS-2-79	1720	8.0	12	1.228[d]	purple	ScS	5.165 ± 2
ScS-2-85	1715	22.0	15.3	1.235[d]	purple	ScS	5.166 ± 2
ScS-2-91	1720	42.0	24	1.239[c]	purple	ScS	5.165 ± 2
				1.236[d]			

[a]Observed temperature, uncorrected.

[b]Total percentage of original sample vaporized.

[c]Results of combustion analysis.

[d]Results of microprobe analysis.

vaporizations from sample ScS-2-51 (S/Sc ≃ 1.05). The product of each vaporization run is labeled in the first column. The percent vaporized in column four is the cumulative total for the successive vaporizations. The compositions of the products were determined by combustion analysis for samples ScS-2-60 and ScS-2-91. Electron microprobe analyses were used to determine the compositions of the other samples using ScS-2-60 as a standard. The value obtained for the composition of ScS-2-91 by the electron microprobe technique (S/Sc = 1.236) agrees with the combustion analysis value (S/Sc = 1.239) to within the experimental uncertainty (± .002). The lattice parameters were obtained by least squares treatment of sin θ values from back reflections obtained on Debye-Scherrer films. The composition, appearance and lattice parameter of sample ScS-2-91 remained unchanged from those for sample ScS-2-85 while a significant percentage of material was vaporized. Further vaporization of sample ScS-2-91 at higher temperatures in the mass spectrometer resulted in unchanged appearance and lattice parameter. Thus the scandium sulfide with this composition (Sc/S ≃ .8065) and lattice parameter (5.165 Å) vaporizes congruently. The final product of the successive vaporizations of the sulfur-rich samples had the same lattice parameter and appearance as the congruently vaporizing sulfide and is assumed to have

that composition. A plot of lattice parameter vs. composition for the successive vaporizations from the monosulfide (ScS-2-51) is shown in Figure 5.1. The datum point at S/Sc = 1.005 was obtained from analysis of a vaporization product of sample ScS-2-171. The lattice parameter decreases linearly with increasing S/Sc ratio (increasing number of scandium vacancies) between the ratios of 1.00 and 1.24.

3. Vaporization of scandium-rich sulfides

Five sulfides were prepared with initial compositions Sc/S of between 1.5 and 4. Seven successive vaporizations of sample ScS-2-75 (Sc/S = 1.46) were performed using an inductively heated tungsten crucible. Table 5.4 lists the results of this study. Phase analysis of the product of each vaporization was performed by the powder diffraction technique. No new phase was found in the region between Sc/S = 1.5 and Sc/S = 1.0. The composition of the products was calculated by assuming that the weight loss by vaporization was due to scandium loss only. According to this analysis the ScS-Sc two phase region, in quenched samples, extends to Sc/S $\leq$ 1.015. Combustion analysis of the sulfide obtained from run 7 (ScS-2-115) gave a composition of Sc/S = 0.90.

Sample ScS-2-93a (Sc/S $\simeq$ 2.0) was heated inductively to

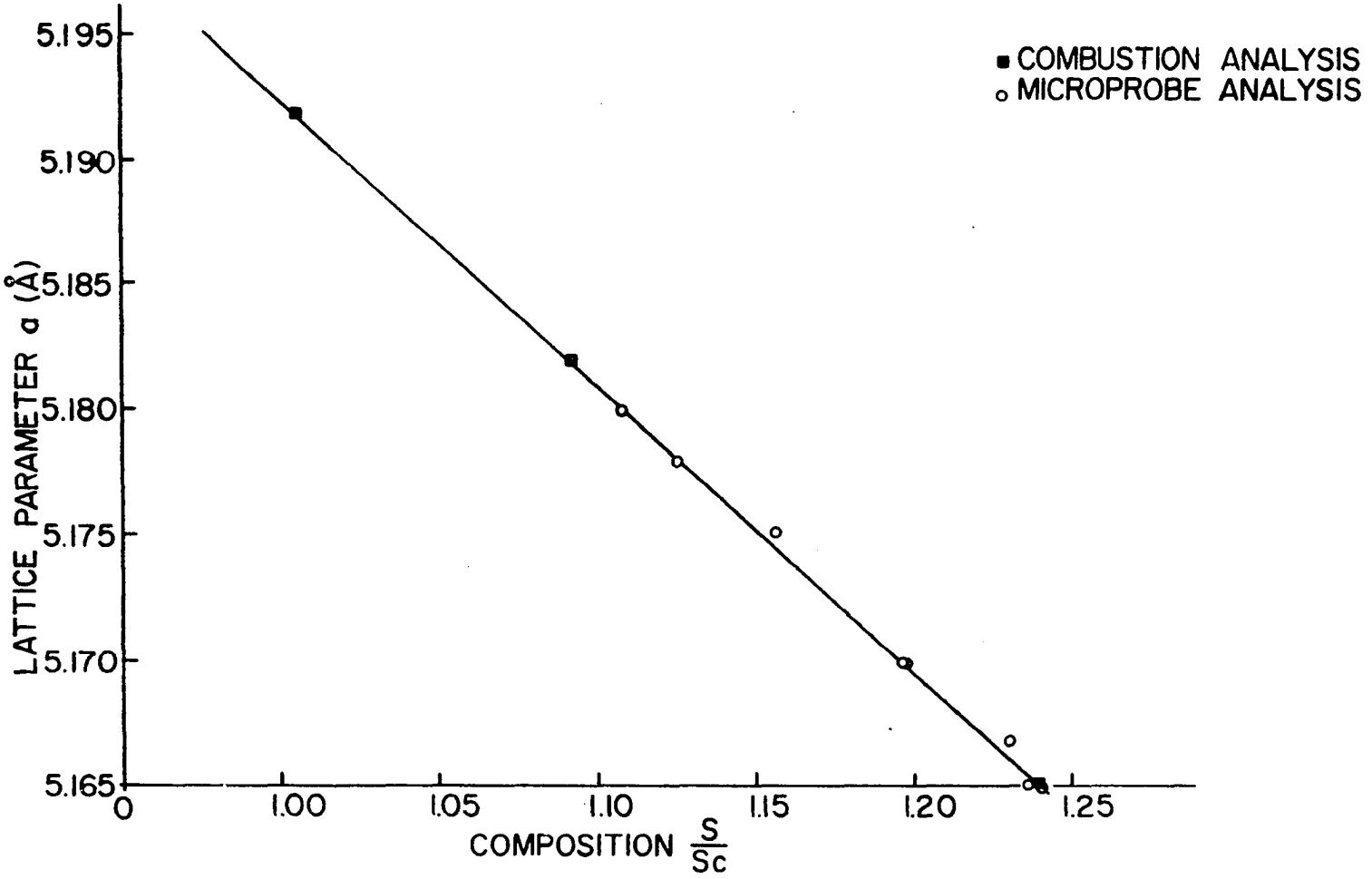

Figure 5.1. Plot of lattice parameter of ScS vs. composition for the successive vaporizations of sample ScS-2-51

Table 5.4. Results of successive vaporization of ScS-2-75 (Sc/S = 1.46)

Run no.	Temp (°C)[a]	Time (hr)	Initial Wt. (mg)	Wt. Loss (mg)	Product (residue)	Appearance	Phases Present	Composition (Sc/S)[b]
1	1375	0.3	174.8	3.0	ScS-2-104	silver-gold	ScS, Sc	1.423
2	1300	0.5	152.0	1.4	ScS-2-105	silver-gold	ScS, Sc	1.401
3	1360	0.7	148.2	4.4	ScS-2-106	silver-gold	ScS, Sc	1.302
4	1365	1.5	136.6	5.6	ScS-2-110	light gold	ScS, Sc	1.227
5	1425	0.25	123.2	7.3	ScS-2-111	gold	ScS, Sc	1.120
6	1430	1.25	108.4	5.6	ScS-2-112	gold	ScS, Sc	1.016
7	1575	3.5	99.0	5.8	ScS-2-115	dark gold	ScS	0.92

[a]Observed temperature, without corrections.

[b]Composition calculated by assuming weight loss was scandium only.

a temperature of 1300°C for one hour. Some scandium was vaporized as evidenced by the deposit on the vacuum line cap. The residue of this vaporization had partially melted. X-ray powder diffraction showed that only phases present in the residue were ScS and Sc metal. Sample ScS-2-93b (Sc/S ≃ 2.5) was heated at 1165°C for 30 minutes followed by heating at 1325°C for 15 minutes. No vapor deposit was observed on the cap for the 1165°C heating and the residue was nonhomogeneous. The 1325°C heating results in a completely melted sample consisting of the monosulfide phase and scandium metal. Sample ScS-2-103 (Sc/S ≃ 3.0) was heated to about 1175°C for one hour. The product, which consisted of the phases ScS and Sc metal only, was pelletized and arcmelted under an atmosphere of argon. The arcmelted sample did not contain any new solid phases. Sample ScS-2-105b (Sc/S ≃ 4.0) was treated in the same manner as sample ScS-2-103; annealing at about 1200°C followed by arcmelting. The absence of phases other than the cubic monosulfide and scandium metal indicates that there are no metal-rich solid phases in the scandium-sulfur system up to 80 mole % scandium, in agreement with the conclusion that $Sc_{.8065}S$ vaporizes congruently and the fact that scandium sulfides containing between 44.6 and 80 mole % scandium preferentially lose scandium when heated.

C. Estimation of Thermodynamic Data for Scandium Sulfides

Thermal data for the vaporization of scandium sulfides were obtained over a particular convenient experimental temperature range. In order to compare thermal data for scandium sulfides with other transition metal sulfides, these data must be converted to those corresponding to a reference temperature (usually either 298 K or 0 K). A knowledge of the absolute entropy at the reference temperature (S^{o}_{298}), and the heat capacity (C_p) of the solid scandium sulfide and the vaporization products are necessary. The heat capacity of a solid above room temperature and at constant pressure can be expressed as a function of temperature by the expression:

$$C_p = a + bT + cT^{-2} \quad , \tag{5.1}$$

where a, b, and c are empirical constants. The relationship between the heat capacity and enthalpy increment and between the heat capacity and entropy increment from the reference temperature (298 K) up to the temperature of interest (assuming there are no phase transitions in this range) may be expressed as follows:

$$H_T^o - H_{298}^o = \int_{298}^{T} C_p dT = a(T-298) + b/2(T^2-298^2)$$

$$- c(1/T-1/298) \quad , \qquad (5.2)$$

$$S_T^o - S_{298}^o = \int_{298}^{T} (C_p/T)dT = a\ln(T/298) + b(T-298)$$

$$- (c/2)(T^{-2}-298^{-2}) \quad . \qquad (5.3)$$

The free energy function (fef) used in the third-law method of thermodynamic data analysis described in Chapter IV can be evaluated for a particular solid substance using the enthalpy increment, entropy increment and absolute entropy at the reference temperature (298 K) by the equation:

$$fef_T = -(H_T^o-H_{298}^o)/T + (S_T^o-S_{298}^o) + S_{298}^o \quad . \qquad (5.4)$$

Thermochemical data for the gas phase products of the vaporization of scandium sulfides can be calculated from known spectroscopic data and molecular parameters.

At the present time no heat capacity data for solid scandium sulfides are available, thus the changes in the required thermoydnamic functions must be estimated. The heat capacity of a solid substance at room temperature may be estimated by "Neumann and Kopp's Rule" which states that the heat capacity of the compound is equal to the sum of

the heat capacities of its constituent elements. Therefore the heat capacity of ScS(s) at 298 K is estimated to be

$$C_p(298\ K)ScS = C_p(298\ K)Sc + C_p(298\ K)S$$

$$= 6.10 + 5.44$$

$$= 11.54 \pm 0.2\ eu \quad , \qquad (5.5)$$

where the heat capacity of Sc(s) was obtained from Dennison et al. (42) and the heat capacity of S(s) was taken from Kelley (43). The heat capacities of these solids at high temperatures may be estimated by the method of Kubaschewski et al. (44). They proposed a value of C_p of 7.25 cal/K per gram atom for the solid at the melting point assuming a linear increase of C_p with temperature. The heat capacity of ScS(s) at an estimated melting point of 2000 K is thus 14.5 cal/K. From the two C_p values for ScS(s) the formula obtained is

$$C_p(ScS) = 11.05 + 1.72 \times 10^{-3}\ T \quad . \qquad (5.7)$$

The heat capacity of $Sc_{.8065}S$ at the melting point of approximately 2200 K is 13.10 cal/K. Thus the C_p formula obtained for the congruently vaporizing scandium sulfide is

$$C_p(Sc_{.8065}S) = 9.93 + 1.44 \times 10^{-3}\ T \quad . \qquad (5.8)$$

The enthalpy increments ($H_T^o - H_{298}^o$) for the two solid scandium sulfides may be calculated by Equations 5.2 and 5.7 or 5.8 (Method 1) in the temperature ranges 298 K to 2000 K, and 298 K to 2200 K for ScS(s) and $Sc_{.8065}S$(s) respectively, the term involving T^{-2} in Equation 5.2 being ignored. Another method (Method 2) of obtaining the enthalpy increments for the solid scandium sulfides involves using the enthalpy increments for scandium metal. Since the scandium sulfides exhibit properties which are in some respects similar to elemental scandium, the enthalpy increments for ScS(s) may be estimated as twice the enthalpy increments for Sc(s) and that for $Sc_{.8065}S$(s) as 1.8065 times the enthalpy increments (omitting phase transformations) for Sc(s) reported in the JANAF Thermochemical Tables (26). A third method for estimating the enthalpy increments of scandium sulfides involves using measured data for a similar refractory sulfide. Heat capacity data of MacLeod and Hopkins (45) for uranium monosulfide were used since US(s) is isostructural with ScS(s), and both ScS and US are metallic compounds. The entropy increments ($S_T^o - S_{298}^o$) for the solid scandium sulfides may also be estimated by three methods. The first method is a calculation using Equations 5.3 and 5.7 or 5.8. Method 2 is to estimate the entropy increments of the sulfides using the entropy increments for Sc(s) as was done in Method 2 (above)

for the enthalpy increment. Method 3 uses the entropy increments from the experimental data for US(s). Table 5.5 lists the values obtained for the enthalpy and entropy increments at various temperatures for ScS(s) by the three estimation methods. Table 5.6 lists the corresponding estimates for $Sc_{.8065}S(s)$.

The absolute entropy of ScS(s) and $Sc_{.8065}S(s)$ at 298 K must also be estimated. The estimation method of Grønvold and Westrum (46) for transition metal chalcogenides was used to estimate S^{o}_{298}. Their method yields a lattice contribution of scandium of 9.7 cal/g-atom K and a sulfur contribution is 3.0 cal/g-atom K. Thus, for ScS(s) a value of 12.7 cal/mole K is obtained for S^{o}_{298} and for $Sc_{.8065}S(s)$ an entropy of 10.8 cal/mole K at 298 K is obtained. A measurement of the magnetic susceptibility of $Sc_{.8065}S(s)$ by H. F. Franzen (47) at Grönigen University indicated that the solid was very weakly paramagnetic. The magnetic contribution to the entropies of the scandium sulfides, therefore, will be neglected. However, since $Sc_{.8065}S(s)$ contains about 20% randomized scandium vacancies in the lattice, a configurational entropy exists for the solid and is taken to be

Table 5.5. Estimated values for the heat content and entropy of ScS(s)

Temperature (K)	$H_T^o-H_{298}^o$ (kcal/mole) Method 1	$H_T^o-H_{298}^o$ (kcal/mole) Method 2	$H_T^o-H_{298}^o$ (kcal/mole) Method 3	$S_T^o-S_{298}^o$ (eu) Method 1	$S_T^o-S_{298}^o$ (eu) Method 2	$S_T^o-S_{298}^o$ (eu) Method 3
1700	17.9	21.5	19.6	21.7	25.0	23.7
1750	18.6	22.6	20.4	22.1	25.6	24.1
1800	19.3	23.6	21.2	22.5	26.25	24.6
1850	20.0	24.6	22.0	22.9	26.9	25.0
1900	20.7	25.7	22.7	23.3	27.4	25.4
1950	21.5	26.8	23.5	23.6	27.95	25.8
2000	22.2	27.9	24.3	24.1	28.5	26.2
2050	22.9	29.0	25.1	24.4	29.0	26.6
2075	23.3	29.6	25.5	24.6	29.25	26.8
2100	23.6	30.0	25.9	24.8	29.5	27.0
2150	24.4	31.1	26.7	25.1	30.0	27.4
2200	25.1	32.2	27.5	25.5	30.5	27.7
2250	25.8	33.3	28.3	25.8	31.0	28.1
2300	26.6	34.4	29.1	26.1	31.5	28.6

Table 5.6. Estimated values for the heat content and entropy of $Sc_{0.8065}S(s)$

Temperature (K)	$H_T^o-H_{298}^o$ (kcal/mole) Method 1	$H_T^o-H_{298}^o$ (kcal/mole) Method 2	$H_T^o-H_{298}^o$ (kcal/mole) Method 3	$S_T^o-S_{298}^o$ (eu) Method 1	$S_T^o-S_{298}^o$ (eu) Method 2	$S_T^o-S_{298}^o$ (eu) Method 3
1700	15.9	19.5	17.7	19.3	22.6	21.4
1750	16.6	20.4	18.4	19.7	23.1	21.8
1800	17.2	21.3	19.1	20.0	23.7	22.2
1850	17.8	22.2	19.8	20.4	24.3	22.6
1900	18.4	23.2	20.5	20.7	24.8	22.9
1950	19.1	24.2	21.2	21.0	25.3	23.3
2000	19.7	25.2	21.9	21.4	25.7	23.7
2050	20.4	26.2	22.6	21.7	26.2	24.0
2075	20.7	26.6	23.0	21.9	26.4	24.2
2100	21.0	27.1	23.4	22.0	26.6	24.4
2150	21.7	28.1	24.1	22.3	27.1	24.7
2200	22.3	29.1	24.8	22.6	27.5	25.0
2250	23.0	30.1	25.5	22.9	28.0	25.4
2300	23.6	31.1	26.3	23.2	28.4	25.8

$$S^{o}_{config} = - R \Sigma X_i \ln X_i$$

$$= - R[0.1935 \ln 0.1935 + 0.8065 \ln 0.8065]$$

$$= .98 \text{ cal/mole K} \quad . \qquad (5.9)$$

The standard entropy at 298 K for the congruently vaporizing scandium sulfide is then 11.8 cal/mole K.

The standard free energy functions of ScS(s) and $Sc_{.8065}S(s)$ can be calculated using Equation 5.4 and the values estimated for the enthalpy and entropy increments and the standard entropy of the solids at 298 K. The values of this function at various temperatures for the two solids are given in Table 5.7. The values used for the enthalpy and entropy increments were those based on the US(s) data (Method 2).

The thermodynamic properties of ScS(g) were calculated from known molecular parameters and spectroscopic data by evaluating the various partition functions (translational, vibrational, rotational and electronic). The equilibrium internuclear distance in the molecule, determined by Marcano and Barrow (48), was 2.1354 Å. The vibrational frequency determined by McIntyre et al. (15), using the matrix isolation technique, was 554 cm^{-1}. They also reported the ground electronic state to be $^2\Sigma^+$, and a $^2\pi$ excited state at about 11,000 cm^{-1}. A $^2\Delta$ band was estimated by T. C. DeVore (49) to occur at about 5,000 cm^{-1}. Using these

Table 5.7. Free energy functions of ScS(s) and $Sc_{.8065}S(s)$

Temperature (K)	fef_T^a(ScS(s)) (cal/mole-deg)	fef_T^a($Sc_{.8065}S(s)$) (cal/mole-deg)
1700	24.87	22.69
1800	25.48	23.27
1900	26.15	23.85
2000	26.75	24.42
2075	27.21	24.81
2100	27.37	24.92
2200	27.90	25.47
2300	28.60	26.06

$^a fef = -(G_T^o - H_{298}^o)/T$.

parameters the translational, vibrational, rotational and electronic contributions to the enthalpy $(H_T^o - H_0^o)$, entropy S_T^o and free energy function (fef) were calculated according to the harmonic oscillator, rigid rotor approximation. The sum of these contributions is given in Table 5.8 for various temperatures. The free energy function calculated here is referred to a reference temperature of 0 K.

Table 5.8. Heat content, entropy and free energy function of ScS(g)

Temperature (K)	$H_T^o - H_0^o$ (cal/mole)	S_T (eu)	fef[a] (eu)
298	2188	56.55	49.31
1930	16850	73.07	64.34
1940	16950	73.12	64.38
1950	17040	73.17	64.43
1960	17140	73.22	64.47
1970	17230	73.27	64.52
1980	17330	73.31	64.56
1990	17430	73.36	64.61
2000	17520	73.41	64.65
2010	17620	73.46	64.69
2020	17710	73.51	64.74
2030	17810	73.55	64.78
2040	17910	73.60	64.82
2050	18000	73.65	64.87
2060	18100	73.70	64.91
2070	18200	73.74	64.95
2080	18290	73.79	64.99
2090	18390	73.84	65.04

[a] $fef = -(G_T^o - H_0^o)/T$.

Table 5.8 (Continued)

Temperature (K)	$H_T^o - H_0^o$ (cal/mole)	S_T (eu)	fef[a] (eu)
2100	18490	73.88	65.08
2110	18580	73.93	65.12
2120	18680	73.97	65.16
2130	18780	74.02	65.20
2140	18870	74.06	65.24
2150	18970	74.11	65.29
2160	19070	74.15	65.33
2170	19160	74.20	65.37
2180	19260	74.24	65.41
2190	19360	74.29	65.45
2200	19450	74.33	65.49
2210	19550	74.38	65.53

D. Knudsen Effusion Vapor Pressure Measurements on $Sc_{.8065}S$

1. Calibration of electron microprobe for scandium

As previously described, scandium metal was vaporized in the target collection apparatus and the vapor was deposited on the aluminum targets. The amount of scandium deposited on each target was calculated from the Knudsen effusion Equation (4.5) using JANAF (26) values for the vapor pressure of scandium at each of the various exposure temperatures in the range 1574 to 1773 K, and other measured parameters. The area of the orifice of crucible RTT-2-172 was 6.22×10^{-3} cm^2 and the distance between orifice and the target measured by a cathetometer was $10.76 \pm .02$ cm. A computer program written by J. G. Edwards (37) was used to calculate the transmission probability (W_p) for the particular orifice arrangement in this experiment. The value obtained for W_p was 4.78×10^{-3} and the Clausing factor of the orifice was determined to be 0.689. The duration of each exposure was measured by an electric timer. The net intensity of the characteristic X-rays of the scandium deposits produced using the electron microprobe technique was determined for each of the 13 targets by subtracting the averaged background counts from the measured scandium counts. Table 5.9 presents the results of this calibration

Table 5.9. Results of scandium calibration of electron microprobe

Target No.	Total[a] Counts	Net Counts	Temp. (K)	Time of Exposure (sec)	Wt. of Sc (μg)
1	9153	8874	1724	3600	24.78
2	2558	2316	1596	6486	6.34
3	4385	4150	1672	3580	11.85
4	12032	11779	1748	3247	32.4
5	2070	1817	1613	3654	4.74
6	8285	8025	1675	6303	21.73
7	3207	2954	1622	5428	8.15
8	3817	3566	1624	6299	9.56
9	12964	12699	1773	2702	37.30
10	5106	4853	1650	6300	14.83
11	9700	9432	1748	2867	28.36
12	1695	1472	1574	3654	3.60
13	6095	5844	1700	3607	18.00

[a]The total scandium counts are the average of six 40-second measurements taken at different positions on the deposit.

experiment. The total scandium counts are the average of six 40-second measurements taken at different positions on the deposit. The standard deviation of the six measurements was generally one percent or less. Figure 5.2 shows the least squares line and the experimental points of the net counts vs. micrograms of scandium. The slope of the line is 343 ± 8 counts/μg and the intercept is 140 ± 170 counts. Thus the amount of scandium on the target can be expressed in terms of the microprobe counts as

$$\mu g\ Sc = \frac{\text{net counts} - 140}{343} \quad . \qquad (5.10)$$

Since scandium deposits were collected at a number of temperatures, the microprobe data can be used to obtain a second-law value for the heat of vaporization of scandium metal. The measured scandium intensity of the deposits is proportional to the vapor pressure of scandium in the Knudsen cell at the particular cell temperature according to the following relation:

$$\text{net counts (Sc)} \propto P_{Sc}\Delta t(44.33A_oW_pM^{1/2}/T^{1/2} \quad . \qquad (5.11)$$

Thus ΔH^o_{298} for vaporization of scandium can be obtained from the slope of the plot of $-R\ \ln(\text{net counts} \cdot T^{1/2}/\Delta t) + \Delta fef$ vs. T^{-1} shown in Figure 5.3. The value obtained for the slope is 88.6 ± 1.0 kcal/mole, which is in satisfactory

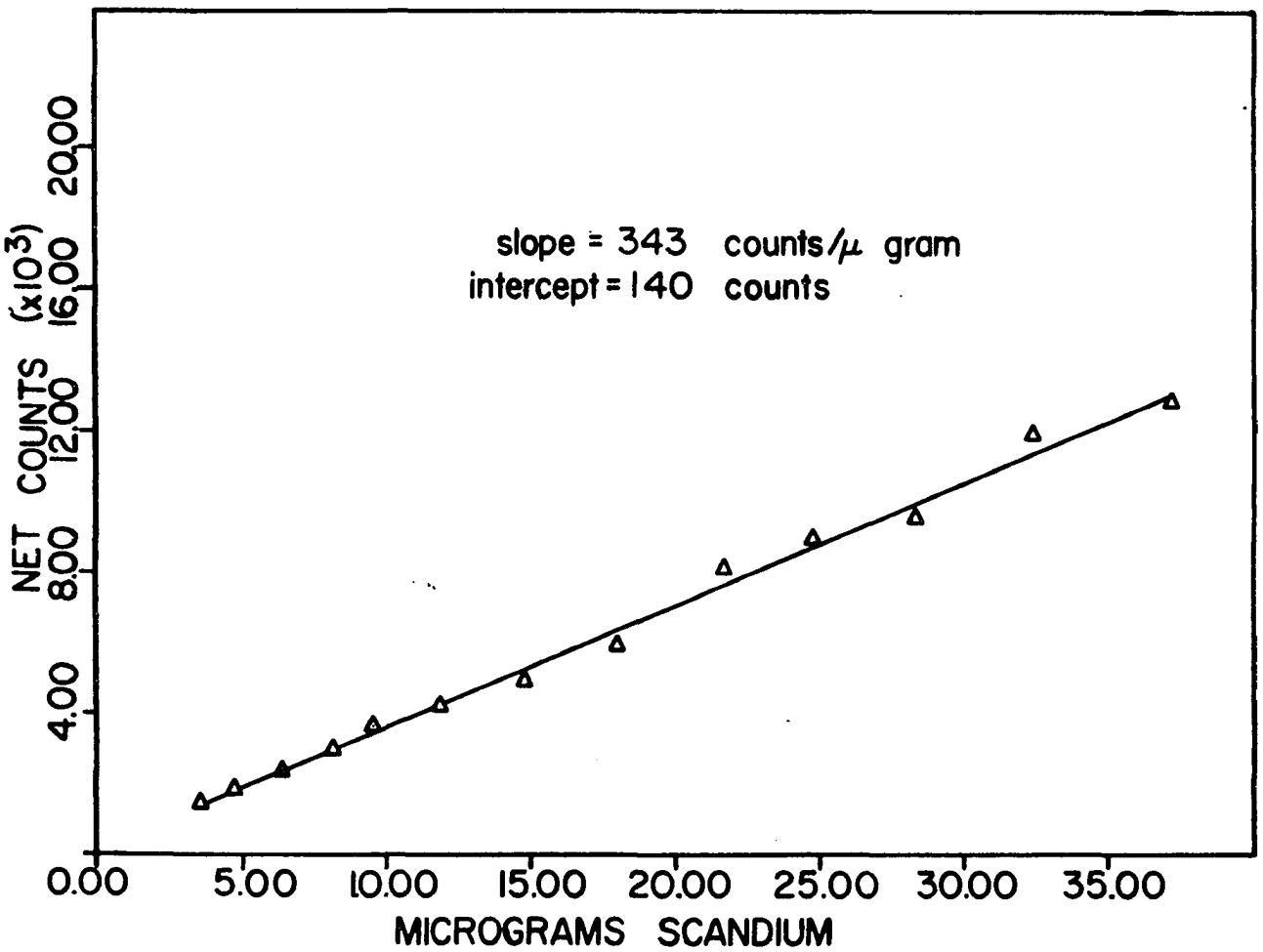

Figure 5.2. Electron microprobe calibration curve for scandium analysis of vapor deposits on aluminum targets

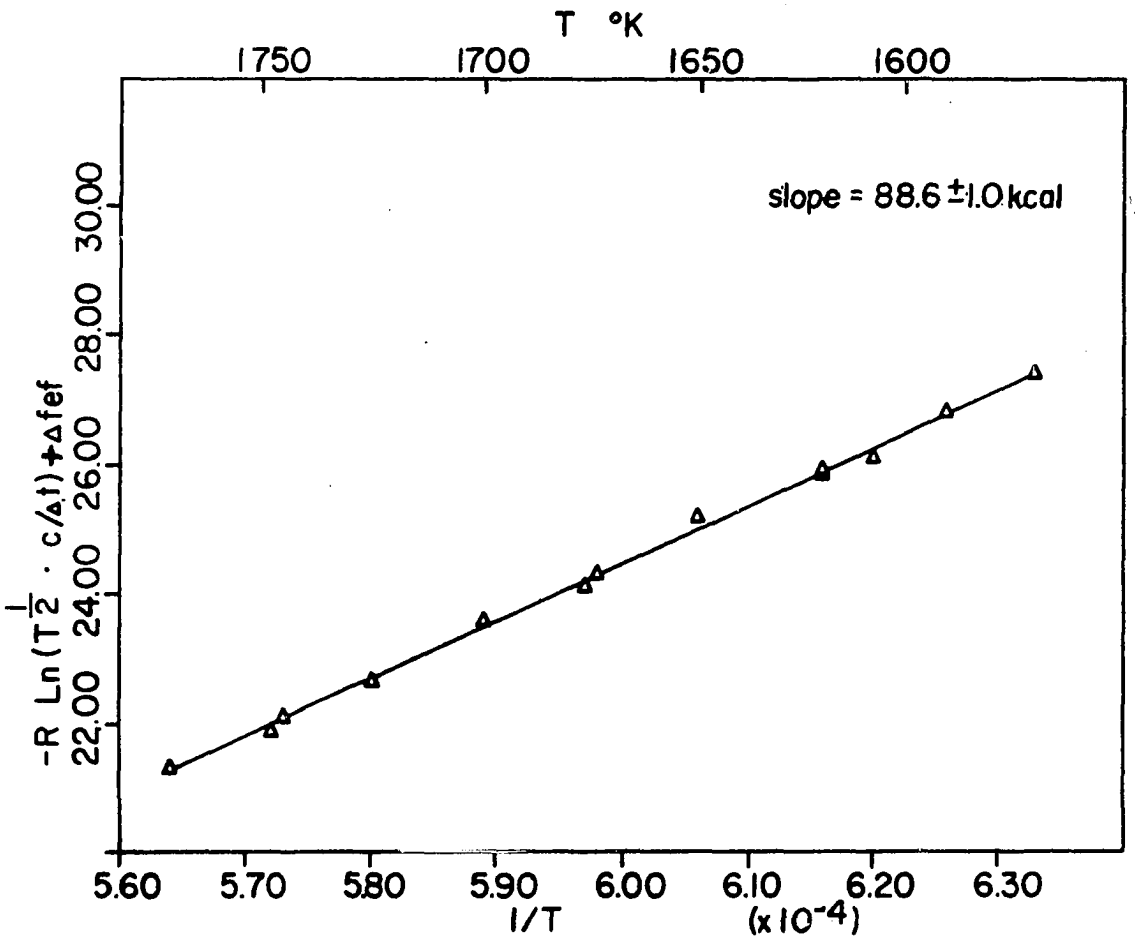

Figure 5.3. Second-law plot for the vaporization of scandium metal using the target collection technique. $P_{Sc} \alpha (T^{1/2} \cdot c/\Delta t)$ where c is the net counts measured by the electron microprobe

agreement with the selected third-law JANAF (26) value of 90.3 ± 1.0 kcal/mole. This analysis indicates that there are no serious systematic errors in the pyrometer calibration, temperature measurement, or microprobe technique of deposited film analysis used in the target collection method of vapor pressure determination.

2. Scandium sulfide target collection experiments

Two target collection experiments on the congruently vaporizing scandium sulfide ($Sc_{.8065}S$) sample ScS-2-91 were performed using the same crucible (RTT-2-172) employed in the scandium vaporization experiment. The distance between the crucible orifice and the target plane was measured and the target collection probability was calculated to be 4.71×10^{-3}. Five targets were collected in the first experiment with the crucible maintained at a constant temperature of 2072 ± 1 K. The targets were exposed for various lengths of time in a range that would produce amounts of condensate having scandium counts in the range of the calibration. The net scandium intensities of the deposits determined by the electron microprobe are plotted against the time of deposition in Figure 5.4. The net scandium counts, as determined by the microprobe, are the averages of four 90-second measurements taken at different positions on the deposits. The slope of the line obtained is 0.330 ± .030 counts/ sec. A

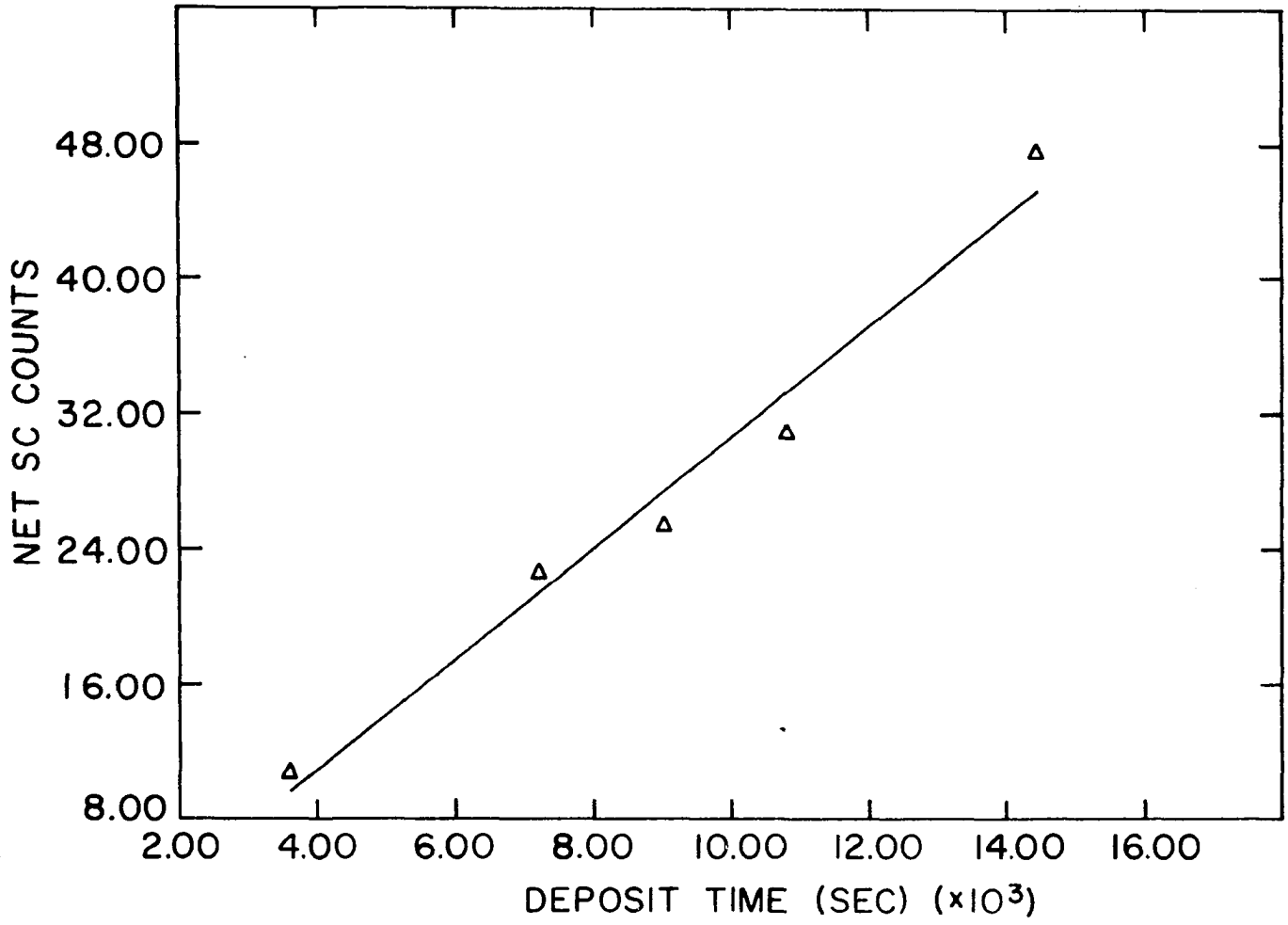

Figure 5.4. Plot of net counts of scandium (as determined by electron microprobe) vs. deposition time, target collection experiment for the vaporization of $Sc_{.8065}S$

10^4-second deposition time results in 3080 scandium counts. The weight of scandium corresponding to this number of counts, obtained from the scandium calibration, Equation 5.10, is 8.57 μg.

The vapor species produced from the vaporization of the congruently vaporizing scandium sulfide cannot be determined from the target collection experiment, therefore neither the partial pressures nor the total vapor pressure can be obtained from these data. However an "effective pressure" (P_E) can be calculated by assuming that the vapor consists entirely of ScS gaseous molecules. The effective pressure can then be calculated by combining the Knudsen equation with Equation 5.10 yielding

$$P_E = \frac{\left[\frac{\text{counts} - 140}{343}\right] \cdot 10^{-6} \cdot T^{1/2}}{\Delta t(44.33\ A_o W_p\ M^{1/2})}\ , \qquad (5.12)$$

where the orifice area A_o and the collection probability W_p have the values 6.22×10^{-3} cm^2 and 4.71×10^{-3} respectively and the molecular weight M is taken to be 77 g/mole (ScS). From the results of the target collection experiment at 2072 K (8.57 μg of scandium collected in 10^4 seconds) an effective pressure of 3.30×10^{-6} atmosphere is obtained.

The purpose of the second target collection experiment

on the congruently vaporizing scandium sulfide was to measure the temperature dependence of the effective pressure. Eighteen targets were collected with deposits from the vapor of the congruently subliming solid in the temperature range 1960 to 2220 K. The temperature was varied in a random order. The amounts of scandium sulfide collected were controlled so that the scandium counts would be in the range of the calibration curve. The results are tabulated in Table 5.10. The data were collected in the order they are listed in the table. The net counts as determined by the microprobe are the average of five 40-second measurements taken at different positions on the deposit. The mass of scandium (in μg) collected on the targets was determined using Equation 5.10. A least squares fit of log P_E vs. T^{-1} was employed in the treatment of the data. The results are shown in Figure 5.5. The least squares linear equation obtained is

$$\log P_E = -(26244 \pm 253)/T + (7.14 \pm .12) \quad , \qquad (5.13)$$

where the errors are standard deviations.

The overall uncertainty introduced into the Knudsen effective pressure was due to combined random and systematic errors in the mass collected (m), the target collection probability (W_p), the time of deposition (t) the temperature measurement (T) and the area of the orifice (A_o). The error

Table 5.10. Results of target collection experiments for $Sc_{.8065}S(s)$

Target No.	Temp. (K)	Deposit Time (sec)	Net Counts	Wt. Loss (μg)	P_E (10^{-6} atm.)
3	2072	10803	2945	8.18	3.02
4	2072	9001	2462	6.77	3.00
6	2120	5251	2606	7.19	5.53
7	2020	16647	2192	5.98	1.42
8	2082	7816	2510	6.91	3.54
9	1960	35017	1997	5.41	0.60
10	2200	2257	3209	8.95	16.30
11	2140	4034	2665	7.94	7.40
12	2000	23070	2141	5.83	0.99
13	2180	2467	2798	7.75	12.90
14	2040	14689	2957	8.21	2.22
15	2220	1742	3045	8.47	20.10
16	1990	27262	2184	5.96	0.86
17	2090	7230	2379	6.53	3.62
18	2160	3242	2495	6.46	8.63
19	1980	30036	1980	5.36	0.70
20	2060	10961	2572	7.09	2.58
21	2170	3035	2876	7.98	10.74
22	2100	6488	2552	7.03	4.36

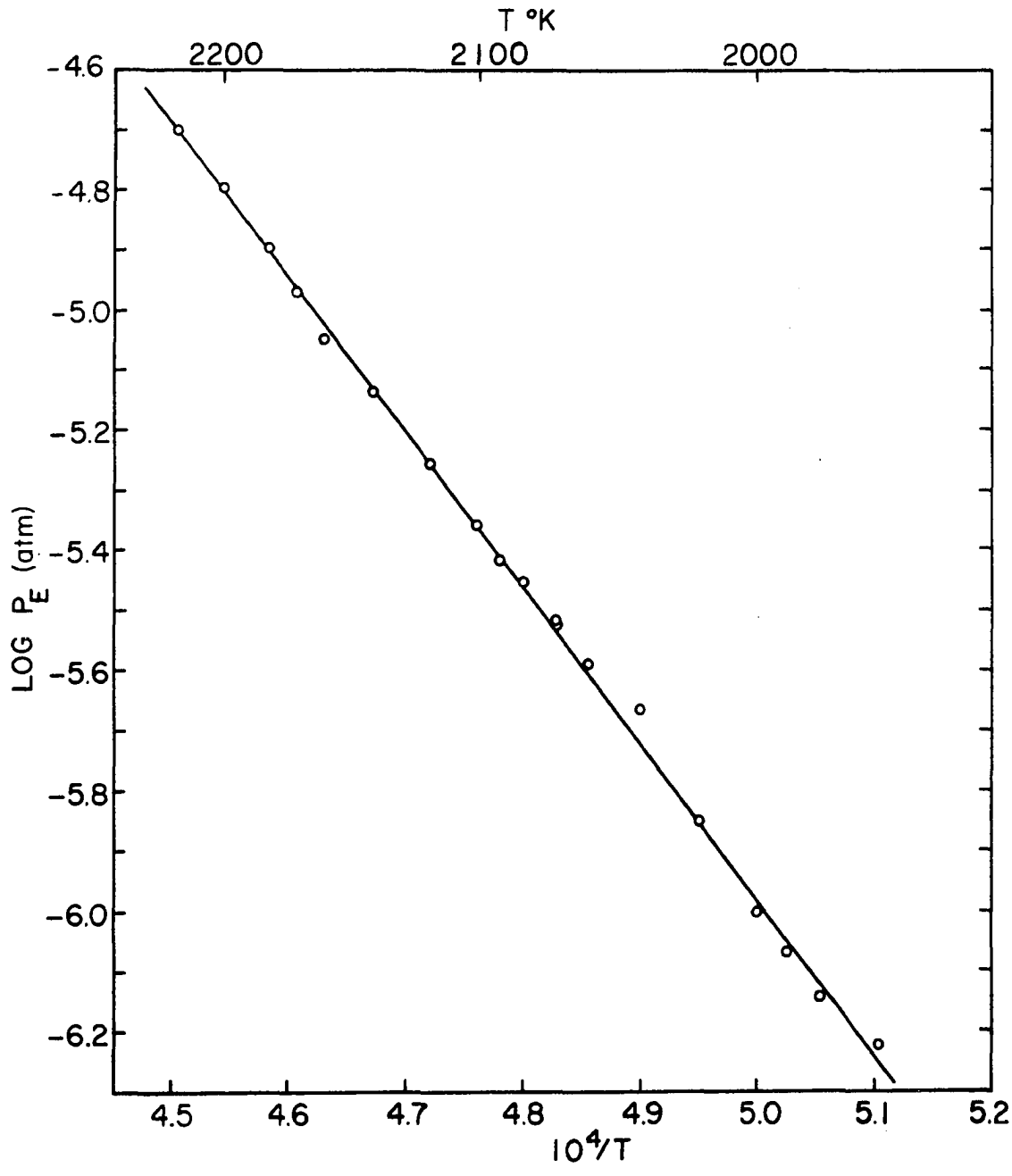

Figure 5.5. Temperature dependence of the effective pressure (P_E) of $Sc_{.8065}S$ determined by target collection experiments

in the mass of scandium collected is estimated to be about ± 6% including errors arising from uncertainties in the electron microprobe calibration curve. The target collection probability error and the error in the orifice area were both estimated to be about ± 2%. The error in the time of exposure was estimated to be less than ± 1% and the error in temperature measurement was ± 0.3%. The resulting error in the effective pressure calculated by the equation

$$(\Delta P_E/P_E)^2 = (\Delta m/m)^2 + (\tfrac{1}{2}\,\Delta T/T)^2 + (\Delta t/t)^2 + (\Delta A/A_o)^2 + (\Delta W_p/W_p)^2 \qquad (5.14)$$

is less than 7%.

E. Mass Spectrometric Data and Results for $Sc_{.8065}S$

1. Determination of vapor species over $Sc_{.8065}S$

The purpose of the first mass spectrometric experiment (MS-1) was to determine the vapor species produced from the vaporization of the congruently subliming scandium sulfide. Shutter closed and shutter open mass scans were obtained on the medium mass range of the spectrometer (masses 10-154) over a temperature range of 1500-1700°C observed. Shutterable ion intensities were observed for mass to charge ratios

of 32, 34, 45, 61, 64, and 77, assumed to arise from the ionization of the species S, H_2S, Sc, ScO, S_2 and SO_2, and ScS respectively. The relative intensities (shutter open minus shutter closed) of these species at about 2000 K using 50 eV ionizing electrons were $I^+(S) > I^+(H_2S) > I^+(Sc) \simeq I^+(ScS) > I^+(S_2) >> I^+(ScO)$. Shutter profiles of the shutterable species observed in this experiment are shown in Figure 5.6. The Sc^+ and ScS^+ ions exhibited very sharp shutter profiles having half-height peak widths of about 1 mm, indicating that they originated from molecular species effusing from the orifice. The S^+ and S_2^+ ions exhibited broad shutter profiles and were not completely shutterable. This observation in addition to the fact the ion peaks for these ions were markedly split especially at the higher temperatures indicates that significant contributions to the ion intensities of S^+ and S_2^+ arose from regions outside of the Knudsen cell. The ion intensity ratio of ScO^+/ScS^+ was found to gradually decrease with time from an initial value of 0.10 down to about 0.02. In order to determine the partial pressures of the ion species from the ion intensities, the electron multiplier gains of the species were determined. The multiplier gain for mass 45 (Sc^+) was measured and found to be 2.8×10^5. The multiplier gain of a reference peak (m/e = 28) was measured immediately before and after the measurement for mass 45 and was found to be 3.5×10^5. The

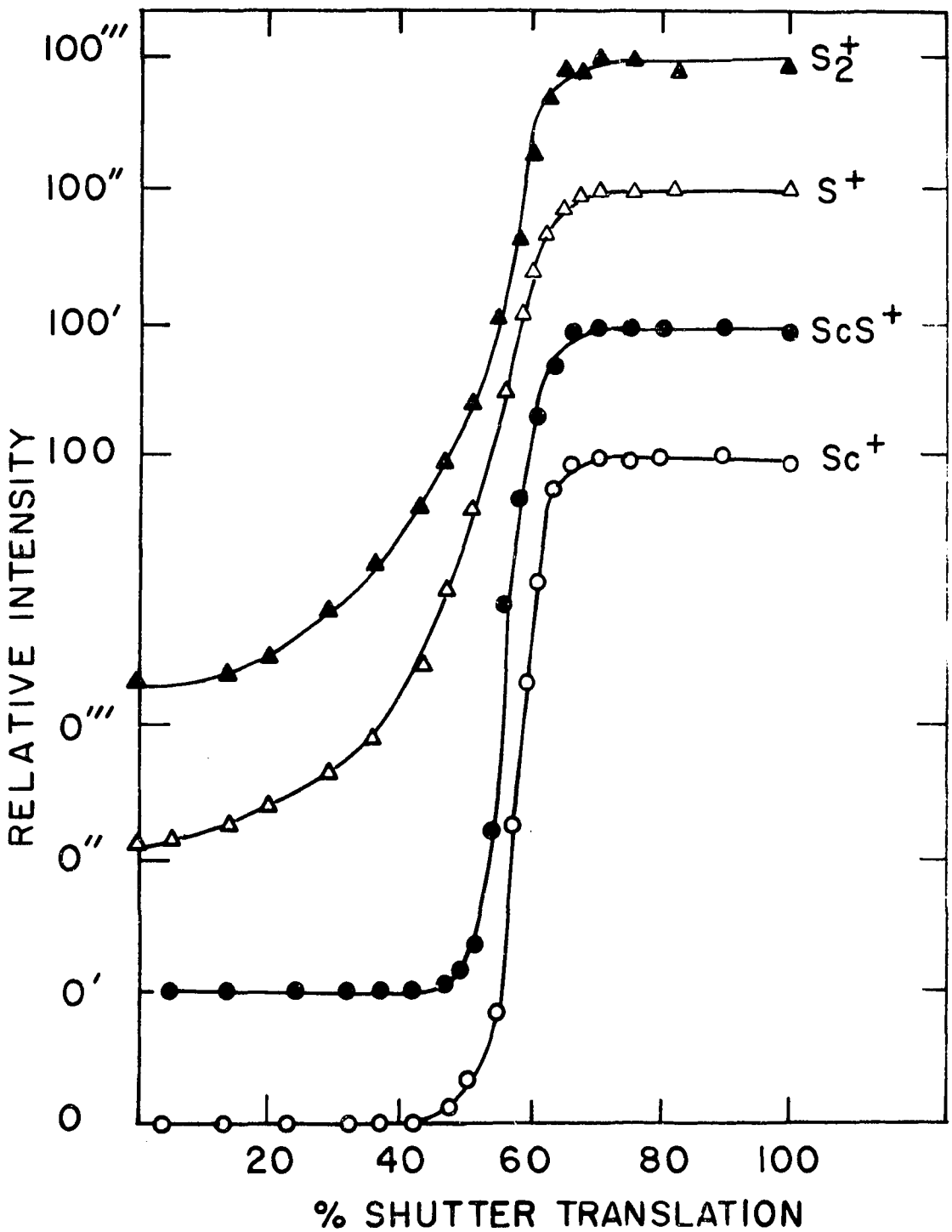

Figure 5.6. Shutter profiles of the shutterable species observed for vaporization of $Sc_{.8065}S$ in experiment MS-1

ratio of gain for mass 28 to that for mass 45 was 1.25. This value is close to the ratio of the reciprocal square roots of their masses as was postulated by Inghram et al. (50) for the variation of multiplier gain with molecular weight. The electron multiplier gain of mass 77 (ScS^+) could not be measured due to lower value of the ion current for this ion on the medium mass range. It was assumed that the reciprocal square root variation between mass and gain would also apply for this ion.

Knowledge of the vapor species present over the congruently vaporizing scandium sulfide enables the vaporization reactions to be written. The two reactions for the vaporization of $Sc_{.8065}S(s)$ are

$$Sc_{0.8065}S(s) = 0.8065\ Sc(g) + S(g) \quad , \qquad (5.14)$$

and

$$Sc_{0.8065}S(s) = 0.8065\ ScS(g) + 0.1935\ S(g) \quad . \qquad (5.15)$$

The dissociation reaction of ScS(g),

$$ScS(g) = Sc(g) + S(g) \quad , \qquad (5.16)$$

is obtained by subtracting Reaction 5.15 from Reaction 5.14. Equilibrium constants and the enthalpy and entropy changes for these reactions can be obtained from measurements of the partial pressures of the observed vapor species as a

function of temperature.

Since reliable partial pressures of S(g) could not be obtained from the ion intensities, the condition for congruent vaporization was used to give values for the partial pressure of S(g) from measured values for the partial pressures of Sc(g) and ScS(g). For congruent vaporization the composition of the solid and the effusing vapor are the same, both having a Sc/S ratio of 0.8065, i.e.

$$0.8065\ n_S = n_{Sc} \quad , \tag{5.17}$$

where n_S and n_{Sc} are the total moles effusing from the cell. Since the major vapor species observed over the congruently vaporizing solid were Sc(g), S(g), and ScS(g), the following relationship between the moles of species can be obtained:

$$0.8065\ n_S = 0.1935\ n_{ScS} + n_{Sc} \quad . \tag{5.18}$$

Using the Knudsen effusion equation the partial pressure of S(g) is given in terms of the partial pressures of the other species as

$$0.8065\ \frac{P_S}{(32)^{1/2}} = 0.1935\ \frac{P_{ScS}}{(77)^{1/2}} + \frac{P_{Sc}}{(45)^{1/2}} \quad . \tag{5.19}$$

2. Pressure calibration of the mass spectrometer

In order to calibrate the mass spectrometer for the evaluation of the partial pressure of each species observed, two silver calibration experiments, MS-2 and MS-3, were performed. In MS-2 4.45 mg of silver were vaporized until completely exhausted at a temperature of 1008°C ± 2°C. The shutter was opened at the beginning of the experiment and remained open during the vaporization. The spectrometer scanned over masses 105-110 at a frequency of about 5 sec/amu using 50 eV ionizing electrons and 2 mA emission current. The resolution was set at the potentiometer value of 6.06 and the extractor, focus and ion energy voltages were 30 volts, 45 volts, and 30 volts respectively. The ion intensity of mass 107 (Ag^+) was measured as a function of time. The ion intensity dropped rapidly to zero upon exhaustion of the silver (5.75 hours). The electron multiplier gain of mass 28 was measured immediately before and after vaporization and was found to be 4.6×10^5 and 4.4×10^5 respectively. The ratio of the multiplier gain of mass 107 to that of mass 28 was determined in experiment MS-4 to be 0.25, thus the gain of the measured silver ion changed from 1.15×10^5 to 1.10×10^5 during the experiment. The function $I^+(^{107}Ag^+)T^{1/2}/\gamma(Ag^+)$ was calculated and is plotted as a function of time in Figure 5.7. The area under this curve was determined to be 2.11×10^{-6} A $K^{1/2}$ sec.

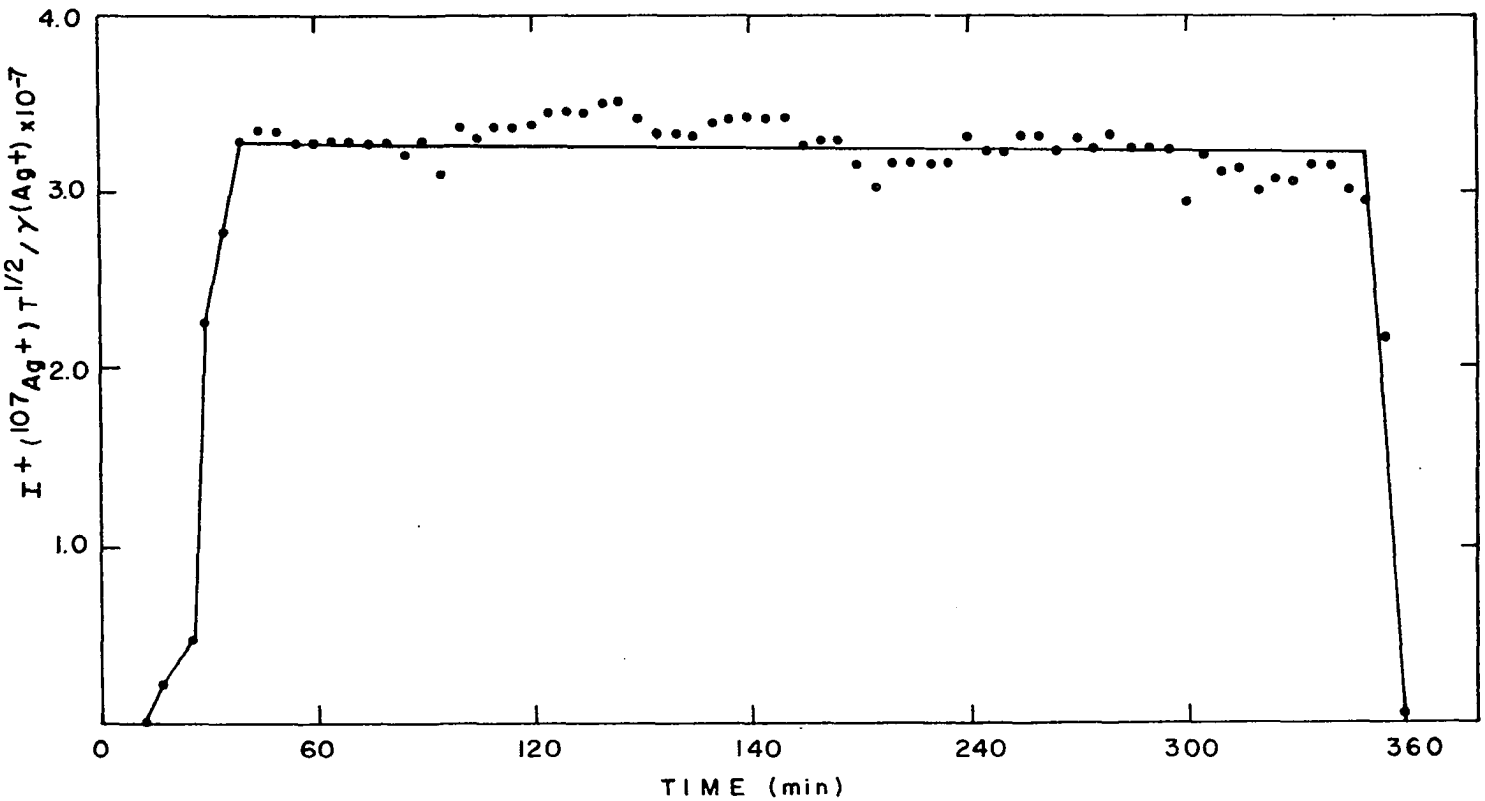

Figure 5.7. Mass spectrometer calibration experiment MS-2, total exhaustion of 4.45 mg of silver at a constant temperature of 1008 ± 2°C. Area under curve is 2.11×10^{-6} $AK^{1/2}$ sec

Substituting this integrated area, along with the experimental parameters $A_o = 8.2516 \times 10^{-3}$ cm^2, W = .6490, M = 107 g/mole, $\Delta g = 4.45 \times 10^{-3}$g, $n(^{107}Ag^+) = .5182$, and $\sigma(Ag^+) = 5.6 \times 10^{-16}$ cm^2 into Equation 4.10, the value of 9.94×10^{-13} atm cm^2/A K is obtained for the machine constant C_m.

Since the machine constant is dependent on the alignment of the crucible and the distance between the crucible and the ion source, experiment MS-3 was performed in order to check the reproducibility. After disassembling the Knudsen cell support, 2.99 mg of silver were placed in the crucible and the cell assembly was realigned. The silver was vaporized at a temperature of 1003 $\pm$ 2°C for 5.67 hr after which time the sample was completely exhausted. The ion intensity of mass 107 (Ag^+) was measured using the same values of the spectrometer parameters as were used in MS-2. The electron multiplier gain for mass 28 was measured before and after vaporization from which the gain for mass 107 was calculated to be 1.32×10^5 at the beginning of the vaporization and 1.16×10^5 at the end. The value obtained for the integral

$$\int_{t_1}^{t_2} I^+(^{107}Ag^+)T^{1/2}/\gamma(Ag^+)dt$$

was 9.1×10^{-7} A $K^{1/2}$ sec which yielded a machine constant

of 10.06×10^{-13} atm cm^2/A K. This is in good agreement with the value obtained from MS-2 and the average value of 1.00×10^{-12} atm cm^2/A K was used for the determination of the vapor pressures of the ion species. Using this machine constant value, the vapor pressure of silver can be calculated from the ion intensities and temperature obtained in experiments MS-2 and MS-3 using the equation

$$P_{Ag} = C_m I^+(Ag)T/\sigma(Ag)\gamma(Ag)n(^{107}Ag) \quad . \qquad (5.20)$$

The pressures obtained were 6.9×10^{-6} atm at 1298 K and 5.8×10^{-6} atm at 1293 K. The vapor pressures of silver in equilibrium with molten silver reported by Hultgren et al. (51) are 1.19×10^{-5} and 1.08×10^{-5} atm at the temperature 1298 K and 1293 K respectively. The calculated pressures of silver are thus less than equilibrium pressures reported in the literature by a factor of 1.7 to 1.9. Since the quantities of silver used were very small (~3 mg) the surface area of the silver was relatively small. This may result in an undersaturation inside the Knudsen cell which would yield a reduced ion intensity and longer exhaustion time than would be expected from the reported vapor pressures. The value of the mass spectrometer constant obtained by the total exhaustion technique is thought to be accurate. The uncertainty in the calibration constant arose mainly from uncertainties in the following: the weight of

silver used (± 2%), the temperature measurement (± 0.3%), the ion intensity measurement (± 3%), the area of the orifice (± 2%), the Clausing factor (± 2%), the multiplier gain (± 5%), and the time required for silver exhaustion (< ± 0.1%). The error in the calibration constant, using the propagation of errors method,

$$(\Delta C/C)^2 = (\Delta m/m)^2 + (\tfrac{1}{2}\Delta T/T)^2 + (\Delta I/I)^2 + (\Delta A_o/A_o)^2 + (\Delta W/W)^2 + (\Delta\gamma/\gamma)^2 + (\Delta t/t)^2 \quad , \qquad (5.21)$$

is about 7%.

3. Measurement of partial pressures over $Sc_{.8065}S$

The purposes of experiments MS-5, MS-6, and MS-7 were to measure the ion intensities of the vapor species over the congruently vaporizing scandium sulfide and determine the partial pressures of these species as functions of temperature. The same crucible that was used for the silver calibration experiment was employed for the scandium sulfide vaporizations. The sulfide sample (ScS-2-91) used in these experiments was characterized as congruently vaporizing.

a. MS-5 In experiment MS-5 an 80 mg sample of ScS-2-91 was loaded into the crucible. The crucible alignment and position were made as close as possible to those in the silver vaporization experiment. Ion intensities were

obtained using 50 eV ionizing electrons and 2 mA emission current. Extractor, focus and ion energy voltages were the same as those used in the silver calibration experiments. The resolution also remained unchanged. Ion intensities (shutter open minus shutter closed) were obtained on the medium range of the mass spectrometer for Sc^+ and ScS^+ over a temperature range of 1957-2197 K. Figure 5.8 shows typical mass spectra obtained for these ions. The scan rate was about 5 sec/amu. The ion intensities of masses 32 (S^+) and 64 (S_2^+) were not measured due to the anomalous shutterability for these ions described in MS-1. Shutterable ion intensities for mass 61 (ScO^+) were only detected at the highest temperatures in the range. ScO^+ intensities were about 2% of the ScS^+ intensities. A total of 28 data were collected at various temperatures for ScS^+ and 27 data were similarly obtained for Sc^+. The temperature was varied randomly during data collection. The electron multiplier gain of the reference ion (m/e = 28) was measured periodically during the run in order that the partial pressures of the ion species could be calculated from the ion intensities. It was found that the multiplier gain of the reference ion decreased with time during the experiment. The ion intensities of ScS^+ and Sc^+ were multiplied by a relative gain, the ratio of the gain at the beginning of the experiment to that obtained at various times during the

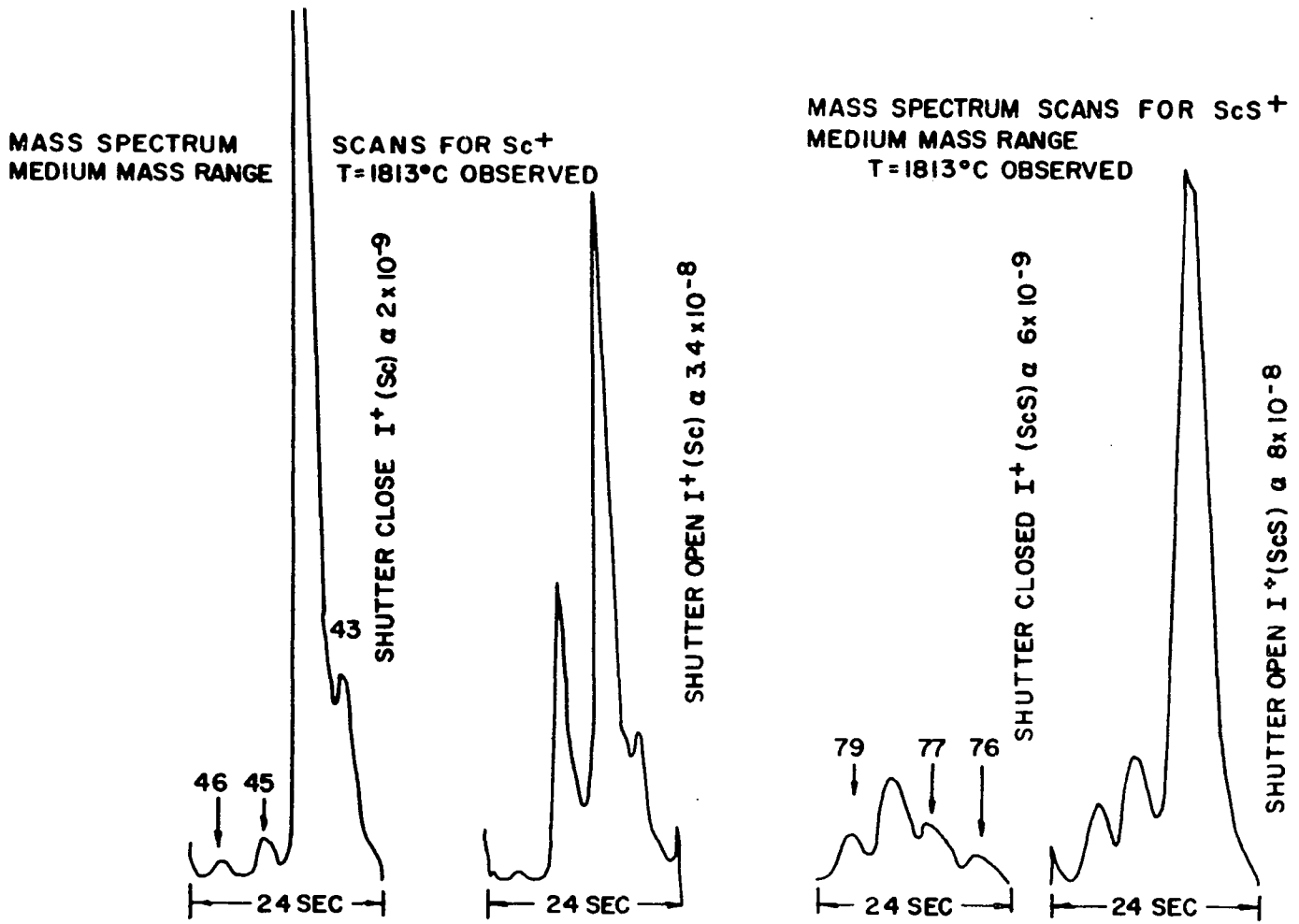

Figure 5.8. Typical mass spectra for ScS^+ (77) and Sc^+ (45) obtained on medium mass range of the quadrupole mass spectrometer in experiments MS-5, MS-6, and MS-7

run. The partial pressures of the two species were calculated from Equation 4.8 using the value of the machine constant determined by silver vaporization (1.00×10^{-12} atm cm^2/A K) and other data given in Table 5.11. The plots of log P vs. 1/T for the gaseous species Sc and ScS along with their least squares lines are shown in Figure 5.9. The equations of the least squares lines obtained are

$$\log P_{Sc}(atm) = -(12000 \pm 800)/T - (.41 \pm .30) \quad (5.22)$$

and

$$\log P_{ScS}(atm) = -(25280 \pm 270)/T + (6.03 \pm .14) \quad (5.23)$$

The uncertainties given are standard deviations.

Table 5.11. Auxiliary data used in the pressure calculation of Sc and ScS in the experiment MS-5

Species	Isotopic Abundance (n_i)	Ionization[a] Cross Section ($10^{-16} cm^2$)	Electron Multiplier[b] Gain (γ_i) (10^5)
Sc(45)	1.00	6.56	2.37
ScS(77)	.95	10.66	1.81

[a]Ionization cross section from Mann's (39) calculation for Sc^+, ScS^+ ionization cross section is sum of that for Sc^+ and S^+.

[b]Electron multiplier gain at the beginning of the experiment determined from gain of mass 28.

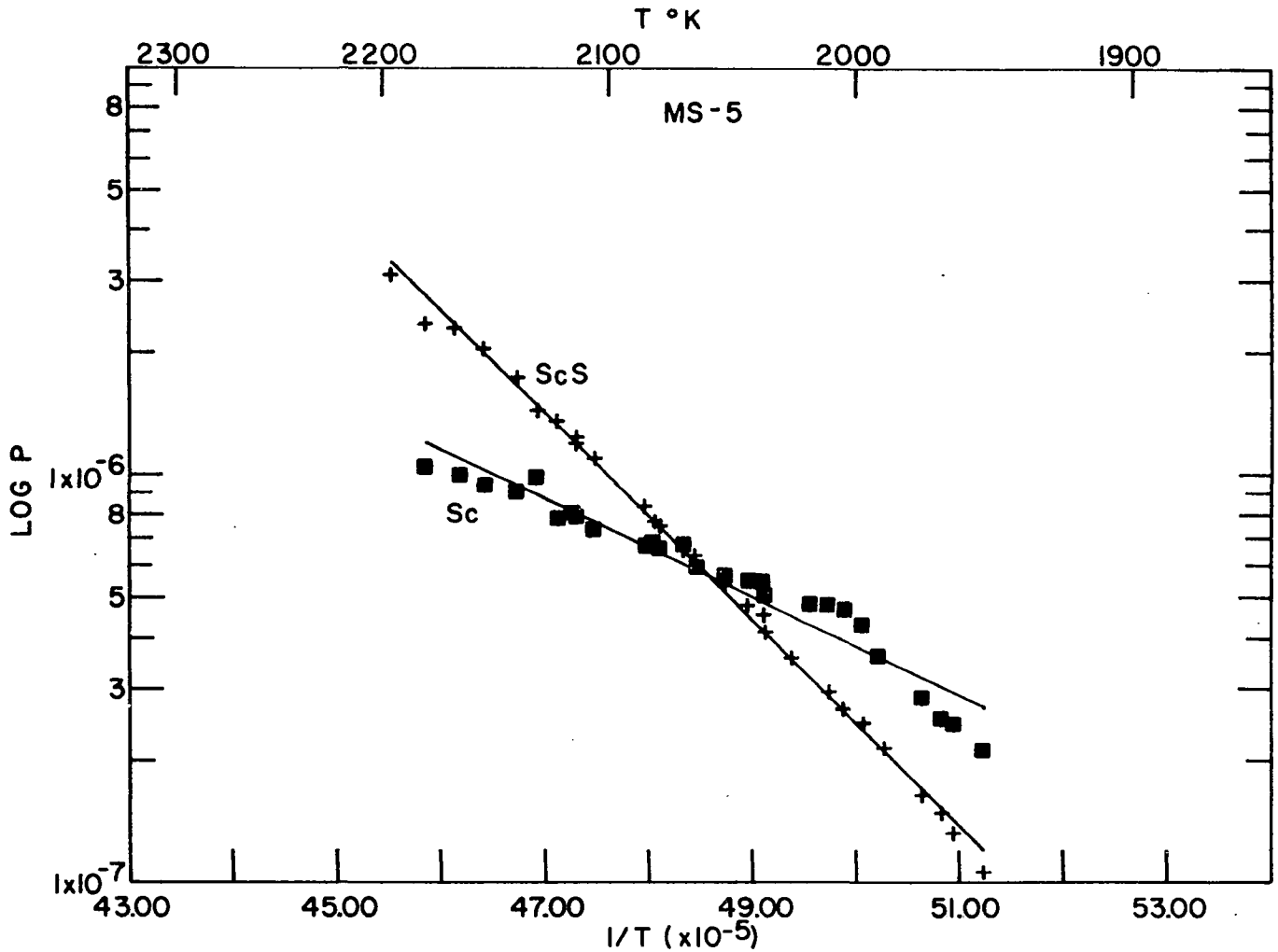

Figure 5.9. Plot of the logarithm of the partial pressures of Sc(g) and ScS(g) over $Sc_{.8065}S(s)$ vs. reciprocal temperature (results of experiment MS-5)

The thermodynamic properties associated with the vaporization reactions of $Sc_{.8065}S(s)$ (reactions 5.14 and 5.15) and the dissociation reaction of ScS(g) (5.16) can be determined from the partial pressures by the second- and third-law treatment of the data. The second-law results were obtained by plotting the logarithm of the equilibrium constant for each vaporization reaction against T^{-1}. It is seen from Equation 4.14 that the slopes and the intercept of the straight line obtained are related to the enthalpy and entropy changes respectively at the midpoint of the experimental temperature range for the corresponding reactions. Since the partial pressure of sulfur over the congruently vaporizing solid was not measured, the congruence Equation 5.19, relating the sulfur partial pressure to the scandium and scandium sulfide partial pressures was used to calculate the sulfur partial pressure and hence the equilibrium constants for the reactions at each of the 27 temperatures obtained in the experiment. The second-law results for the vaporization reactions of $Sc_{0.8065}S(s)$ are given in Table 5.12. The enthalpy changes for the reactions at the reference temperature 298 K were obtained using the $H^{o}_{T}-H^{o}_{298}$ values (estimation Method 2) for the solid, literature values of $H^{o}_{T}-H^{o}_{298}$ for Sc(g) and S(g) and the calculated enthalpy function for ScS(g). The enthalpy change associated with the dissociation of one mole of ScS(g) was

Table 5.12. Second- and third-law results of $Sc_{.8065}S(s)$ vaporization experiment MS-5

Reaction[a]	Midpoint Temp. (K)	ΔH_T^o (II) (kcal)	ΔH_{298}^o(II) (kcal)	ΔH_{298}^o(III) (kcal)
1	2060	109.0 ± 4.6	115.4 ± 4.6	223.5 ± 4.9
2	2060	106.3 ± 1.4	114.4 ± 1.4	133.9 ± 4.5
3	2060	3.3 ± 6	1.2 ± 6	111.0 ± 4.4

[a] 1 $Sc_{.8065}S(s) = .8065\ Sc(g) + S(g)$
2 $Sc_{.8065}S(s) = .8065\ ScS(g) + .1935\ S(g)$
3 $ScS(g) = Sc(g) + S(g)$.

obtained by multiplying the difference between the ΔH values for reactions 5.15 and 5.14 by 1.24.

The third-law method was employed to calculate the enthalpy changes for the vaporization reactions of $Sc_{.8065}S(s)$ at 298 K. The equilibrium constants for the reactions were obtained at each experimental temperature by using the silver calibration constant to obtain the partial pressures of the gaseous species. Thus, using the estimated changes in the free energy functions at each temperature for the corresponding reactions, a value of ΔH_{298}^o was obtained at that temperature using Equation 4.16. The free energy functions for Sc(g) and S(g) were obtained from the

JANAF (26) tabulation. The free energy function of ScS(g) was calculated as previously described and the free energy function of $Sc_{.8065}S(s)$ was estimated as described in Section C of this chapter. Table 5.13 shows the free energy functions of ScS(g), Sc(g), S(g) and $Sc_{.8065}S(s)$ at various temperatures. Values for the functions at intermediate temperatures were obtained by a linear interpolation technique. The third-law results at 298 K are tabulated in the last column of Table 5.12.

During experiment MS-5, it was observed that the ion intensity of masses 42-46 decreased rapidly at the higher crucible temperatures upon opening the molecular beam shutter. It was thought that this was due to the relatively high ion currents of the species CO^+ (44) and Sc^+ (45) causing a deterioration of the electron multiplier gain. Since the multiplier gain was measured only a few times during this run the ion intensity could not be accurately corrected for the change in gain. Thus the results obtained for the Sc second-law slope are grossly in error. The ion intensity of masses 76-79 remained quite constant with time upon opening the shutter. The ScS^+ ion intensities and the ScS second-law slope are thus assumed to be reliable.

Table 5.13. Free energy functions, $-(G_T^o-H_{298}^o)/T$ (cal/mole K)

Temp. K	ScS(g)	Sc(g)	S(g)	$Sc_{.8065}S(s)$
1700	64.52	46.41	45.02	22.69
1800	64.95	46.65	45.26	23.27
1900	64.35	46.88	45.90	23.85
2000	65.74	47.09	45.72	24.42
2100	66.12	47.30	45.94	24.92
2200	66.47	47.51	46.15	25.47
2300	66.84	47.70	46.35	26.06

b. MS-6 In experiment MS-6 the ion intensities were measured as a function of temperature making an effort to measure the multiplier gain immediately before and after each shutter-open mass scan. Another quantity (131 mg) of sample ScS-2-91 was used in this experiment. Thirty-six ion intensity data were collected on each species, Sc^+ and ScS^+, in the temperature range 1915-2197 K using 50 eV ionizing electrons, 2 mA emission current and the same focus, extractor and ion energy voltages used in MS-5. A scan rate of 5 sec/amu was used to scan masses 42-46 and 76-79 on the medium mass range to obtain the Sc^+ and ScS^+ ion intensities respectively. The electron multiplier gains

at the beginning of the experiment were 2.02×10^5 for Sc^+ and 1.54×10^5 for ScS^+. The shutter open ion intensities for Sc^+ were corrected by multiplying by the ratio of the initial multiplier gain to the gain measured after each shutter open scan. The partial pressures of Sc(g) and ScS(g) were obtained from Equation 4.8 using the machine constant value of 1.00×10^{-12} atm cm^2/A K. Figure 5.10 shows the plots of log P vs. T^{-1} for the two species. The equations of the least squares lines obtained are

$$\log P_{Sc}(atm) = -(18636 \pm 372)/T + (2.96 \pm .18) , \quad (5.24)$$

and

$$\log P_{ScS}(atm) = -(25219 \pm 304)/T + (6.05 \pm .15) . \quad (5.25)$$

The uncertainties given are standard deviations.

The second-law results for experiment MS-6 were obtained from a plot of the logarithm of the equilibrium constant for each of the vaporization reactions of $Sc_{.8065}S(s)$, 5.14 and 5.15, versus T^{-1}. The results for the dissociation of ScS(g), reaction 5.16, were obtained from the values for the vaporization reactions as previously described. Table 5.14 gives the second-law results for the reactions 5.14, 5.15 and 5.16. The third-law results were obtained using the free energy functions given

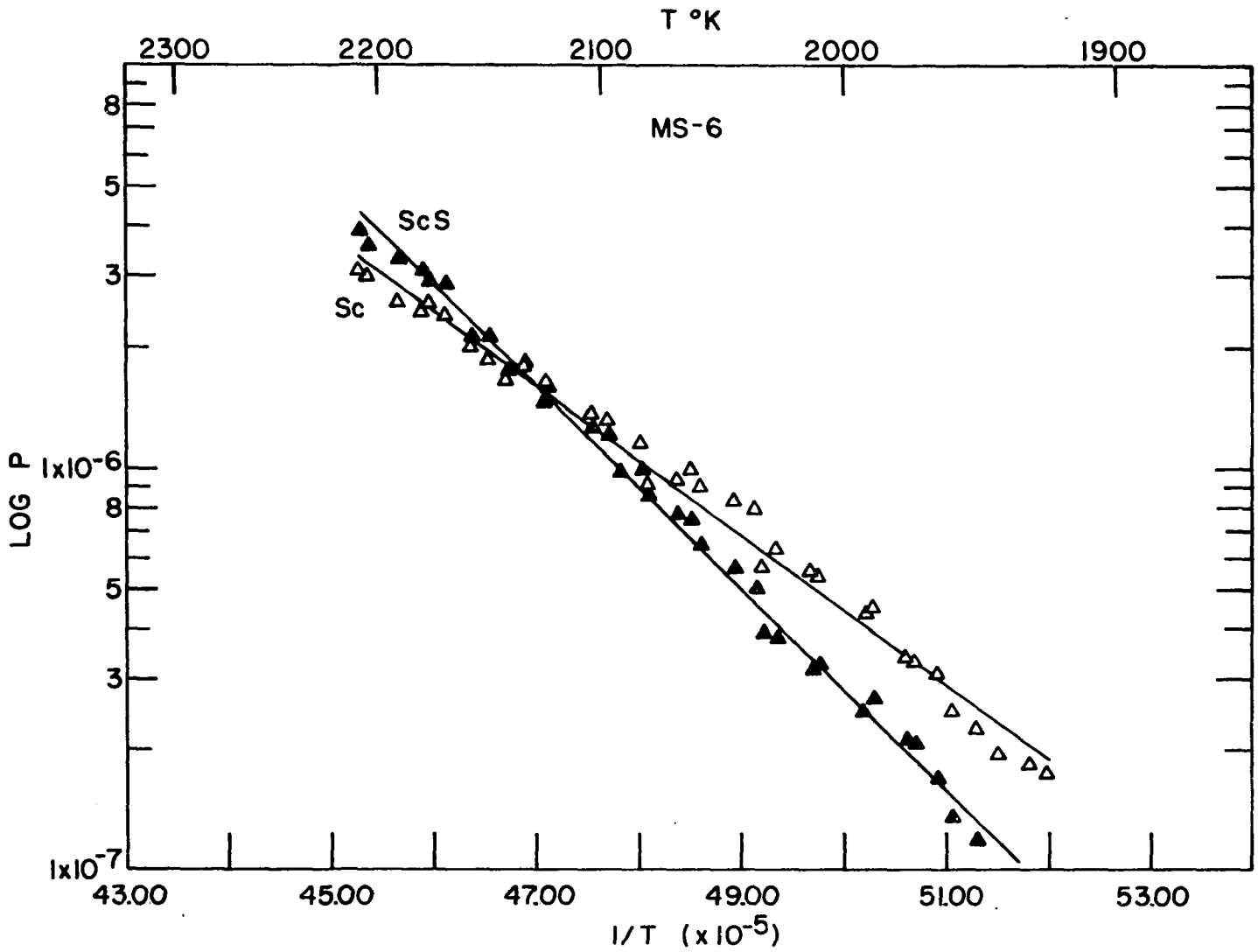

Figure 5.10. Plot of the logarithm of the partial pressures of Sc(g) and ScS(g) over $Sc_{.8065}S(s)$ vs. T^{-1} (results of experiment MS-6)

Table 5.14. Second- and third-law results of $Sc_{.8065}S(s)$ vaporization experiment MS-6

Reaction[a]	Midpoint Temp. (K)	ΔH_T^o (II) (kcal)	ΔH_{298}^o(II) (kcal)	ΔH_{298}^o(III) (kcal)
1	2057	157.4 ± 3.0	163.8 ± 4	224.1 ± 4.9
2	2057	110.2 ± 1.4	118.3 ± 1.4	134.1 ± 4.5
3	2057	58.5 ± 4	57.7 ± 4	111.6 ± 4.4

[a] 1 $Sc_{.8065}S(s) = .8065Sc(g) + S(g)$
2 $Sc_{.8065}S(s) = .8065\ ScS(g) + .1935\ S(g)$
3 $ScS(g) = Sc(g) + S(g)$.

in Table 5.13 and the experimentally determined equilibrium constants for the reactions. The third-law values for ΔH_{298}^o are shown in the last column of Table 5.14.

It was evident in MS-6 that the ion intensity of masses 42-46 and thus the electron multiplier gain for these ions decreased more rapidly than could be measured when the shutter was opened. The value obtained in this experiment for the second-law Sc^+ slope and thus the second-law heats for reactions 5.14, 5.15 and 5.16 are not considered to be reliable. Since the extent of multiplier deterioration is dependent upon crucible temperature (as are $I_{CO_2^+}$ due to outgassing and, of course, I_{Sc^+}), with

greater deterioration at the higher temperatures and very little at the lower temperature, the ion intensities and thus the partial pressures at the lower temperatures in the range are thought to be reliable. Third-law results at the lower temperatures can be considered reliable.

c. MS-7 The scandium sulfide residue from experiment MS-6 was used for experiment MS-7. In this run 36 ion intensity data for ScS^+ and 34 data for Sc^+ were collected in the temperature range 1929-2220 K using 2 mA emission current, 50 eV ionizing electrons and the same values of the focus, extractor and ion energy used in the previous runs. In order to try to reduce the electron multiplier deterioration, mass 44 (CO_2^+) was not in the mass range scanned to obtain the Sc^+ ion intensity. A scan rate of 4 sec/amu was used to scan masses 45-49 and 76-79 on the medium mass range. The electron multiplier gains at the beginning of the experiment were 1.15×10^5 for Sc^+ and 0.87×10^5 for ScS^+. The shutter speed was increased by a factor of two to permit faster collection of intensity data and electron multiplier gains. The electron multiplier gain was measured before the shutter was opened and immediately after it was closed for each ion intensity obtained. The measured ion intensities were corrected for change in multiplier gain. The machine constant value of 1.00×10^{-12} atm cm^2/A K was used in Equation 4.8 to obtain

the partial pressures of Sc(g) and ScS(g). The plots of log P vs. T^{-1} for these two species are shown in Figure 5.11. The least squares lines obtained are

$$\log P_{Sc}(atm) = -(22924 \pm 192)/T + (5.10 \pm .10) , \quad (5.26)$$

and

$$\log P_{ScS}(atm) = -(25655 \pm 165)/T + (6.34 \pm .08) . \quad (5.27)$$

The uncertainties given are standard deviations.

The second-law results for experiment MS-7 were obtained from the slope of the logarithm of the equilibrium constant for each vaporization reaction vs. T^{-1}. Table 5.15 tabulates the second-law results for experiment MS-7. The third-law results were obtained using the free energy functions for the gaseous species and solid $Sc_{.8065}S(s)$ given in Table 5.13 and equilibrium constants at each experimental temperature. The last column of Table 5.15 gives the third-law values obtained for ΔH^{o}_{298} for the specified reactions. Although the agreement between the second- and third-law results is better for experiment MS-7 than for the previous experiments, MS-5 and MS-6, the second-law results are still thought to be in error due to the electron multiplier gain deterioration during the experiment. The third-law results at the lower temperatures are considered to be reliable.

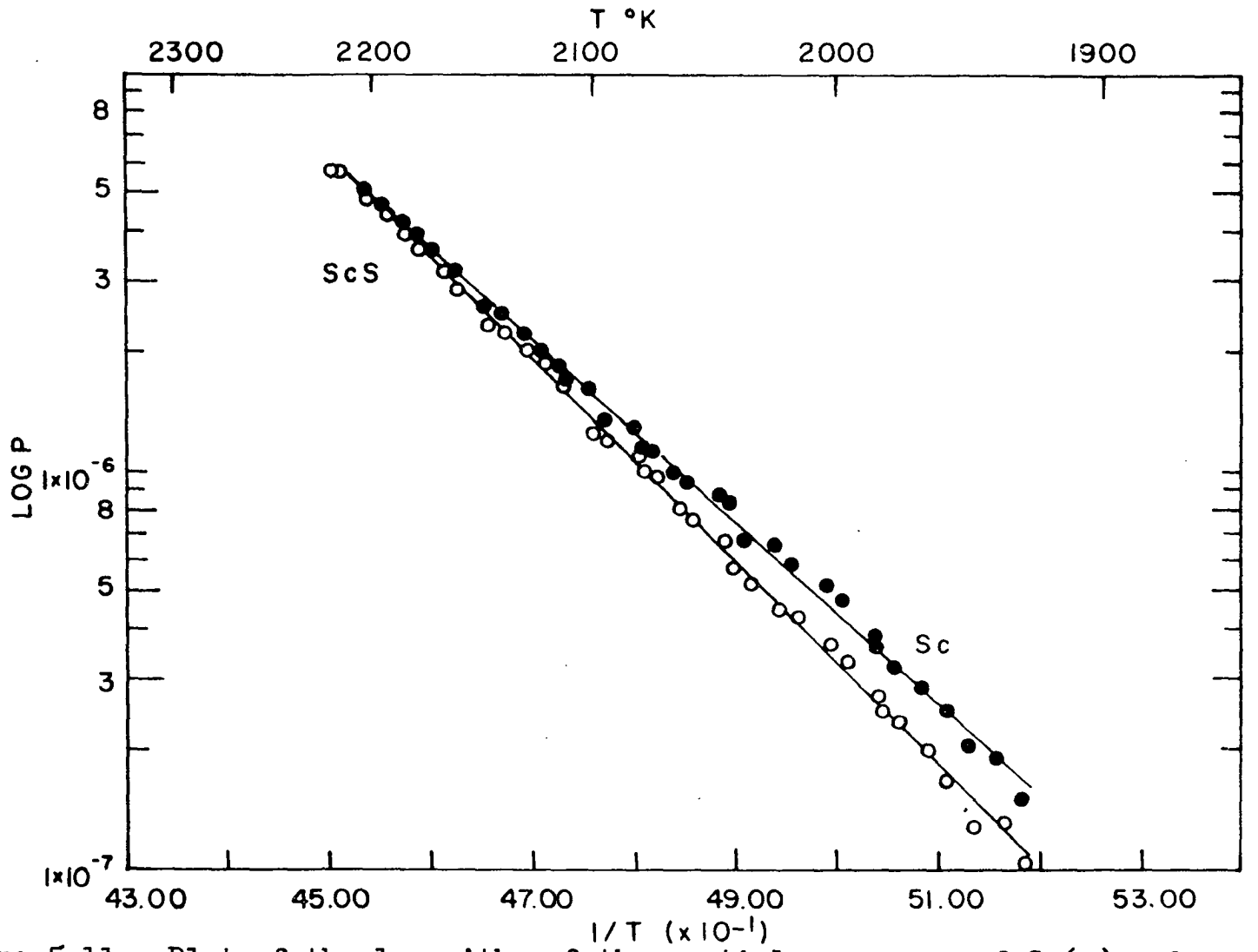

Figure 5.11. Plot of the logarithm of the partial pressures of Sc(g) and ScS(g) over $Sc_{.8065}S(s)$ vs. T^{-1} (results of experiment MS-7)

Table 5.15. Second- and third-law results of $Sc_{.8065}S(s)$ vaporization experiment MS-7

Reaction[a]	Midpoint Temp. (K)	ΔH^o_T (II) (kcal)	ΔH^o_{298}(II) (kcal)	ΔH^o_{298}(III) (kcal)
1	2065	191.1 ± 1.6	197.5 ± 2.0	222.3 ± 4.9
2	2060	115.6 ± .8	123.7 ± 1.5	133.0 ± 4.5
3	2060	93.6 ± 1.8	91.5 ± 2	110.7 ± 4.4

[a] 1 $Sc_{.8065}S(s) = .8065\ Sc(g) + S(g)$
2 $Sc_{.8065}S(s) = .8065\ ScS(g) + .1935\ S(g)$
3 $ScS(g) = Sc(g) + S(g)$.

d. MS-11 The second-law slopes obtained for ScS^+ in the three experiments MS-5, MS-6, and MS-7 are in good agreement but those obtained for Sc^+ are not, presumably due to multiplier deterioration when measuring this ion intensity. Experiment MS-11 was performed on the residue of experiment MS-10. In this experiment ion intensity data were collected for Sc^+ on the low mass range of the spectrometer. Twenty-seven data were collected in the temperature range 1939-2173 K using 50 eV ionizing electrons, 2 mA emission current and focus, extractor, and ion energy values of 30 V, 45 V and 30 V respectively. Figure 5.12 shows a spectrum obtained for Sc^+ with shutter open and closed on

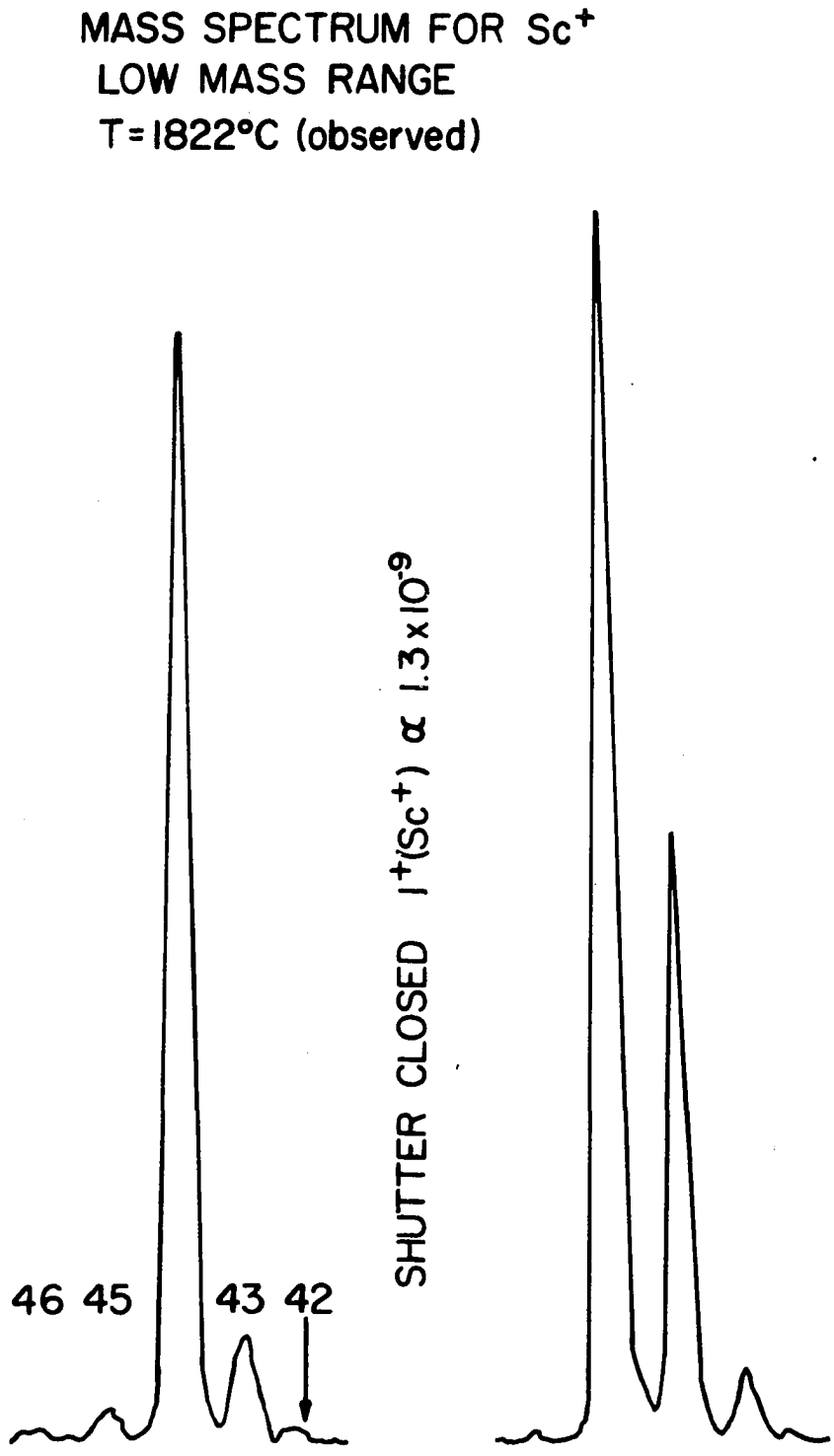

Figure 5.12. Typical mass spectra for Sc^+ (45) obtained on low range of the quadrupole mass spectrometer in experiment MS-11

the low mass range (masses 42-47). The scan rate used was about 5 sec/amu. The resolution between masses 44 and 45 on the low mass range was much better than that obtained on the medium mass range. The ion intensities remained relatively constant for several scans after opening the shutter even at the higher temperatures in the range. The electron multiplier gain for mass 45 was not measured in this experiment but was assumed to be constant during the run. Since the multiplier gain was not measured and the machine constant for the low range of the mass spectrometer was not known, the partial pressure of Sc(g) could not be obtained from the ion intensities. A plot of the logarithm of the ion intensity times the temperature vs. T^{-1} is shown in Figure 5.13. The least squares value obtained for $R\,\partial \ln I_{Sc^+}T/\partial T^{-1}$ is -111.7± 1.0 kcal/mole. Second-law enthalpy changes for reactions 5.14, 5.15, and 5.16 at the temperature T (midpoint of the run) were obtained from the following equations respectively:

$$\Delta H_T^o(5.14) = -0.8065\ R\,\partial \ln I_{Sc^+}T/\partial T^{-1} - R\,\partial \ln I_{S^+}T/\partial T^{-1} \qquad (5.28)$$

$$\Delta H_T^o(5.15) = -0.8065\ R\,\partial \ln I_{ScS^+}T/\partial T^{-1} - 0.1935\ R\,\partial \ln I_{S^+}T/\partial T^{-1} \qquad (5.29)$$

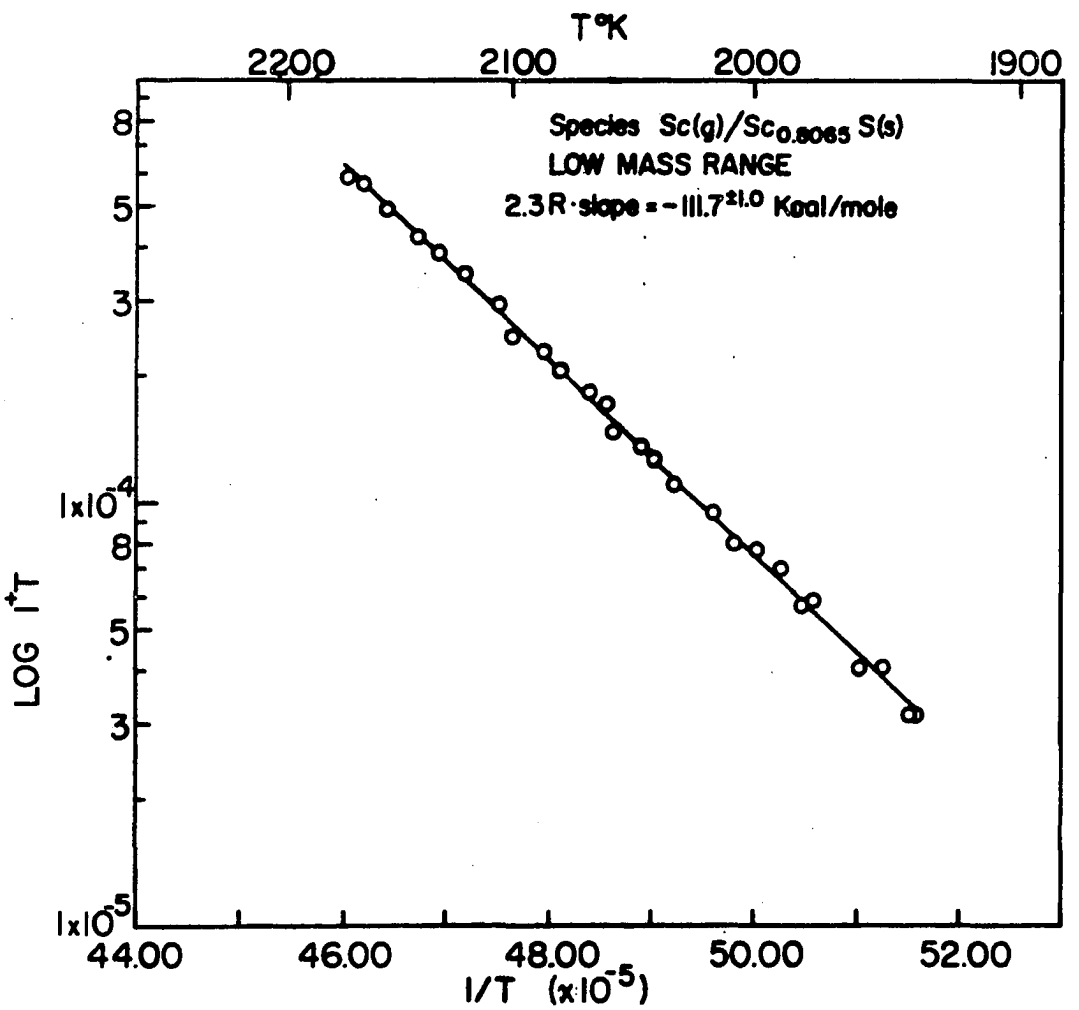

Figure 5.13. Second-law plot of log $I_{Sc^+}T$ vs. T^{-1} for vaporization of $Sc_{.8065}S(s)$ (results of experiment MS-11)

$$\Delta H_T^o(5.16) = 1.24(\Delta H_T^o(5.14) - \Delta H_T^o(5.15)) \quad . \qquad (5.30)$$

The value of $R\,\partial \ln I_{Sc^+}T/\partial T^{-1}$ (-111.7 kcal/mole) was the value determined in this experiment. The value used for $R\,\partial \ln I_{ScS^+}T/\partial T^{-1}$ was the average of the values obtained in experiments MS-5, MS-6, and MS-7 for that quantity (-116.2 kcal/mole). The value of $R\,\partial \ln I_{S^+}T/\partial T^{-1}$ was iteratively calculated assuming congruent vaporization and initial values of -112.0 kcal/mole for $R\,\partial \ln I_{S^+}T/\partial T^{-1}$ and 1×10^{-6} atm for P_S using the procedure described in Appendix B. A value of -113.5 kcal/mole was obtained for the sulfur slope. The second-law results for experiment MS-11 are given in Table 5.16. Since the multiplier gain was not measured in this experiment, the silver calibration could not be applied and thus the third-law method could not be used.

4. Summary of mass spectrometric results

The partial pressures of Sc(g) and ScS(g) over the congruently vaporizing scandium sulfide were evaluated using the silver calibration constant value of 1.00×10^{-12} atm cm^2/A K with the ion intensities obtained for these species as a function of temperature in experiments MS-5, MS-6 and MS-7. Figures 5.14 and 5.15 show plots of log P_{Sc} and log P_{ScS} respectively vs. T^{-1} for the three experiments. The values of $R\,\partial \ln P_{Sc}/\partial T^{-1}$ obtained from plots in Figure

Table 5.16. Second-law results of $Sc_{.8065}S(s)$ vaporization experiment MS-11

Reaction[a]	Midpoint Temp. (K)	ΔH°_{T} (kcal)	ΔH°_{298} (kcal)
1	2065	203.8 ± 1.6	210.2 ± 1.6
2	2065	116.2 ± 1.0	123.8 ± 1.0
3	2065	109.2 ± 1.6	107.1 ± 1.6

[a] 1 $Sc_{.8065}S(s) = .8065\ (c(g) + S(g)$
2 $Sc_{.8065}S(s) = .8065\ ScS(g) + .1935\ S(g)$
3 $ScS(g) = Sc(g) + S(g)$.

5.14 vary from -55.1 to -105.0 kcal/mole. Since in all of the experiments MS-5, MS-6 and MS-7 multiplier deterioration to some degree was observed in the spectrometer scans of mass 45, the values of $R\,\partial \ln P_{Sc}/\partial T^{-1}$ are assumed to be unreliable. The values of $R\,\partial \ln P_{ScS}/\partial T^{-1}$ obtained from the plots shown in Figure 5.15 range from -115.4 to -117.4 kcal/mole. Multiplier deterioration was not a problem in the spectrometer scans of mass 77 thus the values of $R\,\partial \ln P_{ScS}/\partial T^{-1}$ are assumed to be reliable. The average value of the ScS slopes from the three runs is -116.2 kcal/mole. The second law results for the two vaporization reactions of $Sc_{.8065}S(s)$ obtained from the log K_{eq} vs. T^{-1}

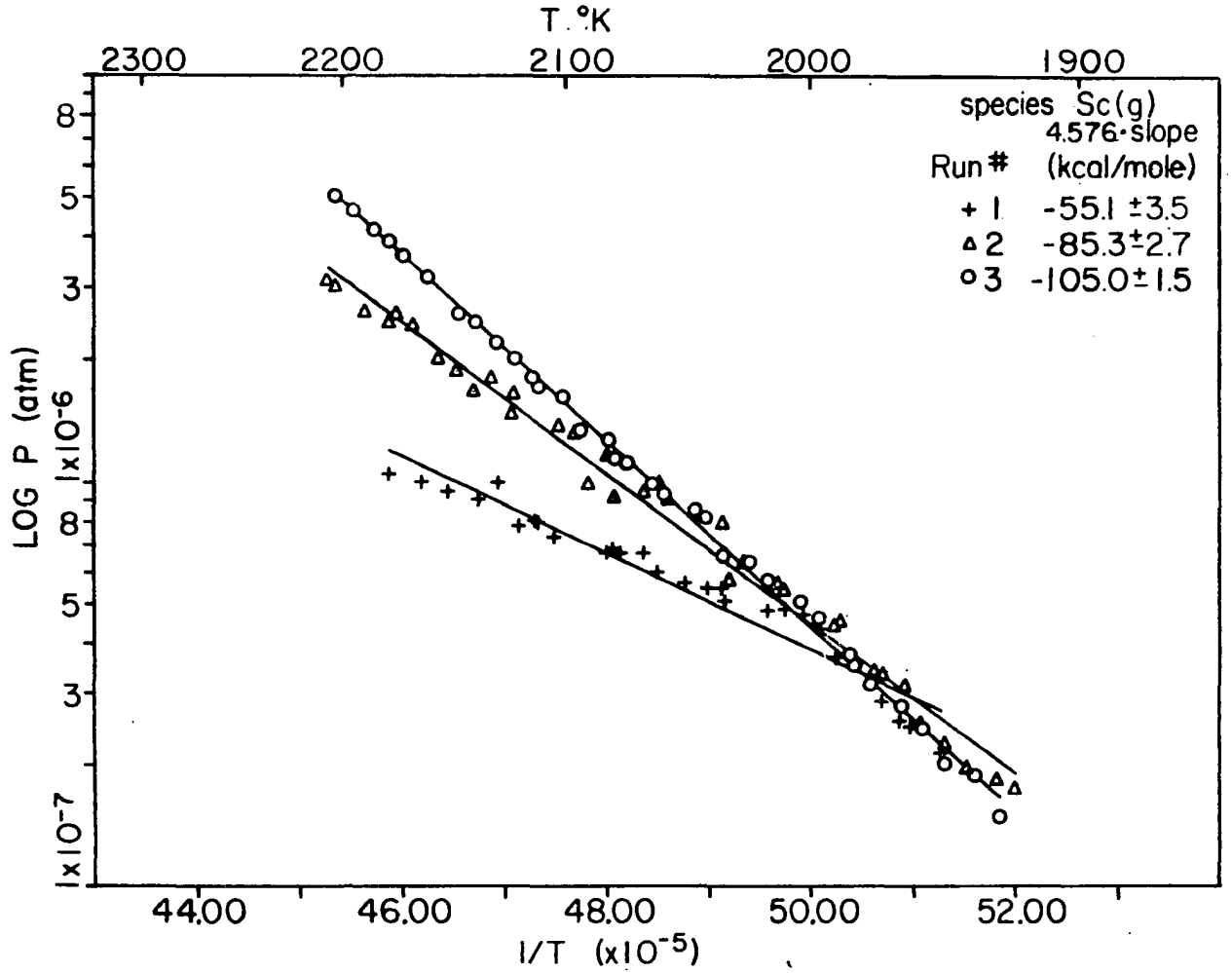

Figure 5.14. Plot of the logarithm of partial pressures of scandium over $Sc_{.8065}S(s)$ versus T-1, results of experiments MS-5 (run #1), MS-6 (run #2), and MS-7 (run #3)

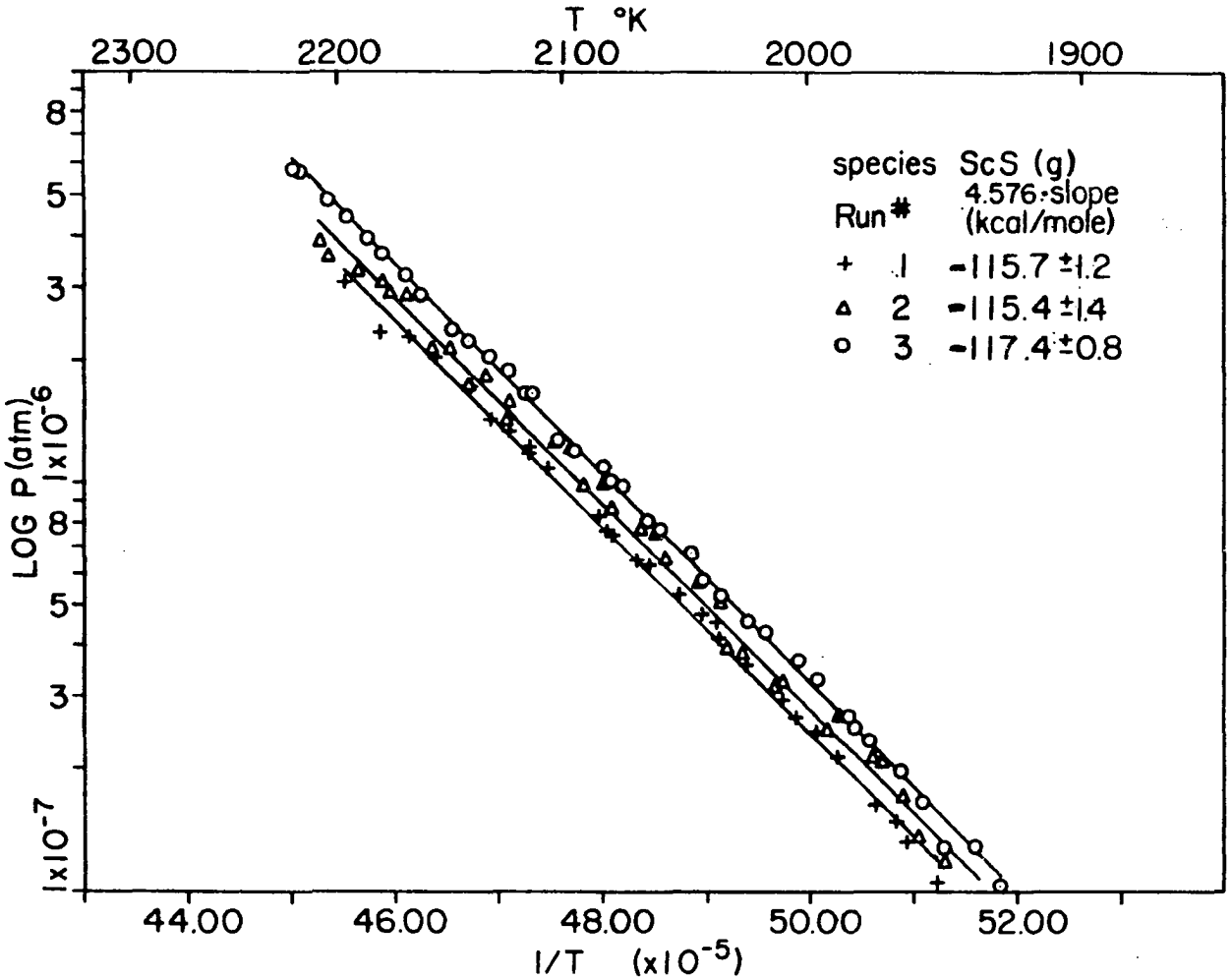

Figure 5.15. Plot of the logarithm of partial pressures of scandium monosulfide over $Sc_{.8065}S(s)$ versus T^{-1}, results of experiments MS-5 (run #1), MS-6 (run #2), and MS-7 (run #3)

plots using data from experiments MS-5, MS-6, and MS-7 are not considered reliable due to the systematic error associated with the $R\,\partial \ln P_{Sc}/\partial T^{-1}$ values. The systematic error in the value obtained for $R\,\partial \ln I_{Sc^+}T/\partial T^{-1}$ from experiment MS-11 is not thought to be serious. Thus the second-law heats obtained using the value of the scandium slope from experiment MS-11 (-111.7 kcal/mole) and the average of the three values obtained for $R\,\partial \ln P_{ScS}/\partial T^{-1}$ are the preferred second-law results. These results together with their standard deviations are given in Table 5.17. The preferred third-law heats for the vaporization reactions of $Sc_{.8065}S$ are obtained by averaging the third-law results from experiments MS-5, MS-6, and MS-7. These average values are given in the last column of Table 5.17. The uncertainties in the third-law values are estimated from uncertainties in the calibration constant and from uncertainties in the free energy function of $Sc_{.8065}S(s)$.

5. Error analysis

Errors in the mass spectrometric determination of vapor pressure and hence in the thermodynamic results for the vaporization of $Sc_{.8065}S(s)$ include: 1) systematic temperature errors, 2) error in mass spectrometric calibration constant, 3) ionization cross section and electron multiplier gain errors, 4) Clausing factor and orifice area

Table 5.17. Preferred second- and third-law mass spectrometric results of $Sc_{.8065}S(s)$ vaporization

Reaction[a]	Midpoint Temp. (K)	$\Delta H_T^{o\,b}$(II) (kcal)	ΔH_{298}^{o}(II) (kcal)	$\Delta H_{298}^{o\,c}$(III) (kcal)
1	2065	203.8 ± 1.6	210.2 ± 1.6	223.4 ± 4.9
2	2065	116.2 ± 1.0	123.8 ± 1.0	133.8 ± 4.5
3	2065	109.2 ± 1.6	107.1 ± 1.6	111.1 ± 4.4

[a] 1 $Sc_{.8065}S(s) = .8065\ Sc(G) + S(g)$
2 $Sc_{.8065}S(s) = .8065\ ScS(g) + .1935\ S(g)$
3 $ScS(g) = Sc(g) + S(g)$.

[b] Obtained from second-law results of experiment MS-11.

[c] Average third-law results of experiments MS-5, MS-6, and MS-7.

errors, 5) chemical composition variation, 6) errors in free energy functions and 7) random errors.

A systematic error in the temperature may be caused by uncertainties in the calibration of the optical pyrometer, window and mirror correction, error in reading the temperatures, a temperature gradient in the crucible, or by a nonideal black body. In the mass spectrometric experiment performed, there was very little deposit on the crucible cap indicating that the temperature gradient in the crucible was not large. It is believed that the

systematic temperature errors in this work arose mainly from reading and calibration of the pyrometer and window and prism corrections. For an experiment carried out over a temperature interval ΔT, the error in the second-law heat, $\delta(\Delta H)$, due to an error in temperature measurement, $\delta(\Delta T)$ is given by the law of propagation of errors

$$\delta(\Delta H)/\Delta H = - \delta(\Delta T)/\Delta T \quad . \tag{5.31}$$

The temperature interval used in all of the vaporization experiments was about 250°. For a 10° error in temperature measurement at one end of the range a 4% error in ΔH would result. The error in the third-law heats due to an error in temperature δT is given by

$$\delta(\Delta H^{\circ}_{298}) = \delta T(R \ln K_{eq} + \Delta fef) \quad . \tag{5.32}$$

Thus, the error in ΔH°_{298} for reactions 5.14, 5.15 and 5.16 resulting from a 10° temperature error would be 1.0, 0.6 and 0.5 kcal respectively.

The error estimated in the mass spectrometric constant was about 7%. This error would be introduced into the third-law pressure calculations of the gaseous species and hence into the third-law heats. The error in the third-law values for ΔH°_{298} for reactions 5.14, 5.15, and 5.16 would be about .30 kcal/mole.

The error in the electron multiplier gain measurements,

excluding the error resulting from the rapid gain deterioration observed in several experiments, is estimated to be about 10%. Mann's values for the ionization cross sections of Ag^+ and Sc^+ are assumed to be accurate to within 10%, although the value estimated for the ionization cross section of ScS^+ may be grossly in error. The error in the third-law values of ΔH^o_{298} resulting from a 10% error in both the ionization cross section and the multiplier gain would be about 0.6 kcal/mole for reactions 5.14, 5.15 and 5.16.

Since the same crucible was used for the silver calibration experiment and the scandium sulfide experiments, the error in the Clausing factors and orifice area would cancel. It was assumed that the crucible alignment was reproducible in the experiments.

Any change in the stoichiometry of the congruently vaporizing scandium sulfide during the mass spectrometric experiments would cause a systematic error in the second-law heats of the vaporization reactions. Powder patterns of the residue of various experimental runs, in which the sample was quenched from various temperatures in the range, yielded lattice parameters of about $5.165 \pm .002$ Å. This is the value corresponding to a composition S/Sc = 1.24. Thus, errors caused by variation in chemical composition would be negligible.

Errors in the enthalpy and entropy increments for Sc(g), S(g), ScS(g) and $Sc_{.8065}S(s)$ would introduce errors in the second-law heats at the reference temperature, and errors in the free energy functions of these species would result in errors in the third-law heats. For $Sc_{.8065}S(s)$, the error in $H^{o}_{2050}-H^{o}_{298}$ is estimated to be about $\pm$ 1 kcal/mole and the error in $S^{o}_{2050}-S^{o}_{298}$ is estimated to be about $\pm$ 1.2 eu. The error in the estimation of S^{o}_{298} for $Sc_{.8065}S(s)$ is thought to be $\pm$ 1.0 eu and the error in the estimation of the free energy function of the solid is about $\pm$ 1.5 eu. Since the molecular parameters of ScS(g) have been accurately determined, the errors in the thermodynamic properties of the gas are negligible compared to those for the solid. Thus, errors from uncertainties in thermodynamic properties would yield second-law errors of about 1.0 kcal/mole for reactions 5.14 and 5.15. The errors in the third-law values of ΔH^{o}_{298} for reactions 5.14 and 5.15 would be about 3 kcal/mole.

Random errors in second-law heats were evaluated as standard deviations of the least squares fit of the data. The total uncertainties in the second-law values of ΔH^{o}_{298} are $\pm$ 10.6, $\pm$ 6, and $\pm$ 5.5 kcal/mole for reactions 5.14, 5.15, and 5.16 respectively. The total uncertainties in the third-law results for the heats are $\pm$ 4.9, $\pm$ 4.5, and $\pm$ 4.4 kcal/mole for reactions 5.14, 5.15 and 5.16

respectively. By a comparison of the errors associated with the two methods of data treatment, it is evident that any systematic temperature dependent errors would introduce large uncertainties in the second-law heats, and any uncertainties in free energy functions would cause large errors in the third-law heats.

F. Comparison Between Mass Spectrometric Results and Target Collection Experiments on $Sc_{.8065}S$

Mass spectrometric investigation of the vaporization of $Sc_{.8065}S(s)$ demonstrated that the vapor species formed over the solid are Sc(g), S(g) and ScS(g). In the calculation of the effective pressure of $Sc_{.8065}S(s)$ using the target collection technique, it was assumed that ScS(g) was the only vapor species. However, the scandium collected on the targets arises from both ScS(g) and Sc(g), and thus the rate at which scandium is collected should equal the rate at which ScS molecules are collected plus the rate at which Sc atoms are collected, i.e.,

$$Z_{Sc}(\text{total}) = Z_{ScS} + Z_{Sc} \quad . \tag{5.33}$$

Thus, the partial pressures of ScS(g) and Sc(g) inside the Knudsen cell are related to the effective pressure by the equation,

$$P_E/(77)^{1/2} = P_{ScS}/(77)^{1/2} + P_{Sc}/(45)^{1/2} \quad . \qquad (5.34)$$

The relationship between the partial pressures of P_{Sc}, P_{ScS}, and P_S resulting from congruent vaporization is

$$.8065\ P_S/(32)^{1/2} = P_{Sc}/(45)^{1/2} + .1935\ P_{ScS}/(77)^{1/2} \quad . \qquad (5.19)$$

The equilibrium between ScS(g) and Sc(g) and S(g) provides another relationship between the partial pressures of the species. This relation can be written as follows:

$$P_{Sc}P_S/P_{ScS} = e^{-\Delta G^o_{diss}/RT} \quad , \qquad (5.35)$$

where the free energy change associated with dissociation of the sulfide molecule is given by

$$\Delta G^o_{diss} = \Delta H^o_{diss} - T\Delta S^o_{diss} \quad . \qquad (5.36)$$

The partial pressures P_{Sc}, P_S, and P_{ScS} can thus be obtained at each temperature at which a target was collected by solving Equations 5.34, 5.19, and 5.35 using the experimental P_E values and calculated ΔG^o_{diss} values. ΔG^o_{diss} can be calculated at any temperature using the dissociation energy of ScS(g) at 0 K of 113.4 kcal/mole reported by Coppens et al. (13) together with reported enthalpy increments and entropies for Sc(g) and S(g) and calculated enthalpy increments and

entropies for ScS(g). Table 5.18 lists the values obtained for the partial pressures of Sc and ScS from the target collection effective pressures and compares them with the mass spectrometrically determined pressures. The values of P_{Sc} obtained by the two methods are in good agreement, but the ratios P_{Sc}/P_{ScS} disagree. The P_{Sc}/P_{ScS} ratio obtained in the target collection experiment is determined by the value used for the dissociation energy of ScS(g). In the mass spectrometric work, P_{Sc}/P_{ScS} is determined by the ratio K_{ScS}/K_{Sc}, since the relationship between the partial pressures and the ion current temperature product is

$$I_i T = K_i P_i / C_m \quad , \tag{5.37}$$

where K_i contains the ionization cross section and multiplier efficiency. Thus, the ratio K_{ScS}/K_{Sc} is given by

$$K_{ScS}/K_{Sc} = \sigma_{ScS}\,\gamma_{ScS}/\sigma_{Sc}\gamma_{Sc} \quad . \tag{5.38}$$

In the evaluation of P_{ScS}, it was assumed that σ_{ScS} could be approximated by the sum of σ_{Sc} and σ_S obtaining σ_{ScS}/σ_{Sc} = 1.63. Assuming that the value obtained for γ_{ScS}/γ_{Sc} of .764 is correct, a ratio σ_{ScS}/σ_{Sc} = .74 is required to give the target collection value for P_{Sc}/P_{ScS}. This value of the ionization cross section ratio is reasonable according to results of Steiger and Cater (52) for YS(g) and recent evidence (53, 54) that ionization cross sections of uranium dioxide,

Table 5.18. Comparison of partial pressures calculated from target collection and mass spectrometric experiments

Temp. (K)	P_{ScS}(TC) (10^{-6}atm)	P_{Sc}(TC) (10^{-6}atm)	$\frac{P_{Sc}}{P_{ScS}}$(TC)	P_{ScS}(MS) (10^{-6}atm)	P_{Sc}(MS) (10^{-6}atm)	$\frac{P_{Sc}}{P_{ScS}}$(MS)
1960	0.35	0.19	.54	0.18	0.25	1.4
2000	0.56	0.33	.59	0.32	0.42	1.3
2040	1.34	0.68	.51	0.57	0.73	1.3
2080	2.06	1.13	.55	1.04	1.28	1.2
2120	3.16	1.81	.57	1.71	2.02	1.2
2160	4.92	2.92	.59	2.87	3.26	1.1
2200	9.52	5.19	.55	4.74	5.31	1.1

monoxide, and metal gases increase in that order.

Enthalpy changes for the vaporization reactions 5.14 and 5.15 can be obtained from the target collection partial pressures by calculating the equilibrium constants for the reactions as a function of temperature. As discussed in Chapter IV, the slope of a plot of $-R \ln K_{eq} + \Delta fef$ vs. T^{-1} gives a second-law value for ΔH^{o}_{298} for the reaction. The intercept of this plot should be at the origin. However, if the function $-R \ln K_{eq} + \Delta fef + S^{o}_{298}(Sc_{.8065}S)$ is plotted vs. T^{-1}, the intercept is the entropy of the solid at 298 K. Figure 5.16 shows this plot in which $K_{eq} = P^{.8065}_{Sc} P_S$, the

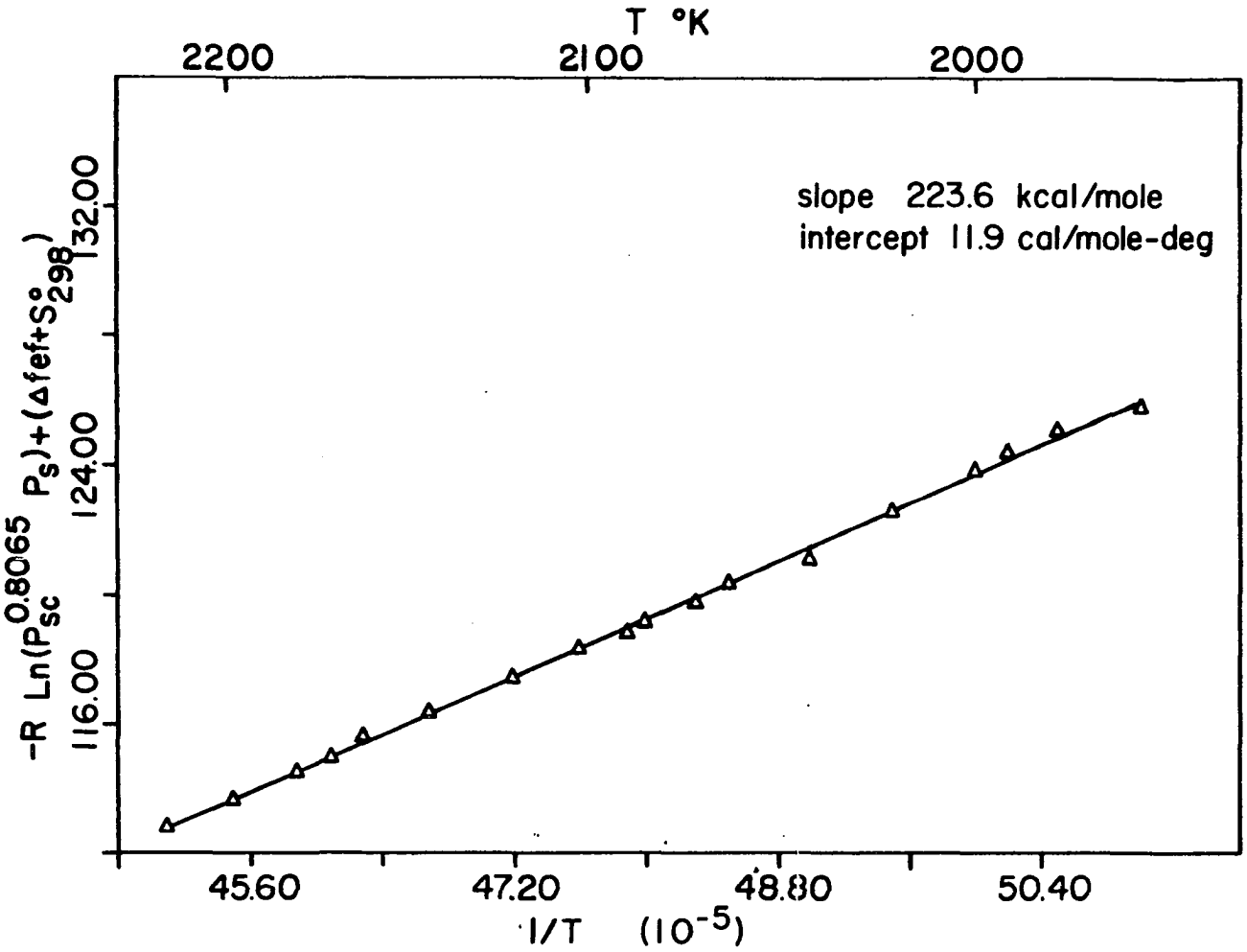

Figure 5.16. Plot of $-R \ln(P_{Sc}^{.8065} P_S) + \Delta fef + S^\circ_{298}(Sc_{.8065}S)$ vs. T^{-1}, partial pressures over $Sc_{.8065}S(s)$ obtained from target collection data

equilibrium constant for reaction 5.14, is obtained from the target collection data. The value of ΔH^{o}_{298} obtained for the reaction is 223.6 ± 1.9 kcal/mole and the value obtained for the entropy of $Sc_{.8065}S(s)$ at 298 K is 11.9 ± .9 eu. The enthalpy change is in good agreement with the third-law value obtained from the mass spectrometric data and the entropy of the congruently vaporizing sulfide agrees well with the estimated value of 11.8 eu. Combining the target collection value for the heat of reaction for reaction 5.14 with the CSD value of the dissociation energy, of ScS(g), a value of 131.3 kcal is obtained for the enthalpy change at 298 K associated with reaction 5.15. Table 5.19 compares the results obtained from the target collection experiment on the vaporization of $Sc_{.8065}S(s)$ with the mass spectrometric results.

G. Mass Spectrometric Results for the Vaporization of ScS

It has been determined from vaporization experiments using the rf induction heating system that stoichiometric scandium monosulfide preferentially loses scandium when heated in vacuum above 1600°C. The purpose of the mass spectrometric investigation of the vaporization of ScS(s) was to obtain partial pressure data for Sc(g) and ScS(g) above the stoichiometric solid, and as a function of time

Table 5.19. Comparison of target collection and mass spectrometric results for the vaporization of $Sc_{.8065}S(s)$

Reaction[a]	Mass Spectrometric ΔH^o_{298}(II) (kcal)	Mass Spectrometric ΔH^o_{298}(III) (kcal)	Target Collection ΔH^o_{298} (kcal)	Target Collection ΔS^o_{298} (eu)
1	210.2 + 10.6	223.4 ± 4.9	223.6 ± 2	61.9 ± 1.0
2	123.8 + 6	133.8 ± 4.5	131.3 ± 2	41.5 ± 1.5
3	107.1 + 6	111.1 ± 4.4	114.4[b]	25.2 ± .5

[a] 1 $Sc_{.8065}S(s) = .8065\ Sc(g) + S(g)$
2 $Sc_{.8065}S(s) = .8065\ ScS(g) + .1935\ S(g)$
3 $ScS(g) = Sc(g) + S(g)$.

[b] Value reported by Coppens et al. (13).

as the composition (Sc/S) of the solid changed from 1.0 to 0.8065. In experiment MS-9 ion intensity data were collected for Sc^+ on the medium mass range as a function of temperature upon vaporizing a sample having a composition ScS = 1.01. The temperature range used in this experiment was 1414 - 1601 K. This range is sufficiently low such that the composition change during the experiment is very small. The rate of mass loss from the crucible at the highest temperature in the range calculated from the Knudsen Equation 4.4 is 4.6×10^{-8} g/sec or 1×10^{-9} moles/sec assuming the

mass loss is only scandium. Thus, if the sample was heated for one hour at 1600 K, 3.6×10^{-6} moles of scandium would be vaporized. Since 85.3 mg of sample was present at the beginning of this experiment, 0.3 mole % of scandium would be lost if the samples were vaporized at 1600 K for one hour. Actually 25 ion intensity data for Sc^+ were collected over the temperature range 1414-1601 K in about 5 hours. The data were collected at temperatures varied randomly in the range to minimize any temperature dependent errors due to variation in the composition of the solid. No observable ion intensity for ScS^+ was detected in this temperature range. The electron multiplier gain for Sc^+ at the beginning of the run was 1.85×10^5 and at the end of the run was 1.7×10^5. Gain deterioration was not observed in the scans for Sc^+ over the temperature range used in this experiment. The partial pressure of Sc(g) was calculated from Equation 4.8 using a value of 1.77×10^5 for the multiplier gain and the machine constant value of 1.0×10^{-12} atm cm^2/A K. The plot of log P_{Sc} vs. T^{-1} and the least squares line are shown in Figure 5.17. The slope $R\, \partial \ln P_{Sc}/\partial T^{-1}$ obtained is -85.0 ± 1.0 kcal and the intercept is $11.1 \pm .3$ cal/K. The least squares is extrapolated to a temperature of 2035 K yielding a value for P_{Sc} of 3×10^{-4} atm at that temperature.

The purpose of experiments MS-8 and MS-10 was to obtain

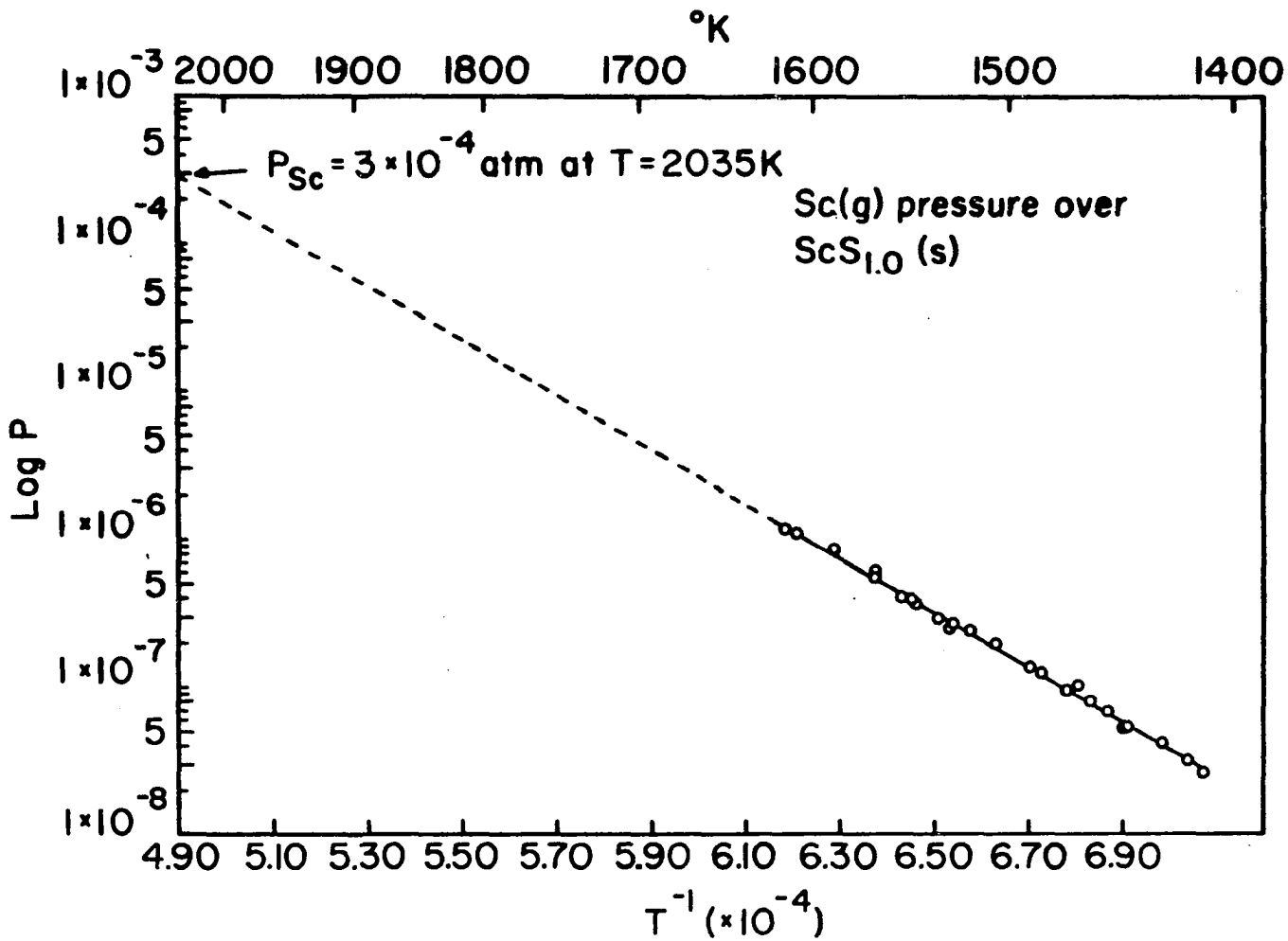

Figure 5.17. Plot of the logarithm of the partial pressure of scandium over ScS(s) vs. T^{-1}, results of experiment MS-9

ion intensity data for Sc^+ and ScS^+ over a scandium sulfide sample with composition varying from an initial Sc/S value of 1.0 to the congruently vaporizing composition. An 89.5 mg sample of ScS-2-175 (S/Sc = 1.006) was used for experiment MS-8. The sample was outgassed at about 1400 K for 24 hours after which time the shutter was opened and the temperature increased to 2035 ± 3 K. Ion intensity data were collected for Sc^+ and ScS^+ for about eight hours until a constant ion current was obtained. The composition was then assumed to be that of the congruently vaporizing solid. Due to instrumental problems associated with the high pressures resulting from the rapid temperature increase, measurable ion intensities could not be obtained until 1.5 hours after the beginning of the run. The multiplier gains which originally deteriorated upon increase of temperature continued to improve during the run. Partial pressures of Sc(g) and ScS(g) were calculated from the respective values of I^+T/γ using the calibration constant value of 1.0×10^{-12} atm cm^2/A K. Figure 5.18 shows the plots of P_{Sc} and P_{ScS} as a function of time. Since data were not obtained in the early part of the run in which the pressure variation was greatest, extrapolation of the partial pressures to time = 0 or Sc/S = 1.0 would yield large errors, especially for P_{Sc} which varies very sharply during this time interval. Since the partial pressure of

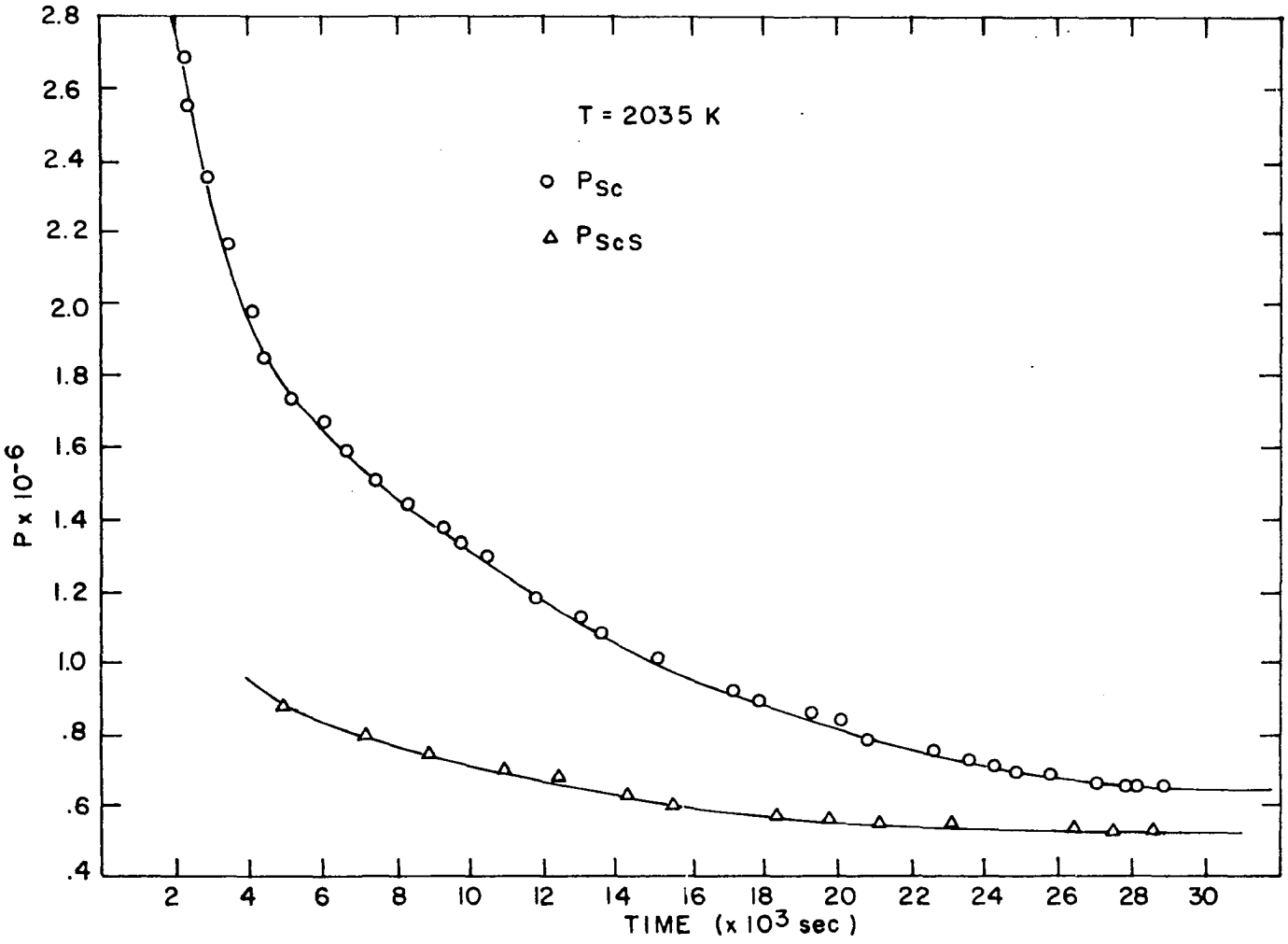

Figure 5.18. Partial pressures of scandium and scandium sulfide as a function of time upon vaporization of Sc(s) at 2035 K, results of experiment MS-8

ScS(g) is less sensitive to composition variation, this method could give a reasonably accurate value for P_{ScS} over the stoichiometric solid.

In experiment MS-10, an attempt was made to measure the ion intensity of ScS^+ more rapidly after the vaporization of the stoichiometric monosulfide was started. The residue of experiment MS-9 (Sc/S $\simeq$ 1.0) was used. The temperature of the sample was rapidly increased from 1400 to 2035 K. The shutter was opened and the spectrometer scanned mass 75-79 until a constant ion current was obtained. Measurable ion intensities were obtained about 40 minutes after initiating the experiment. Partial pressures were obtained from the ion intensities and are plotted against time of vaporization in Figure 5.19. The curve obtained from this plot was extrapolated to the origin of the time axis yielding a value for P_{ScS} of $1.6 \pm .4 \times 10^{-6}$ atm. The value of P_{ScS} obtained by this method depends on how the curve is extrapolated, however 1.25×10^{-6} atm would certainly be a lower limit. An upper limit for P_{ScS} over the stoichiometric solid can be obtained by application of the Gibbs-Duhem equation using the value of P_{Sc} over the 1:1 composition determined by extrapolation of the log P_{Sc} vs. T^{-1} plot (experiment MS-9). The integrated form of the Gibbs-Duhem equation, Equation 4.20, using the following partial pressures at 2035 K : $P_{Sc}(x=.8065) = 6.65 \times 10^{-7}$ atm,

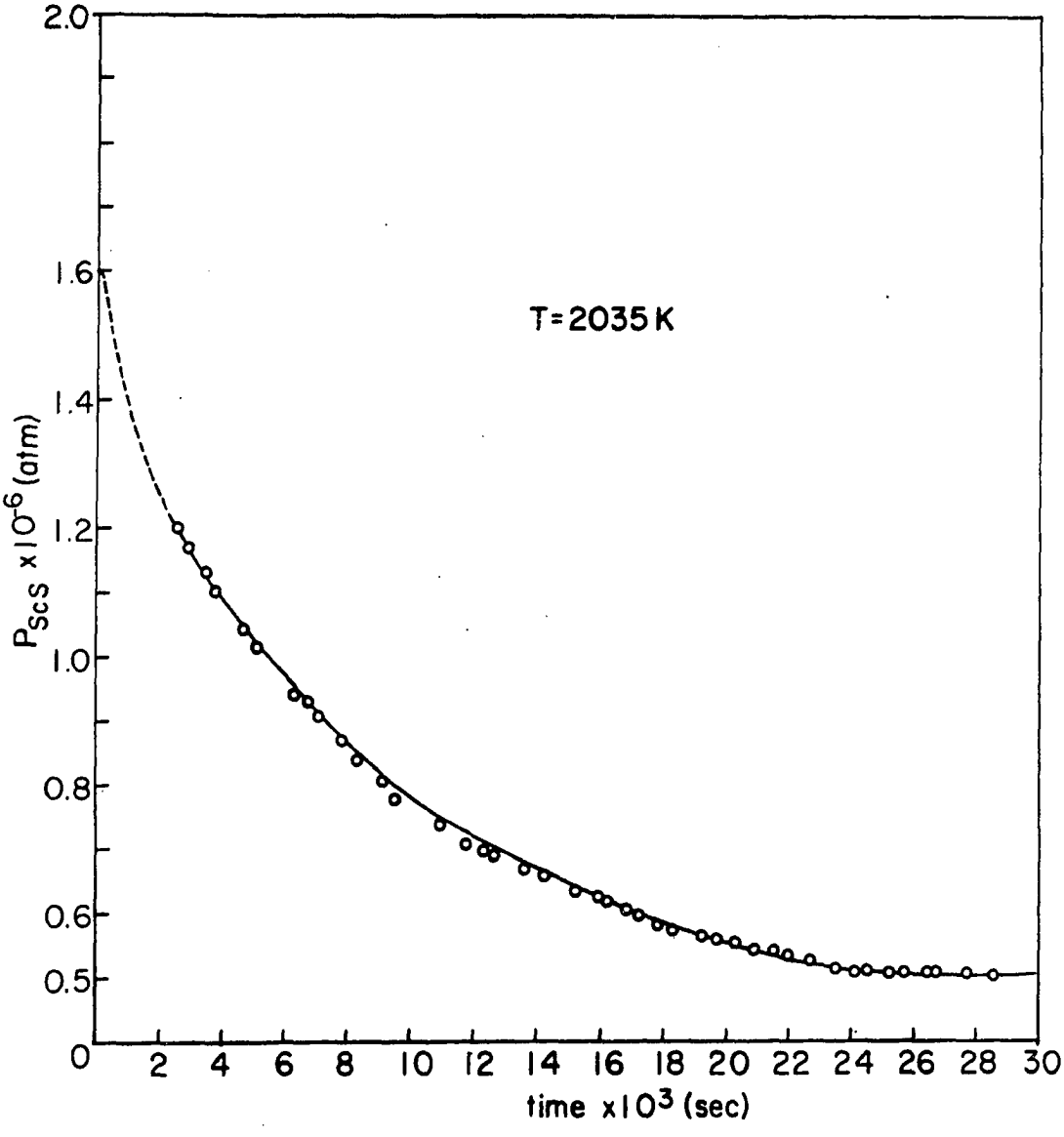

Figure 5.19. Partial pressure of scandium sulfide as a function of time upon vaporization of ScS(s) at 2035 K, results of experiment MS-10

$P_{ScS}(x=.8065) = 5.6 \times 10^{-7}$ atm, becomes

$$\frac{P_{ScS}(x=1.0)}{5.6 \times 10^{-7}} = \left[\frac{P_{Sc}(x=1.0)}{6.65 \times 10^{-7}}\right]^{.1935} \cdot e^{-A} \quad , \qquad (5.39)$$

where A is a positive area of integration. Table 5.20 lists the results obtained for $P_{ScS}(x=1.0)$ using two values for $P_{Sc}(x=1.0)$; the value obtained by extrapolation of the log P_{Sc} vs. T^{-1} plot, 3×10^{-4} atm, and the vapor pressure of pure scandium metal at 2035 K, 1.1×10^{-3} atm (upper limit for $P_{Sc}(x=1.0)$. The upper limit for $P_{ScS}(x=1.0)$ with $P_{Sc}(x=1.0) = 3 \times 10^{-4}$ atm is 1.78×10^{-6} atm, and with $P_{Sc}(x=1.0) = 1.1 \times 10^{-3}$ atm is 2.25×10^{-6} atm. Thus, $P_{ScS}(x=1.0)$ has a lower limit of 1.25×10^{-6} atm and an upper limit of 2.25×10^{-6} atm with the value of 1.6×10^{-6} atm considered accurate within $\pm$ 30%.

The partial pressure of Sc(g) and ScS(g) obtained over the stoichiometric scandium sulfide may be used to calculate thermodynamic properties associated with reactions between the stoichiometric solid and the congruently vaporizing sulfide. The following reaction may be considered:

$$Sc_{.8065}S(s) + .1935\ Sc(g) = ScS(s) \quad . \qquad (5.40)$$

This process is the result of the sum of the two reactions,

$$Sc_{.8065}S(s) + .1935\ Sc(g) = ScS(g) \quad , \qquad (5.41)$$

Table 5.20. $P_{ScS}(x=1.0)$ values calculated from the Gibbs-Duhem equation

$P_{Sc}(x=1) = 3 \times 10^{-4}$ atm		$P_{Sc}(x=1) = 1.1 \times 10^{-3}$ atm	
A	$P_{ScS(x=1)}$ $\times 10^{-6}$atm	A	$P_{ScS}(x=1)$ $\times 10^{-6}$atm
0	1.78	0	2.25
.1	1.67	.1	2.12
.2	1.51	.2	1.92
.3	1.32	.3	1.74
.4	1.24	.4	1.57
		.5	1.42
		.6	1.29

and

$$ScS(g) = ScS(s) \quad . \tag{5.42}$$

The standard free energy changes for reactions 5.41 and 5.42 are $-RT \ln P_{ScS}/P_{Sc}^{.1935}$ and $RT \ln P^{o}_{ScS}$ respectively, where P_{ScS} and P_{Sc} are the partial pressures over $Sc_{.8065}S(s)$ and P^{o}_{ScS} is the partial pressure of ScS(g) over ScS(s). Thus, the standard free energy change for reaction 5.40 is given by

$$\Delta G^{o}_{T} = -RT \ln P_{ScS}/P_{Sc}^{.1935} + RT \ln P^{o}_{ScS} \quad . \qquad (5.43)$$

Since the value of $P^{o}_{ScS} = 1.6 \times 10^{-6}$ atm was obtained at 2035 K, ΔG^{o} for reaction 5.40 is calculated at that temperature using values for P_{ScS} and P_{Sc} of 5.4×10^{-7} atm and 6.8×10^{-7} atm respectively. The value obtained is $\Delta G^{o}_{2035} = -7.7 \pm 1$ kcal. The enthalpy change ΔH^{o}_{2035} for reaction 5.40 can be calculated from the equation

$$\Delta H^{o}_{2035} = \Delta G^{o}_{2035} + T\Delta S^{o}_{2035} \quad , \qquad (5.44)$$

where

$$\Delta S^{o}_{2035} = S^{o}_{2035}(ScS(s)) - S^{o}_{2035}(Sc_{.8065}S(s)) - .1935\ S^{o}_{2035}(Sc(g)) \quad . \qquad (5.45)$$

The entropy of Sc(g) at 2035 K can be obtained from the JANAF Tables (26) and the entropies of the solids ScS(s) and $Sc_{.8065}S(s)$ at 2035 K can be obtained from the values estimated at 298 K by the method of Grønvold and Westrum, which yielded a value in good agreement with the value of the entropy of $Sc_{.8065}S(s)$ obtained from the target collection data, with estimated entropy increments from 298 to 2035 K for the solids. Since the entropy of Sc(g) is well known and since the same estimation method was used to obtain entropies for the solids, the value obtained for

ΔS°_{2035} of -5.1 eu is thought to be accurate to ± 0.5 eu. Thus, the value obtained for the enthalpy change at 2035 K for reaction 5.40 is -17.9 ± 2 kcal. The atomization reaction of ScS(s) can be obtained by combining reaction 5.40 with reaction 5.14 as follows:

$$Sc_{.8065}S(s) = .8065Sc(g) + S(g) \qquad \Delta H^{\circ}_{2035} = 215.3 \pm 4 \text{ kcal}$$

$$- \underline{Sc_{.8065}S(s) + .1935Sc(g) = ScS(s)} \qquad \underline{\Delta H^{\circ}_{2035} = -17.9 \pm 2 \text{ kcal}}$$

$$ScS(s) = Sc(g) + S(g) \qquad \Delta H^{\circ}_{2035} = 233.2 \pm 5 \text{ kcal} , \quad (5.46)$$

where the enthalpy change at 2035 K for reaction 5.14 was obtained from the target collection value of ΔH°_{298} using enthalpy increments between 298 and 2035 K for the reactant (estimated) and the products (literature). The value obtained for the standard enthalpy change at 2035 K for reaction 5.46 can be combined with the appropriate enthalpy functions for Sc(g) and S(g) and an estimated enthalpy increment for ScS(s) (same estimation method used for $Sc_{.8065}S(s)$) yielding ΔH°_{298} = 240.2 ± 5 kcal for that reaction. An experimental value for the enthalpy of formation of ScS(s) can be obtained by combining the enthalpy change at 298 K for reaction 5.46 with the enthalpy changes for the reactions

$$Sc(s) = Sc(g) \quad \Delta H^{\circ}_{298} = 90.3 \pm 1.0 \text{ kcal/mole} \qquad (5.47)$$

and

$$S(s) = S(g) \quad \Delta H^{\circ}_{298} = 66.68 \pm .6 \text{ kcal/mole} \qquad (5.48)$$

yielding $\Delta H^{\circ}_{298} = -82.8 \pm 5$ kcal for the reaction

$$Sc(s) + S(s) = ScS(g) \quad . \qquad (5.49)$$

The entropy of formation of ScS(s) at 298 K can be calculated from S°_{298} for crystalline sulfur, 7.63 eu, and solid scandium, 8.28 eu, and the value of S°_{298} for ScS(s), 12.7 eu, estimated by the method of Grøvold and Westrum yielding

$$\Delta S^{\circ}_{f,298} \text{ of ScS(s)} = -3.2 \pm 1.0 \text{ eu} \quad . \qquad (5.50)$$

Thus, the standard free energy of formation of ScS(s) is

$$\Delta G^{\circ}_{f,298} \text{ of ScS(s)} = -82 \pm 5 \text{ kcal/mole} \quad . \qquad (5.51)$$

VI. DISCUSSION

A. Ordering of Vacancies in $Sc_{.8065}S$ (Second Order Phase Transition)

The congruently vaporizing scandium sulfide has been characterized as $Sc_{.8065}S(s)$ having nearly 20% scandium vacancies from the stoichiometric monosulfide. The absence of superstructure lines in X-ray powder patterns or superstructure spots in Weissenberg photographs of samples with this composition which were quenched from high temperatures (above 1500°C) indicates that the congruently vaporizing solid has the rocksalt structure with random scandium vacancies at high temperature. A sample of congruently vaporizing scandium sulfide which was quenched from high temperatures was annealed at 500°C in a closed, evacuated quartz tube for about an hour. X-ray powder diffraction revealed that the product of this treatment had the rhombohedral $Sc_{1.37}S_2$ structure. Thus, the scandium vacancies which are randomly distributed in the sodium chloride structure at high temperature order at lower temperatures. The fact that the ordering is the same for the congruently vaporizing composition (S/Sc = 1.24) as for the $Sc_{1.37}S_2$ (S/Sc = 1.46) composition indicates that the $Sc_{1.37}S_2$ structure exists over a wide range of composition (at least to S/Sc = 1.24 and possibly to S/Sc = 1.0

as postulated by Dismukes and White (10)). The $Sc_{1.37}S_2$ structure is a partially disordered scandium-deficient rocksalt structure in which the vacancies appear in alternate scandium layers in the 111-direction of the cubic cell. The phase transition from the rhombohedral structure (s.g. $R\bar{3}m$) to the rocksalt structure (s.g. $Fm3m$) could occur with composition by continuously filling the vacant scandium lattice sites or with temperature by randomizing the vacancies over all scandium lattice sites. The results of the vaporization of scandium sulfide sample ScS-1-179 ($1.24 < S/Sc < 1.5$) show that the $Sc_{1.37}S_2$ structure was obtained for samples quenched from 1500°C and below, while the rhombohedral superstructure lines were not present in samples quenched from above 1560°C. This indicates that the phase transition occurs at some temperature in this interval for the particular composition of this sample. The two structures were not observed to coexist in any of the samples obtained by quenching various compositions from temperatures between 1260°C and 2000°C. Thus, it is possible that the phase transition between these structures is second order. The Landau theory for second order phase transitions can be applied to the NaCl to $Sc_{1.37}S_2$ structure change. The Landau theory (55) requires that a number of symmetry conditions must hold in order for a phase transition to be second order. These conditions are:

1. The symmetry group of one structure must be a subgroup of the symmetry group of the other.
2. The distortion of the crystal from the higher symmetry to the lower symmetry must correspond to a single irreducible representation of the space group of higher symmetry.
3. The third order terms in expansion of the free energy of the crystal must vanish by symmetry.
4. The symmetry operations in the group of the wave vector must include a center of symmetry or symmetry planes and axes intersecting in a point, and the representation to which the distortion corresponds must be singly degenerate.

The Landau conditions have been recently discussed by Franzen (56). The space group of the $Sc_{1.37}S_2$ structure, $R\bar{3}m$, is a subgroup of the space group $Fm3m$ with the $R\bar{3}m$ group having one-fourth of the symmetry operations of the cubic group. The distortion of the cubic structure arising from the ordering of the scandium vacancies results in a doubling of the body diagonal, and thus corresponds to one of the vectors in the star of $\{\frac{1}{2}, \frac{1}{2}, \frac{1}{2}\}$ (point L in the Brillouin zone). Jaap Fulmer (57) has obtained basis functions for the four equivalent distortions and has shown that the particular distortion of the NaCl structure which results in the $R\bar{3}m$ space group corresponds to the

$\hat{\tau}_1$ singly degenerate small irreducible representation (Kovalev (58)) of the space group Fm3m at point L in the Brillouin zone. He has further shown that there are no third order combinations of the coefficients of the basis functions which remain invariant under the symmetry operations of the cubic space group. Since point L in the Brillouin zone has $\bar{3}$m symmetry, a center of symmetry is present in the group of the wave vector and since the small irreducible representation is singly degenerate, the fourth condition of Landau is met and a second order phase transition is allowed. Thus, since no region of coexistence of the ScS and $Sc_{1.37}S_2$ phases was observed experimentally and all of the Landau criteria for second order phase transitions are met, a second order phase transition between these two phases could occur, although it is not possible to demonstrate that such a second order transition in fact does occur.

B. Comparison of Experimental Results with Born-Haber Calculations

Born-Haber calculations have been used to obtain estimates of the thermodynamic properties of a number of transition-metal sulfides. Moody and Thomas (59) using the Kapustinskii equation, Equation 4.27, for the lattice energy calculated by this thermochemical cycle an enthalpy

of formation of ScS(s). They obtained a value for $\Delta H^{o}_{f,298}$ of -76 kcal/mole which agrees rather well with the experimental value obtained in this work of -82.8 kcal/mole. However, the close agreement between the experimental and calculated lattice energies does not necessarily indicate that this solid is purely ionic. In order to further test the ability of the ionic model to describe the bonding in the scandium sulfides, a Born-Haber calculation can be used to obtain a value for the enthalpy change for the reaction,

$$ScS(s) = Sc_{.8065}S(s) + .1935\ Sc(g) \quad , \qquad (6.1)$$

between the stoichiometric and congruently vaporizing compositions of scandium monosulfide. The Born-Haber cycle employed for this purpose is shown below.

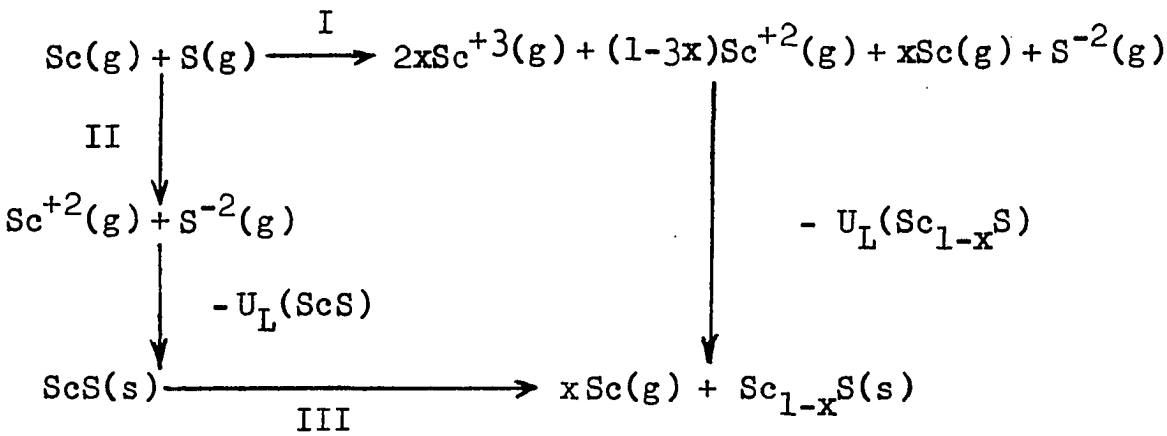

In this diagram when x = .1935, process III is the reaction

6.1. The enthalpy change for this reaction can be obtained from the enthalpy difference of two reaction paths starting with one mole each of gaseous Sc and S atoms. Thus,

$$\Delta H^{o}_{III} = (\Delta H^{o}_{I} - U_L(Sc_{.8065}S) - (\Delta H^{o}_{II} - U_L(ScS)) , \quad (6.2)$$

where $U_L(Sc_{.8065}S)$ and $U_L(ScS)$ are the lattice energies for the congruently vaporizing and stoichiometric solids respectively. These lattice energies can be calculated using Equation 4.26. For ScS(s), z_1 and z_2 both have the value 2 and r_o = 2.5925 Å yielding a value for $U_L(ScS)$ of 775.5 kcal/mole. For $Sc_{.8065}S(s)$, there are about 20% fewer scandium ions in the solid than sulfur ions. Therefore, in order for the crystal to be electrically neutral, 48% of the scandiums must have a +3 valence and 52% a +2 valence. Thus, $z_1 = .48(3) + .52(2) = 2.48$ where the Sc^{+3} and Sc^{+2} ions are evenly distributed over the occupied scandium lattice sites. In the defect sulfide, however, there are only .8065 N_o scandium ions per mole of solid. Thus, for $Sc_{.8065}S(s)$ Nz_1z_2 has the same value as it does for ScS(s) and the value obtained for $U_L(Sc_{.8065}S(s))$ is 777.6 kcal/mole for r_o = 2.583 Å. Since $\Delta H^{o}_{I} = 2x(I_1 + I_2 + I_3) + (1 - 3x)(I_1 + I_2) - E_S$ and $\Delta H^{o}_{II} = I_1 + I_2 - E_S$ where I_1, I_2 and I_3 are the first, second and third ionization potentials respectively for scandium and E_S is the electron affinity of sulfur, Equation 6.2 for ΔH^{o}_{III} with

$x = .1935$ becomes

$$\Delta H^{o}_{III} = .387\ I_3 - .1935(I_1 + I_2) - 2.1 \text{ kcal}$$

$$= 132.4 \text{ kcal} \quad . \qquad (6.3)$$

The enthalpy change for this reaction obtained from the equilibrium vapor pressure measurements over the stoichiometric and congruently vaporizing compositions was $+ 17.9 \pm 2$ kcal. The Born-Haber calculation thus yields an enthalpy change about 115 kcal greater than the experimental value and much too great to be compensated for by $T\Delta S$. This ionic model predicts that the monosulfide with composition $Sc/S = .8065$ would not be produced from the stoichiometric solid even at high temperatures.

C. Comparison of Thermodynamic Properties of ScS with Related Compounds

A comparison of the thermodynamic properties of scandium monosulfide with those for other binary transition-metal monosulfides may reveal trends across a transition series. This will aid in predicting thermodynamic properties for monosulfides of metals which have as yet been uninvestigated and may also provide an insight into the nature of the bonding in these sulfides. The values obtained for the atomization enthalpy and heat of formation

of ScS(s) are compared with reported values for other fourth row binary monosulfides in Table 6.1. The heats of atomization for the corresponding metals are also tabulated. The general trend is that the $\Delta H^{o}_{a,298}$ values for the first row transition-metal sulfides initially increase with increasing atomic number. There is a rather large increase from CaS to ScS, a smaller increase from ScS to TiS, an increase from TiS to VS and then a decrease to MnS. No thermodynamic data have been reported for CrS(s), however the value of $\Delta H^{o}_{a,298}$ for this solid would be expected to lie between the values for VS(s) and MnS(s). The trend observed for the $\Delta H^{o}_{a,298}$ values of the sulfides is similar to that found for the atomization enthalpies for the corresponding metals. Brewer (64) has explained this trend for the metals as relating to the variation in bonding energy per gram atom of the metal in the appropriate valence state with the number of d electrons. According to Brewer, the valence state bonding enthalpy per unpaired d electron for both the $d^{n-2}sp$ and $d^{n-1}s$ valence states decreases from scandium to manganese as an increased number of d electrons are crowded around an atom until a minimum in the bonding energy per electron is reached, when five d electrons per metal atom are used for bonding. Figure 6.1 shows the plot of the bonding enthalpy per unpaired electron in the valence state gaseous atom versus the number of unpaired electrons

Table 6.1. Comparison of thermodynamic properties of some fourth row metals and monosulfides[a]

Element	$\Delta H^{o}_{a,298}(M)$[b] (kcal/mole)	$\Delta H^{o}_{a,298}(MS)$ (kcal/mole)	$\Delta H^{o}_{f,298}(MS)$ (kcal/mole)
Ca	42.6 ± .4	224 ± 4 (60)	-114 ± 2 (60)
Sc	90.3 ± 1.0	240 ± 5	-83 ± 4
Ti	112.3 ± .5	243 ± 2 (61)	-63 ± 2 (61)
V	123.0 ± .2	259 ± 5 (62)	-69 ± 5 (62)
Cr	95.0 ± 1.0	--[c]	--[c]
Mn	67.7 ± 1.0	188 ± 4 (63)	-52 ± 4 (63)

[a]Reference numbers are given in parentheses.

[b]From JANAF Tables (26).

[c]No data available.

obtained by Brewer for the first transition series. Thus, the total bonding energy in kilocalories per gram atom of the element in a particular valence state, for example the $d^{n-2}sp$ (hcp) valence state, varies as fcllows:

Ca(85) Sc(135) Ti(157) V(165) Cr(158) Mn(120) .

The bonding energy of a metal in a particular valence state is, according to this scheme, the sum of the heat of vaporization from the ground electronic state plus the promotion

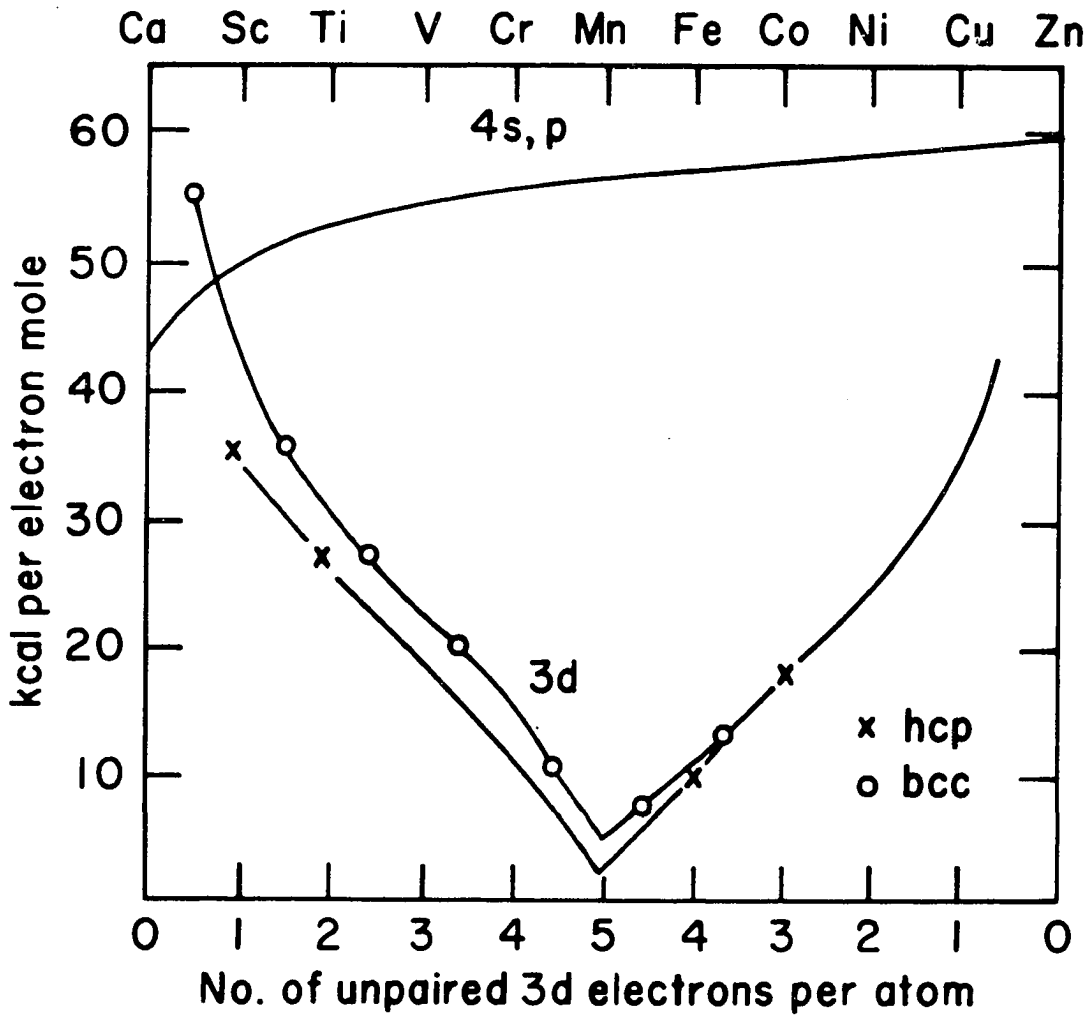

Figure 6.1. Valence-state bonding enthalpy per unpaired electron in kilocalories per gram atom (from Brewer (64)); upper curve plots bonding enthalpy of 4s or 4p electrons and bottom curve plots the bonding enthalpy of the 3d electron against the number of unpaired d electrons

energy in the gaseous atom from the ground state to the valence state. The promotion energy to the $d^{n-2}sp$ valence state does not vary substantially for the gaseous metal atoms from calcium to manganese. Thus, the initial variation in the heat of atomization across the first transition series is very similar to the variation in the bonding energy for those elements. Since the trend in the heats of atomization for the monosulfides is similar to that for the corresponding metals, it appears that the bonding energy of the transition metal d electrons contributes significantly to the stabilities of the monosulfides.

Thermodynamic properties for solid phases in the scandium sulfur system have been estimated by comparison with reported values for other Group III A sulfides. Mills (65) estimated a value for the heat of formation of ScS(s) at 298 K of -108 ± 10 kcal/mole using the following relationship

$$\frac{\Delta H^{o}_{f,298}(ScS(s))}{\Delta H^{o}_{f,298}(Sc_2O_3(s))} \simeq \frac{\Delta H^{o}_{f,298}(YS(s))}{\Delta H^{o}_{f,298}(Y_2O_3(s))} \simeq \frac{\Delta H^{o}_{f,298}(LaS(s))}{\Delta H^{o}_{f,298}(La_2O_3(s))} . \qquad (6.4)$$

The values of $\Delta H^{o}_{f,298}$ for $Sc_2O_3(s)$, $Y_2O_3(s)$ and $La_2O_3(s)$ of -152.0, -151.8, and -143.0 kcal/g-atom O respectively were taken from a tabulation by Brewer and Rosenblatt (66).

$\Delta H^{o}_{f,298}$ for YS(s) of -109 kcal/mole was determined by Steiger and Cater (52) and $\Delta H^{o}_{f,298}$ for LaS(s) of -105 kcal/mole was reported by Cater and Steiger (67). The experimental value for $\Delta H^{o}_{f,298}$ for ScS(s) of -83 $\pm$ 5 kcal/mole obtained in this work is considerably lower than the estimated value. The fact that the oxide-sulfide comparison does not work well for estimating the enthalpy of formation for ScS(s), but is in good agreement with reported heats of formation for YS(s) and LaS(s), and the fact that the stoichiometric yttrium and lanthanum monosulfides vaporize congruently while stoichiometric scandium monosulfide is unstable at high temperatures with respect to a reaction producing a defect monosulfide with composition Sc/S = .8065, may be attributed to the difference in the extent to which the d electron contributes to the bonding in the ScS(s) with respect to that in YS(s) and LaS(s). The bonding energy associated with the d electron on Sc, Y, and La can be obtained from the difference in the valence state bonding energies given by Brewer (64) between Sc and Ca, Y and Sr, La and Ba yielding 40, 64 and 58 kcal/per g-atom respectively. The results obtained by adding these values to the atomization enthalpies of CaS(s), SrS(s) and BaS(s) are given in column five of Table 6.2. These results are in excellent agreement with the reported atomization enthalpies of YS(s) and LaS(s), however

Table 6.2. Atomization enthalpies of Group II and Group III A monosulfides[a]

Group II	$\Delta H^{o}_{a,298}$(II) (kcal/mole)	Group III A	ΔBE[b] (kcal/g-atom)	$\Delta H^{o}_{a,298}$(II) + ΔBE (kcal/mole)	$\Delta H^{o}_{a,298}$(III) (kcal/mole)
CaS(s)	224 ± 2 (60)	ScS	40	264	240 ± 5[c]
SrS(s)	214 ± 3 (68)	YS	64	278	278 ± 2 (52)
BaS(s)	217 ± 2 (68)	LaS	58	275	275 ± 3 (67)

[a]Reference numbers given in parentheses.

[b]Difference in valence state bonding energies between Group III A and Group II metals, from Brewer (64).

[c]This work.

the value obtained in this work for the heat of atomization of ScS(s) is 24 kcal less than the calculated value. It is suggested here that the scandium 3d electron is not as effectively involved in metal-metal bonding in ScS(s) as are the 4d electron of yttrium and the 5d electron of lanthanum in yttrium monosulfide and lanthanum monosulfide respectively due to the relatively limited radial extent of the 3d orbitals compared to that for the 4d and 5d orbitals.

It would be of interest to compare the thermodynamic properties of ScS(s) with those for other scandium monochalcogenides. Although both ScSe(s) (69) and ScTe(s) (70) are reported to exist, no vaporization or thermodynamic data are available. Leary and Wahlbeck (71) determined that $Sc_2Se_3(s)$ vaporized congruently. They measured an effective vapor pressure over the solid but did not obtain equilibrium constants or enthalpy changes for the vaporization reactions.

D. Bonding in ScS(s)

The failure of the Born-Haber calculation to explain the formation of the defect scandium sulfide from the stoichiometric monosulfide indicates that the ionic bonding model, in which scandium is divalent in ScS(s) and a mixture of divalent and trivalent ions in $Sc_{.8065}S(s)$, is

not adequate for this solid. Further results which indicate a nonionic bonding character for scandium monosulfide have been provided by X-ray photoelectron spectroscopy. Franzen et al. (72) have measured the binding energy for an electron in both the metal and sulfur $2p^{3/2}$ orbitals for $ScS_{1.01}$ and $ScS_{1.24}$. They obtained binding energies for a $2p^{3/2}$ scandium electron in $ScS_{1.01}$ and $ScS_{1.24}$ of 402.15 and 402.20 eV respectively. These values are essentially the same and within the uncertainty of the measurement are indistinguishable from the value reported by Baker and Betteridge (73) of 402 eV for the binding energy of elemental scandium. Since the shift in the binding energy is proportional to the charge on the ion, the observed scandium shifts indicate very little charge on Sc in these compounds, although the amount of shift per unit charge is not known for scandium. The sulfur shifts have been demonstrated (74, 75) to be a rather sensitive measure of charge transfer with the 2p level shifting about 5 eV per charge. The observed binding energies for an electron in the sulfur $2p^{3/2}$ orbital in $ScS_{1.01}$ and $ScS_{1.24}$ were 162.5 and 162.2 eV respectively. The binding energy reported by Franzen and Sawatzky (76) for the 2p sulfur level in elemental sulfur is 163.7 eV. Thus, the sulfur shifts are 1.2 and 1.5 eV respectively corresponding to about -0.3 units of charge on the sulfur ions. The fact that the magnitude of

the sulfur charge is considerably less than 2, as would be expected for purely ionic bonding, suggests that the charge on the S^{-2} ions is largely delocalized into scandium 3d orbitals by a mixing of the valence and conduction bands.

The ESCA results show that there is relatively little charge transfer between the scandium and sulfur atoms in both stoichiometric scandium monosulfide and a defect scandium monosulfide. These results are similar to those found by Franzen and Sawatzky (76) in an ESCA study of VS(s) and indicate that these compounds may better be thought of as intermetallic rather than ionic compounds.

The bonding in transition-metal monochalconides has been discussed by Franzen (77). He proposed that a delocalized, directional, covalent bonding description similar to that proposed by Rundle (78) for MX compounds (in which M is a transition metal and X is C, N, or O), was consistent with the metallic conductivity, brittleness, high melting points comparable to the constituent metals, and the Pauli paramagnetic behavior observed for these chalcogenides. In this description the bonding in these compounds is primarily between metal and nonmetal atoms. In order to account for this strong interaction, Rundle (78) applied the valence bond model of chemical bonding to the transition-metal carbides, nitrides and oxides having the rocksalt structure. Rundle proposed that the p^3

orbital combination could utilize each orbital in bonding to two symmetrically equivalent coordinated atoms (two ligand per orbital bonding) with the appropriate symmetry for octahedral coordination. In scandium monosulfide (rocksalt structure) both atoms are octahedrally coordinated. Franzen (79) considered various orbital combinations suitable for two ligand per orbital bonding in trigonal prismatic and trigonal antiprismatic configurations. The lowest lying configuration appropriate to scandium in an octahedron (trigonal antiprism) is sd^2 and the lowest lying atomic configuration appropriate to sulfur in that coordination is p^3. In this scheme after promotion the three valence electrons of scandium and four valence electrons of sulfur are available for bonding. Six valence electrons are used in the valence band consisting of the sd^2 orbital combination from scandium and the p^3 orbital combination from sulfur. The remaining valence electron may be delocalized in the conduction band consisting principally of scandium d orbitals. However, these metal-metal interactions would be very weak, since the Sc-Sc distances in the NaCl structure are quite long (3.67 Å) and the 3d orbitals have a rather limited radial extent.

A qualitative MO scheme may also be used to describe the bonding in the scandium sulfides. In a discussion of the bonding in covalent transition-metal monocarbides,

mononitrides and monoxides having the NaCl-type structure, Denker (80) considers the molecular orbitals for an isolated MX_6 isolated octahedron in which both σ-type and π-type cation-anion bonding are possible. A molecular orbital energy level diagram (qualitative) for σ and π cation-anion bonding of an octahedral complex, MX_6, O_h symmetry, is shown in Figure 6.2. Each molecular orbital participating in bonding contributes one bonding and one antibonding level. In substances with eight valence electrons, such as CaS, ScN, and TiC, all of the bonding and nonbonding levels are occupied. In the absence of band overlap, these compounds would be insulators or semiconductors. Compounds with more valence electrons, e.g. TiN, TiO, and ScS, partially fill higher-lying antibonding levels and should be metallic. In this MO scheme stoichiometric scandium monosulfide with 9 valence electrons would have one electron in an antibonding orbital. This would tend to destabliize the octahedral configuration somewhat for ScS with respect to that for CaS. Reducing the valence electron concentration (v.e.c.) of scandium monosulfide however would tend to stabilize the MX_6 configuration. The existence of scandium vacancies would decrease the effective number of valence electrons and thus strengthen the σ and π scandium-sulfur bonding in an octahedral configuration.

The molecular orbital scheme is undoubtedly too simple

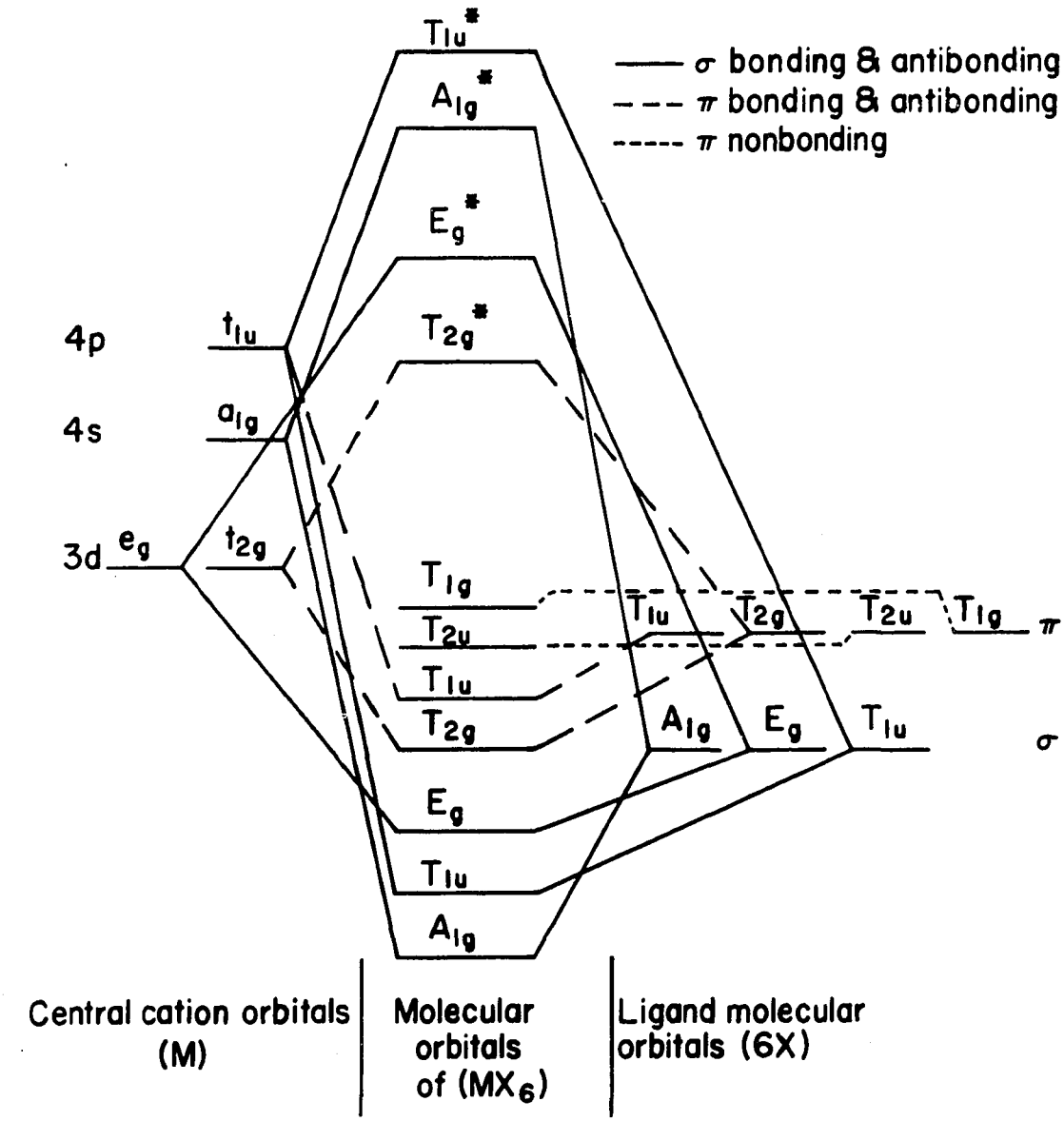

Figure 6.2. Qualitative molecular-orbital energy-level diagram for σ and π cation-anion bonding of an octahedral complex MX_6, O_h symmetry (energy not to scale)

a model for the bonding in a nonmolecular solid. The model does not include metal-metal interactions. A band structure calculation is needed in order to include additional solid state interactions and obtain an accurate density of states for the solid. This has not at present been done for scandium monosulfide, however energy band calculations have been performed on a number of transition-metal monocarbides, mononitrides and monoxides with the NaCl-type structure. Energy band calculations by Ern and Switendick (81) for TiC, TiN and TiO have revealed overlapping valence and conduction bands. They also determined that both metal-nonmetal and metal-metal interactions were important. The density-of-states obtained for these solids indicates that the Fermi energy lies across bonding levels in TiC (8 v.e.c.) but lies across antibonding levels in TiN (9 v.e.c.) and TiO (10 v.e.c.). The existence of lattice vacancies in TiN and TiO would reduce the effective number of valence electrons and thus depopulate antibonding levels stabilizing the NaCl-type structure (providing that the energy required to create a lattice vacancy is low enough). Because the Fermi energy of TiC lies only across bonding levels, vacancies would not be expected to stabilize this crystal. Since stoichiometric scandium monosulfide is a metallic rocksalt-structure solid having nine valence electrons, it is thought that the Fermi level in this

compound may also lie across antibonding states. The experimental results which show an increased stability of ScS with 20% scandium vacancies definitely support this contention. Assuming that there are no sulfur vacancies, the effective number of valence electrons in the congruently vaporizing monosulfide ($Sc_{.8065}S$) is 8.4. The maximum stability for scandium sulfide with the rocksalt structure occurs at this valence electron concentration. Calcium monosulfide which also has the rocksalt structure has eight valence electrons and would not require lattice vacancies to stabilize the structure. Nonstoichiometry has not been reported for calcium monosulfide. The fact that the valence electron concentration of the congruently vaporizing scandium monosulfide is between eight and nine is in agreement with the proposal that the 3d electron cannot fully participate in metal-metal bonding in this compound. The existence of lattice vacancies has not been reported for congruently vaporizing yttrium monosulfide or lanthanum monosulfide, which are isotypic and isoelectronic with ScS. The fact that the NaCl-type structure is stable with a valence electron concentration of nine for these compounds is also consistent with the contention that the d electrons in these solids are more effectively involved in metal-metal bonding.

VII. BIBLIOGRAPHY

1. F. Jellinek, in Inorganic Sulphur Chemistry, edited by G. Nickless (Elsevier, Amsterdam, 1968), Chapter 19.

2. G. B. Samsonov, High Temperature Compounds of Rare Earth Metals with Nonmetals (Consultants Bureau, New York, 1965).

3. L. Pauling, The Nature of the Chemical Bond, 3rd Edition (Cornell University Press, Ithaca, N.Y., 1960).

4. R. E. Rundle, in Intermetallic Compounds, edited by J. H. Westbrook (John Wiley and Sons, Inc., New York, N.Y., 1967), Chapter 2.

5. W. Hume-Rothery, in Phase Stability in Metals and Alloys, edited by P. S. Rudman, J. Stringer and R. Jaffee (McGraw-Hill, New York, 1967), Chapter 1.

6. L. Brewer, in Electronic Structure and Alloy Chemistry of the Transition Elements, edited by P. A. Beck (Interscience, New York, N.Y., 1963), Chapter 8.

7. W. Klemm, K. Meisel and H. U. von Vogel, Z. Anorg. Allgem, Chem., 190, 123 (1930).

8. A. A. Men'kov, L. N. Komissarova, Yu. P. Simanov and V. I. Spitsyn, Dokl. Akad. Nauk SSSR, 141, 364-367 [transl.: Doklady Chem., 141, 1137-1140 (1961)].

9. H. Hahn, Special Publication No. 12 (The Chemical Society, London, 1958).

10. J. P. Dismukes and J. G. White, Inorg. Chem., 3, 1220-1228 (1964), and J. G. White and J. P. Dismukes, Acta Cryst., 16, Suppl., 1963 A24.

11. J. P. Dismukes, J. Phys. Chem. Solids, 32, 1689-1691 (1971).

12. G. V. Lashkarev, V. A. Obolonchik, S. V. Radzikovskaya, V. P. Fedorchenko and T. M. Mikhlina, Ukr. Fiz. Zh., 15, 1560-1562 (1970).

13. P. Coppens, S. Smoes and J. Drowart, Trans. Faraday Soc., 63, 2140-2148 (1967).

14. R. P. Steiger and E. D. Cater, High Temp. Science, submitted for publication.

15. N. S. McIntyre, K. C. Lin and W. Weltner, Jr., J. Chem. Phys., 56, 5576-5582 (1972).

16. Bruce Randolph Conard, Ph.D. thesis, Iowa State University, 1969 (unpublished).

17. John George Smeggil, Ph.D. thesis, Iowa State University, 1969 (unpublished).

18. F. H. Spedding and B. J. Beaudry, J. Less-Common Metals, 25, 61-73 (1971).

19. K. Yvon, W. Jeitscho and E. Parthé, A FORTRAN Program for the Intensity Calculation for Powder Patterns (1969 version), University of Pennsylvania, 1969 (unpublished).

20. H. P. Hanson, F. Herman, J. D. Lea and S. Skillman, Acta Cryst., 17, 1040 (1964).

21. J. W. Colby, MAGIC IV - A Computer Program for Quantitative Electron Microprobe Analysis, Bell Telephone Laboratories, 1967 (unpublished).

22. F. A. Shunk, Constitution of Binary Alloys, Second Supplement (McGraw-Hill Book Co., New York, 1969).

23. R. P. Elliott, Constitution of Binary Alloys, First Supplement (McGraw-Hill Book Co., New York, 1965).

24. R. J. Thorn and G. H. Winslow, Recent Developments in Optical Pyrometry, ASME unpublished paper No. 63-WA-224, 1963.

25. E. D. Cater, USAEC Report No. COO-1182-30 (1969) (unpublished); in Techniques of Metal Research, edited by R. F. Bunshah (Wiley-Interscience, New York), Vol. IV, Part 1, Chapter 2A.

26. JANAF Thermochemical Tables, edited by D. R. Stull and H. Prophet (The Dow Chemical Company, Midland, Michigan, 1972), Supplement No. 38.

27. P. W. Gilles, in The Characterization of High-Temperature Vapors, edited by J. L. Margrave (John Wiley and Sons, Inc., New York, 1967), Chapter 2.

28. W. A. Chupka and M. G. Inghram, J. Phys. Chem., 59, 100 (1955).

29. M. G. Inghram and J. Drowart, in Proceedings of an International Symposium on High Temperature Technology (McGraw-Hill, New York, 1960).

30. R. T. Grimley, in Characterization of High Temperature Vapors, edited by J. L. Margrave (John Wiley and Sons, Inc., New York, 1967), Chapter 8.

31. J. Drowart and P. Goldfinger, Angewandte Chemie, International Edition, 6, No. 7 (1967).

32. W. Paul, H. P. Reinhard and U. von Zahn, Z. Physik, 152, 143 (1958).

33. E. G. Rauh, R. C. Sadler and R. J. Thorn, USAEC Report No. ANL-6563, 1962 (unpublished).

34. Thomas Peter Owzarski, M.S. thesis, Iowa State University, 1973 (unpublished).

35. M. Knudsen, Ann. Physik, 28, 999 (1909).

36. S. Dushman and J. M. Lafferty, Scientific Foundations of Vacuum Technique, 2nd Edition (John Wiley and Sons, Inc., New York, 1966).

37. J. G. Edwards, Ph.D. thesis, Oklahoma State University, 1964 (unpublished).

38. J. W. Otvos and D. P. Stevenson, J. Amer. Chem. Soc., 78, 546-551 (1956).

39. J. B. Mann, J. Chem. Phys., 46, 1646-51 (1967).

40. M. Gryzinski, Phys. Rev., 138, A336-358 (1965).

41. A. F. Kapustinskii, Quart. Rev., 10, 283-294 (1956).

42. D. H. Dennison, K. A. Geschneider and A. H. Daane, J. Chem. Phys., 44, 4273-82 (1966).

43. K. K. Kelley, Bureau of Mines Bulletin, 584, 157 (1960).

44. O. Kubaschewski, E. L. Evans and C. B. Alcock, Metallurgical Thermochemistry, 4th Edition (Pergamon Press, New York, 1967), Vol. I.

45. A. C. MacLeod and S. W. J. Hopkins, Proc. Brit. Ceram. Soc., 8, 15 (1967).

46. F. Grønvold and E. F. Westrum, Jr., Inorg. Chem., 1, 36-48 (1962).

47. H. F. Franzen, Iowa State University, private communication.

48. M. Marcano and R. F. Barrow (unpublished), reported by R. F. Barrow and C. Cousins in Advances in High Temperature Chemistry, edited by L. Eyring (Academic Press, New York, 1971), Vol. 4.

49. T. C. DeVore, Ph.D. thesis, Iowa State University, 1975 (unpublished).

50. M. G. Inghram, R. J. Hayden and D. C. Hess, U.S. Nat. Bureau of Standards Circular, 552, 257 (1953).

51. R. Hultgren, R. L. Orr, P. D. Anderson and K. K. Kelley, Selected Values of Thermodynamic Properties of Metals and Alloys (John Wiley and Sons, Inc., New York, 1963).

52. R. A. Steiger and E. D. Cater, High Temp. Science, submitted for publication.

53. P. E. Blackburn and P. M. Danielson, J. Chem. Phys., 56, 6156 (1972).

54. A. Pattoret, J. Drowart and S. Smoes, Trans. Faraday Soc., 65, 98 (1969).

55. L. D. Landau and E. M. Lifshitz, Statistical Physics (Pergamon Press Ltd., London, 1962), Chapter 14.

56. H. F. Franzen, The Landau Theory of Phase Transitions, Iowa State University, unpublished paper.

57. Jaap Fulmer, Grönigen University, The Netherlands, private communication.

58. O. V. Kovalev, Irreducible Representations of the Space Groups (Gordon and Breach, Science Publishers, Inc., New York, 1964).

59. G. J. Moody and J. D. R. Thomas, J. Chem. Soc., 1964, 1417 (1964).

60. R. D. Freeman, Thermo. Properties of Binary Sulfides, Oklahoma State University Res. Foundation Report No. 60, Stillwater, Okla. (1962).

61. J. G. Edwards, H. F. Franzen and P. W. Gilles, J. Chem. Phys., 54, 545 (1971).

62. T. P. Owzarski and H. F. Franzen, J. Chem. Phys., 60, 1113 (1974).

63. H. Wiedemeier and P. W. Gilles, J. Chem. Phys., 42, 2765 (1965).

64. L. Brewer, Science, 161, 115 (1968).

65. K. C. Mills, Thermodynamic Data for Inorganic Sulfides Selenides and Tellurides (Butterworths and Co. Ltd., London, 1974).

66. L. Brewer and G. Rosenblatt, in Advances in High Temperature Chemistry, edited by L. Eyring (Academic Press, New York, 1969), Vol. 2, Chapter 1.

67. E. D. Cater and R. P. Steiger, J. Phys. Chem., 72, 2231 (1968).

68. E. D. Cater and E. W. Johnson, J. Chem. Phys., 47, 5353 (1967).

69. F. Hulliger and G. W. Hull, Jr., Solid State Comm., 8, 1379-1382 (1970).

70. L. H. Brixner, J. Inorg. Nucl. Chem., 15, 199-201 (1960).

71. H. J. Leary, Jr. and P. G. Wahlbeck, High Temp. Science, 1, 277-286 (1969).

72. H. F. Franzen, J. McCreery, R. J. Thorn and M. X. Umaña, Iowa State University, unpublished.

73. A. D. Baker and D. Betteridge, Photoelectron Spectroscopy, Chemical and Analytical Aspects (Pergamon Press Ltd., Oxford, 1972).

74. K. Siegbahn, C. Nordling, A. Fahlman, R. Nordbert, K. Hamrin, J. Hedman, G. Johansson, T. Bergmark, S. E. Karlsson, I. Lindgren and B. Linberg, ESAC-Atomic, Molecular and Solid State Structure Studies by Means of Electron Spectroscopy (Uppsala, 1967).

75. K. Siegbahn, Phil. Trans. Roy. Soc. Lond., A268, 33 (1970).

76. H. F. Franzen and G. A. Sawatzky, J. Solid State Chem., submitted for publication.

77. H. F. Franzen, J. Inorg. Nucl. Chem., 28, 1575 (1966).

78. R. E. Rundle, Acta Cryst., 1, 180 (1948).

79. H. F. Franzen, Hybrid Orbitals for Two Ligand per Orbital Bonding. Application to Vandium Monosulfide, Iowa State University, unpublished paper.

80. S. P. Denker, J. Less-Common Metals, 14, 1-22 (1968).

81. V. Ern and A. C. Switendick, Phys. Rev., 137, 1927A (1965).

VIII. ACKNOWLEDGMENTS

The author wishes to express his sincere appreciation to Professor H. F. Franzen for his encouragement, suggestions and enthusiastic interest throughout the course of this research.

The author is also extremely grateful to Thomas Owzarski for communicating his expertise on the operation of the mass spectrometer.

The author is indebted to many of the personnel of the Ames Laboratory, particularly: Fran Laabs, who performed the electron microprobe analysis of scandium sulfide samples and target deposits; Harlan Baker for preparing the surface of the targets; Gary Wells and members of the research shop for construction of crucibles and apparatus; and Edgar Moore of the glassblowing shop for construction of the target collection apparatus.

Also, the author wishes to express appreciation to the members of Dr. Franzen's high temperature laboratory for their assistance and helpful discussions.

IX. APPENDIX A: IN SITU CALIBRATION OF THE AUTOMATIC OPTICAL PYROMETER

The Leeds and Northrup automatic optical pyrometer (ALPN 13994) was calibrated using the same arrangement for measuring temperature used in the target collection experiments. The automatic pyrometer was sighted through a window and prism, having a combined correction constant of $1.43 \times 10^{-5}\ K^{-1}$, onto the black-body hole of the inductively heated tungsten crucible. At various settings of the Electromax IV controller, the millivolt output of the automatic pyrometer was compared with the temperature measured by sighting the disappearing filament pyrometer (ALPN 9415) through a window and mirror, having a combined correction constant of 1.53×10^{-5} K, into the orifice in the top of the tungsten crucible. The target magazine and liquid nitrogen dewar were replaced with a flat pyrex plate for this purpose. The results of this calibration are tabulated in Table A.1.

Table A.1. Calibration[a] of M range of automatic optical pyrometer (ALPN 13994) against manual optical pyrometer (ALPN 9415)

Set point[b]	Output of Auto. Pyr.[c] (mv)	Observed Temp. Manual Pyr.[d] °C	Corrected Temp. Manual Pyr.[e] °C
2900	30.49 ± .03	1245 H	1236
3000	31.40 ± .03	1281 H	1270
3100	32.29 ± .02	1313 H	1302
3200	33.18 ± .02	1338 H	1328
3300	34.09 ± .01	1369 H	1359
3400	35.01 ± .01	1402 H	1393
3500	35.94 ± .01	1430 H	1422
3600	36.86 ± .01	1463 H	1455
3700	37.79 ± .01	1487 H	1481
3800	38.72 ± .01	1515 H	1510
3900	39.63 ± .01	1540 H	1537
4000	40.59 ± .01	1569 H	1567

[a]Automatic optical pyrometer calibrated with same arrangement used for temperature measurement in target collection experiments.

[b]Set point of Electromax controller.

[c]Automatic pyrometer sighted through a window and prism having a combined correction constant of $.143 \times 10^{-4}$ K^{-1}.

[d]Pyrometer drum reading.

[e]Temperature correction includes sectored wedge calibration and correction constant of window and mirror ($.153 \times 10^{-4}$ K^{-1}).

Table A.1 (Continued)

Set point[b]	Output of Auto. Pyr.[c] (mv)	Observed Temp. Manual Pyr.[d] °C	Corrected Temp. Manual Pyr.[e] °C
4100	41.55 ± .01	1593 H	1593
4200	42.48 ± .01	1620 H	1618
4300	43.39 ± .01	1652 XH	1643
4400	44.30 ± .02	1678 XH	1667
4500	45.33 ± .01	1713 XH	1693
4600	46.35 ± .01	1741 XH	1724
4700	47.36 ± .01	1773 XH	1754
4800	48.42 ± .01	1809 XH	1789
4900	49.42 ± .01	1835 XH	1638

X. APPENDIX B: ITERATIVE PROCEDURE FOR CALCULATING THE SULFUR SLOPE

An equation relating the sulfur slope, $R\,\partial \ln I_{S^+}T/\partial T^{-1}$, to the experimentally determined scandium and scandium sulfide slopes was obtained as follows: The congruence equation,

$$\frac{0.8065\ P_S}{\sqrt{32}} = \frac{P_{Sc}}{\sqrt{45}} + \frac{.1935\ P_{ScS}}{\sqrt{77}} \qquad (A.1)$$

was differentiated with respect to T^{-1}, yields

$$\frac{.8065}{\sqrt{32}}\frac{\partial P_S}{\partial T^{-1}} = \frac{1}{\sqrt{45}}\frac{\partial P_{Sc}}{\partial T^{-1}} + \frac{.1935}{\sqrt{77}}\frac{\partial P_{ScS}}{\partial T^{-1}} \quad . \qquad (A.2)$$

This equation can be expressed as

$$\frac{.8065\ P_S}{\sqrt{32}}\frac{\partial \ln P_S}{\partial T^{-1}} = \frac{P_{Sc}}{\sqrt{45}}\frac{\partial \ln P_{Sc}}{\partial T^{-1}} + \frac{.1935\ P_{ScS}}{\sqrt{77}}\frac{\partial \ln P_{ScS}}{\partial T^{-1}} \quad . \qquad (A.3)$$

Rearrangement of this equation with multiplication by R yields

$$R\frac{\partial \ln P_S}{\partial T^{-1}} = \frac{\frac{P_S}{\sqrt{45}}\frac{R\,\partial \ln P_{Sc}}{\partial T^{-1}} + \frac{.1935\ P_{ScS}}{\sqrt{77}}\frac{R\,\partial \ln P_{ScS}}{\partial T^{-1}}}{\sqrt{32}/.8065\ P_S} \quad , \qquad (A.4)$$

where $R\,\partial \ln P_S/\partial T^{-1} = R\,\partial \ln I_{S^+}T/\partial T^{-1}$.

Enthalpy changes, ΔH_1 and ΔH_2, respectively for the reactions

$$Sc_{.8065}S(s) = .8065\ Sc(g) + S(g) \quad , \tag{A.5}$$

and

$$Sc_{.8065}S(s) = .8065\ ScS(g) + .1935\ S(g) \quad , \tag{A.6}$$

are obtained from the sulfur, scandium, and scandium sulfide slopes as follows:

$$\Delta H_1 = .8065\ R\,\partial \ln P_{Sc}/AT^{-1} + R\,\partial \ln P_S/\partial T^{-1} \quad , \tag{A.7}$$

and

$$\Delta H_2 = .8065\ R\,\partial \ln P_{ScS}/\partial T^{-1} + .1935\ R\,\partial \ln P_S/\partial T^{-1} \quad . \tag{A.8}$$

The free energy changes, ΔG_1 and ΔG_2, for reactions A.5 and A.6 respectively are

$$\Delta G_1 = \Delta H_1 - T\Delta S_1 = -RT \ln(P_{Sc}^{.8065}P_S) \quad , \tag{A.9}$$

and

$$\Delta G_2 = \Delta H_2 - T\Delta S_2 = -RT \ln(P_{ScS}^{.8065}P_S^{.1935}) \quad . \tag{A.10}$$

The sulfur pressure, P_S, can be expressed in terms of the free energy changes by combining Equations A.7 and A.8 with

Equation A.1 to obtain

$$P_S = \frac{.24\sqrt{32}}{\sqrt{45}} \frac{e^{-\Delta G_2/RT}}{P_S^{.24}}^{1.24} + \frac{1.24\sqrt{32}}{\sqrt{45}} \frac{e^{-\Delta G_1/RT}}{P_S^{I.24}}^{1.24} . \quad (A.11)$$

The procedure for obtaining the iterative sulfur slope and the partial pressures was as follows: Enthalpy changes ΔH_1 and ΔH_2 were obtained from Equations A.7 and A.8 by using an initial estimate for the sulfur slope at a temperature of 2060 K, the midpoint of the temperature range used on the measurement of the scandium and scandium sulfide slopes, with the measured values for these slopes. The free energy changes ΔG_1 and ΔG_2 were then calculated from ΔH_1 and ΔH_2 and computed values for ΔS_1 and ΔS_2 at 2060 K. A value for the sulfur pressure was obtained from Equation A.11 using the ΔG values and initial estimate of the sulfur pressure. A scandium pressure, P_{Sc}, and a scandium sulfide pressure, P_{ScS}, were obtained from the sulfur pressure and the values for ΔG_1 and ΔG_2 by using Equations A.9 and A.10 respectively. A new value for the sulfur slope was obtained from Equation A.4. The procedure was repeated until successive sulfur slopes agreed to within .1%.